

**DESIGN AND MODELING OF A PORTABLE HEMODIALYSIS SYSTEM**

A Thesis  
Presented to  
The Academic Faculty

By

Jeffrey Carter Olson

In Partial Fulfillment  
Of the Requirements for the Degree  
Master of Science in Mechanical Engineering

Georgia Institute of Technology

May 2009

## DESIGN AND MODELING OF A PORTABLE HEMODIALYSIS SYSTEM

Approved by:

Dr. David W. Rosen, Chair  
George W. Woodruff School of Mechanical Engineering  
*Georgia Institute of Technology*

Dr. David N. Ku  
George W. Woodruff School of Mechanical Engineering  
*Georgia Institute of Technology*

Dr. Christiaan J.J. Paredis  
George W. Woodruff School of Mechanical Engineering  
*Georgia Institute of Technology*

Date Approved: 2009 March 26

To my family.

## ACKNOWLEDGEMENTS

Firstly, I am very grateful of the support of the Carlos and Marguerite Mason Foundation. Without such support, this work would not have been possible.

I would like to acknowledge my advisor, Dr. David Rosen, for providing guidance during the completion of this work. Writing a thesis is a daunting task; I have been fortunate to work with an advisor who could provide insightful advice, valuable opinions, and the proper amount of interference.

I thank the rest of my reading committee, Drs. David Ku and Chris Paredis, for their advisement. Dr. Ku, as an advisor to the research group of which this thesis is a product, has provided me with helpful advice regularly for the last two years. It is not easy for a mechanical engineer to solve medical problems; his expertise has guided me many times.

In addition to Drs. Rosen and Ku, I would like to thank the rest of the “kidney project” team: Yong Yang, Jason Weaver, and Jane Kang. I have had a lot of fun working with Yong day in and day out on trying to improve hemodialysis over the last two and a half years. I am very grateful for Jason’s laboratory work – I am not sure if I could have completed this work if I had to handle blood regularly.

These last two and a half years I have been apart of a community known as the Systems Realization Laboratory. I have met too many great people in the lab to list all of them, but I would like to specifically acknowledge Christopher Williams and Jamal Wilson. Chris was one of the first SRL members I became acquainted with, and as a senior member, was always willing to provide me with excellent advice – even if it meant a two-hour phone call the night before his Virginia Tech application was due. Jamal’s help over the last two years has been invaluable. We have gone

through countless dry erase markers together in our joint research efforts. I hope that someday our professional paths cross again.

Lastly, I would like to thank the people I dedicated this work to – my family. In life, I have always known that I have had the support of the ones who have known me the longest – my father, my mother, my sister – throughout all of my adventures.

## TABLE OF CONTENTS

<b>Acknowledgements</b> .....	<b>iv</b>
<b>List of Tables</b> .....	<b>x</b>
<b>List of Figures</b> .....	<b>xii</b>
<b>List of Symbols and Abbreviations</b> .....	<b>xvii</b>
<b>Summary</b> .....	<b>xix</b>
<b>1 Motivation for Modeling and Designing a Hemodialysis System</b> .....	<b>1</b>
1.1 Renal replacement therapies .....	1
1.2 Research questions and hypothesis.....	2
1.3 Validation and verification strategy .....	4
<b>2 Present Work in Renal Replacement</b> .....	<b>5</b>
2.1 A brief history of renal replacement .....	5
2.1.1 The first dialyzer designed for human use.....	6
2.1.2 The first trial of dialysis on a human.....	6
2.1.3 The drum dialyzer and the first successful renal replacement therapy .....	7
2.1.4 The coil and twin coil dialyzer .....	9
2.1.5 The development of reusable vein access .....	10
2.1.6 Successful treatment of chronic renal failure .....	10
2.1.7 Single-pass dialysis and home hemodialysis .....	10
2.1.8 The hollow fiber dialyzer .....	11
2.2 Peritoneal dialysis.....	11
2.3 Hemofiltration.....	14
2.4 Bioartificial kidneys .....	16
2.5 MEMS renal replacement research .....	18
2.6 Computational efforts .....	19
2.7 Wearable renal replacement therapy.....	21
2.8 Conclusion.....	22
<b>3 Conceptual Development</b> .....	<b>23</b>
3.1 Basic physiology of the human kidney.....	23
3.2 Functional analysis of current renal replacement therapies.....	27

3.2.1	Review of current renal replacement therapies.....	27
3.2.2	Performance assessment of hemodialysis and hemofiltration.....	30
3.3	Functional analysis of the human kidney .....	34
3.3.1	Decomposition of human kidney function .....	34
3.3.2	Behavioral assessment of kidney .....	34
3.3.3	Decomposition of the kidney into subsystems .....	35
3.3.4	Functional assessment of the behavior of subsystems.....	36
3.3.5	Compiled functional analysis .....	38
3.3.6	High-level functional results.....	38
3.4	Requirements list for a renal replacement device .....	39
3.5	Functional analysis of renal replacement.....	41
3.5.1	Development of function structures and working principles .....	42
3.5.2	Analysis of working principles .....	43
3.6	Concept formation .....	51
3.6.1	A bio-inspired renal replacement therapy .....	51
3.6.2	A portable traditional hemodialysis system.....	53
3.7	Comparison and discussion of performance.....	55
3.7.1	A bio-inspired hemodialysis system.....	55
3.7.2	A portable traditional hemodialysis system.....	58
3.8	Conclusion.....	59
<b>4</b>	<b>Creation of a System Model .....</b>	<b>61</b>
4.1	System model objectives .....	61
4.1.1	Identify parameters that have the largest impact on system weight.....	62
4.1.2	Determine the relationship between blood and dialysate flow rate .....	62
4.1.3	Determine feasible treatment schedules of a portable system .....	62
4.2	Hemodialysis components.....	63
4.2.1	Dialyzer .....	64
4.2.2	Dialysate.....	65
4.3	Fundamentals of dialyzer physics .....	65
4.3.1	Fick's Law .....	66
4.3.2	Overall mass transfer coefficient.....	67
4.3.3	The concentration difference .....	68
4.3.4	Dialysance.....	69
4.4	Dialyzer design .....	73

4.5	Modeling pump power requirements.....	75
4.5.1	Overview of different types of pumps .....	75
4.5.2	Estimating the pressure drop across the dialyzer.....	76
4.5.3	Relating the pressure drop to pump power requirements.....	80
4.6	Exploring the primary equations of a hemodialysis system.....	84
4.6.1	System parameters.....	85
4.6.2	Precursory analysis of the Michaels equation .....	86
4.6.3	Effect of dialyzer size in the Michaels equation.....	87
4.7	Modeling Hemodialysis in Simulink.....	91
4.7.1	Step-by-step procedure used in the model.....	93
4.7.2	Other considerations of the model.....	101
4.7.3	Assumptions in the model .....	102
4.8	Conclusion.....	104
<b>5</b>	<b>Model Verification and Proposed Scenarios.....</b>	<b>106</b>
5.1	Validation of the hemodialysis system model.....	106
5.1.1	Laboratory setup .....	106
5.1.2	Validation via laboratory tests .....	109
5.1.3	Validation via published hemodialysis data.....	111
5.2	Modeling basic hemodialysis scenarios.....	112
5.2.1	Basic system with no recirculation or urea generation.....	113
5.2.2	Basic system with recirculation but no urea generation .....	115
5.2.3	Basic system with urea generation and no recirculation .....	118
5.2.4	Basic system with recirculation and urea generation.....	119
5.3	Steady state behavior and sample size.....	121
5.3.1	Initial BUN selection and steady state behavior.....	121
5.3.2	Examining the effects of sample size in the model.....	125
5.4	Modeling hemodialysis.....	128
5.4.1	Recreating a typical clinical hemodialysis scenario .....	129
5.4.2	A daily hemodialysis schedule without recirculation.....	131
5.4.3	A daily hemodialysis schedule with recirculation.....	134
5.4.4	Recommended system configurations .....	138
5.5	Conclusion.....	145
<b>6</b>	<b>Closure and Contributions.....</b>	<b>147</b>
6.1	Answering the research questions.....	147

6.1.1	Research question one.....	147
6.1.2	Research question two .....	149
6.1.3	Research question three .....	150
6.2	Contributions.....	151
6.2.1	A functional analysis of kidney behavior and a related renal replacement therapy concept.....	151
6.2.2	A thorough one-compartment model of hemodialysis.....	152
6.2.3	Relating a time constant to a given set of hemodialysis inputs.....	153
6.2.4	Feasible concepts of a portable hemodialysis system.....	154
6.3	Scope and limitations of this research.....	154
6.4	Future work.....	155
6.4.1	Dialysate regeneration.....	156
6.4.2	System optimization and sensitivity analysis.....	156
6.4.3	Improved pump design.....	156
6.4.4	Dialyzer-free dialysis.....	157
<b>Appendix A: Glossary.....</b>		<b>158</b>
<b>Appendix B: Simulink Code.....</b>		<b>161</b>
<b>References .....</b>		<b>177</b>

## LIST OF TABLES

Table 1-1. Organization of research questions.....	4
Table 2-1. Solute concentration in a typical hemofiltration fluid (Forni & Hilton, 1997). .....	15
Table 2-2. Experimental results from Gura et al. (2007). .....	21
Table 3-1. Summary matching functional relationship between hemodialysis and hemodiafiltration against the human kidney. ....	33
Table 3-2. The functional difference between the human kidney and clinical dialysis. ....	42
Table 3-3. Morphological chart for bioinspired concept.....	52
Table 3-4. Morphological chart for portable hemodialysis system.....	53
Table 3-5. Renal replacement therapy comparison.....	56
Table 4-1. Selected pump data (Omega).....	82
Table 4-2. Various dialyzers and their clearance rates (Baxter Healthcare Corporation).....	85
Table 4-3. The inputs of the system model. ....	94
Table 4-4. The parameters calculated by the system model.....	94
Table 4-5. The output from the model of the first four minutes from a simulation. ....	101
Table 5-1. The simulations in Section 5.1. ....	113
Table 5-2. Input parameters associated with Figure 5-7.....	113
Table 5-3. Output parameters associated with Figure 5-7. ....	113
Table 5-4. Input parameters associated with Figure 5-8.....	116
Table 5-5. Output parameters associated with Figure 5-8. ....	116

Table 5-6. Input parameters associated with Figure 5-10.....	119
Table 5-7. Output parameters associated with Figure 5-10.....	119
Table 5-8. The curve fit equations for the plots in Figure 5-14.....	123
Table 5-9. The scenarios modeled in this section.....	129
Table 5-10. Input parameters used for simulation in Figure 5-18.....	131
Table 5-11. Output parameters of simulation in Figure 5-18.....	131
Table 5-12. Input parameters associated with Figure 5-19.....	132
Table 5-13. Output parameters associated with Figure 5-19.....	132
Table 5-14. Input parameters associated with Figure 5-21.....	135
Table 5-15. Output parameters associated with Figure 5-21.....	135
Table 5-16. Input parameters associated with Figure 5-22.....	138
Table 5-17. Output parameters associated with Figure 5-22.....	138
Table 5-18. Input parameters for a best-case scenario.....	142
Table 5-19. Output parameters for a best-case scenario.....	142
Table 5-20. Input parameters for a realistic scenario.....	142
Table 5-21. Output parameters for a realistic scenario.....	143
Table 5-22. Input parameters for a worst-case scenario.....	144
Table 5-23. Output parameters for a worst-case scenario.....	145

## LIST OF FIGURES

Figure 2-1. Abel's dialyzer (Abel, Rowntree, & Turner, 1913).....	6
Figure 2-2. Haas' 1924 dialyzer (Gottschalk & Fellner, 1997).....	7
Figure 2-3. The Kolff drum dialyzer (Gottschalk & Fellner, 1997). .....	8
Figure 2-4. The first Kolff dialyzers ready to be sent around the world following the end of World War II, September 1944 (Kolff, 1965).....	9
Figure 2-5. A shell-and-tube hollow fiber dialyzer. ....	11
Figure 3-1. The figure on the left shows a complete nephron. In the figure on the right, the dark-red glomerulus is surrounded by the pink Bowman's capsule, forming the renal corpuscle. ....	24
Figure 3-2. A functional model of waste removal in the kidney.....	25
Figure 3-3. Functional performance of hemodialysis.....	28
Figure 3-4. A hemodialysis circuit (YassineMrabet, 2008).....	28
Figure 3-5. A typical hemodiafiltration circuit (Asahi Kasei Medical Company). ....	30
Figure 3-6. Simple system model of the human kidney.....	34
Figure 3-7. Model of the overall behavior of the human kidney.....	35
Figure 3-8. Structural decomposition of the human kidney. ....	35
Figure 3-9. Kidney subsystem interactions.....	36
Figure 3-10. Standalone behaviors of each of the kidney subsystems. All figures are in mmol/day. ....	37
Figure 3-11. Hierarchical function representation of the human kidney. ....	38
Figure 3-12. High-level function of the human kidney.....	39

Figure 3-13. Function structures and solution principles of an RRT.....	43
Figure 3-14. Specific working principles for a renal replacement therapy concept.....	51
Figure 3-15. A bio-inspired renal replacement therapy (RRT) concept.....	52
Figure 4-1. A typical hemodialysis circuit (YassineMrabet, 2008).....	63
Figure 4-2. The flow path of the blood during hemodialysis. ....	63
Figure 4-3. A typical dialyzer. The blood enters on the right and travels through thousands of tiny tubules before exiting on the left. The dialysate enters on the bottom left, fills the spacing around the tubules and exits on the bottom right. ....	64
Figure 4-4. The number of solutes passing through the membrane depends on the thickness of the membrane ( $\Delta x$ ), the ratio of the number of solutes on each side ( $\Delta C$ ), the size of the membrane ( $A$ ), and the diffusivity constant ( $D$ ). ....	66
Figure 4-5. The expected pressure drop according to the Hagen-Poiseuille equation in 0.16 m length dialyzers of various tubule inner diameters. ....	78
Figure 4-6. The expected pressure drop according to the Hagen-Poiseuille equation in tubules of 250 $\mu\text{m}$ in dialyzer of lengths of 0.1 m, 0.15 m, and 0.2 m at various flow rates. ....	79
Figure 4-7. The efficiency of various peristaltic pumps from the same manufacturer. ....	84
Figure 4-8. The relationship between the blood and dialysate flow rates with respect to overall dialyzer clearance. The $K_0A$ was 1000 mL/min and the dialysate flow rate ( $Q_D$ ) was 250 mL/min.....	87
Figure 4-9. The relationship between the size of the dialyzer and overall dialyzer clearance at various blood and dialysate flow ratios. ....	88
Figure 4-10. Various dialyzer sizes are compared at an 80 mL/min blood flow rate. ....	89
Figure 4-11. The overall dialyzer clearance at four different dialysate flow rates. ....	90
Figure 4-12. A screenshot of the Matlab Simulink model.....	93

Figure 4-13. The trade-off dialysate flow rate. The maximum clearance is 100 mL/min (at  $Q_D > 200$  mL/min), and the trade-off clearance is 95 mL/min (at  $Q_D = 114$  mL/min).....95

Figure 5-1. The laboratory setup. From left to right: the blood reservoir (1), the blood pump (2), the dialyzer (3), the dialysate pump (4), and the dialysate reservoir (5). ..... 107

Figure 5-2. The dialysate reservoir seen early in (left) and later in (right) dialysis when the dialysate recirculated through the dialyzer. .... 108

Figure 5-3. A close-up of the dialyzer after dialysis. Porcine blood has filled the baffle at the entrance of the dialyzer and the thousands of tubules that run the length of the dialyzer. Dialysate flows counter to the blood and exits in the tube on the right..... 109

Figure 5-4. Single-pass mode: 450 mL of porcine plasma through a ( $K_0A = 450$  mL/min) dialyzer at 100 mL/min and dialysate flow rate of 150 mL/min. The light gray line is the model and the dark gray line is the experimental results. .... 110

Figure 5-5. Recirculation mode: 750 mL of porcine plasma through a dialyzer ( $K_0A = 450$  mL/min) at 100 mL/min. A fixed volume of 500 mL of dialysate was recirculated through the dialyzer at 150 mL/min. The light gray line is the model and the dark gray line is the experiment results..... 111

Figure 5-6. The one-compartment Matlab model (dashed line) compared to the published results (solid line) of Ziólko et al. (2000). ..... 112

Figure 5-7. A simple dialyzer circuit without dialysis recirculation or urea generation. The predicted BUN drops below 1 mg/L after 63 minutes. See Table 5-2 for a detailed list of the parameter values..... 114

Figure 5-8. A simple dialysis circuit with dialysate recirculation, but no urea generation. .... 115

Figure 5-9. Two liters of dialysate are used in single-pass for 19 minutes, and then the dialyzer is shut off. The dotted line is the same parameters, but the 2 L is allowed to recirculate for the full 80 minutes..... 117

Figure 5-10. A simple dialysis circuit with no dialysate recirculation, but a constant urea generation rate of 17.3611 mg/min. The dotted line is the expected performance when there is no urea generation..... 118

Figure 5-11. Comparing dialysate recirculation to single-pass. Both simulations used approximately the same volume of dialysate..... 120

Figure 5-12. Regardless of the initial BUN, after several days the daily BUN cycle is the same. The only difference between the plots is the initial BUN – every other parameter ( $K_0A$ ,  $Q_B$ ,  $Q_D$ , etc.) is the same..... 122

Figure 5-13. When the peaks of the simulation corresponding to an initial BUN of 70 mg/dL are connected (dashed line) an exponential curve is formed..... 123

Figure 5-14. The daily peaks of each plot in Figure 5-12 are plotted. A simple exponential curve accurately describes how each plot decays to the same steady state conditions. .... 124

Figure 5-15. The published hemodialysis input data (Figure 5-6) is modeled at three different time intervals: 1 min, 10 min, and 0.1 min. .... 126

Figure 5-16. Two different sampling sizes are plotted. The 10-minute interval line (grey, long dashes) is able to predict the final BUN calculated equally as accurate as when using 1-minute intervals..... 127

Figure 5-17. The discrepancy between the two plots of Figure 5-16 are plotted. As time increases, the difference between the two plots decreases. .... 128

Figure 5-18. The model predicting the results of traditional hemodialysis. The patient is dialyzed every other day for two hours..... 130

Figure 5-19. A daily hemodialysis schedule with a limited blood flow rate. .... 133

Figure 5-20. A daily home hemodialysis schedule with a reduced urea generation rate of 6.25 g/day. The dotted line is 12.5 g/day urea generation rate. .... 134

Figure 5-21. Daily hemodialysis with a fixed amount (12 L) of dialysate recirculating per treatment. The dotted line is the same simulation without recirculation (which uses more than 12 L of dialysate, but equal treatment time)..... 136

Figure 5-22. A fixed volume of dialysate (12.36 L) is run in single-pass mode (light line) and recirculation mode (dark line). The treatment time for the single-pass simulation was shorter (2 h vs. 3 h)..... 137

Figure 5-23. The best-case scenario. .... 140

Figure 5-24. A realistic scenario. .... 141

Figure 5-25. The worst-case scenario..... 144

## LIST OF SYMBOLS AND ABBREVIATIONS

CKD	Chronic Kidney Disease	–
RRT	Renal Replacement Therapy	–
CAPD	Continuous Ambulatory Peritoneal Dialysis	–
CCPD	Continuous Cycler-assisted Peritoneal Dialysis	–
GDP	Glucose Degradation Products	–
pH	power of Hydrogen	–
ICU	Intensive Care Unit	–
$S_D$	Seiving Coefficient	–
$q$	mass flux	mg/min
MEMS	Micro Electro-Mechanical Systems	–
Da	Daltons	–
TMP	Trans-Membrane Pressure	mmHg
$K_0$	overall mass transfer coefficient	cm/min
$A$	effective surface area	$m^3$
$K$	clearance	ml/min
$J$	flux	mg/min
$\mathbb{D}$	diffusion coefficient	–
$\Delta C$	concentration difference	mg/mL
$C_{BI}$	incoming blood concentration	mg/mL
$C_{BO}$	outgoing blood concentration	mg/mL
$C_{DI}$	incoming dialysate concentration	mg/mL
$C_{DO}$	outgoing dialysate concentration	mg/mL
$\Delta C_I$	incoming concentration difference	mg/mL

$\Delta C_D$	outgoing concentration difference	mg/mL
$D$	diffusive dialysance	-
$Q_B$	blood flow rate	mL/min
$Q_D$	dialysate flow rate	mL/min
$K_0A$	dialyzer properties	mL/min
$R_0$	overall membrane resistance	Pa/mL/min
$R_B$	blood-side membrane resistance	Pa/mL/min
$R_M$	internal membrane resistance	Pa/mL/min
$R_D$	dialysate-side membrane resistance	Pa/mL/min
$R$	tubule radius	$\mu\text{m}$
$\eta$	fluid viscosity	Pa
$L$	tubule length	m
$\Delta P$	pressure drop	Pa
$V_B$	blood volume	L
$V_D$	dialysate volume	L
BUN	Blood Urea Nitrogen	mg/dL
$\dot{G}$	urea generation rate	mg/min
$\alpha$	trade-off coefficient	-
$GFR\%$	residual kidney function	-
$K_{UF}$	ultrafiltration clearance	mL/min
$p_B$	dialyzer blood pressure	mmHg
$p_D$	dialyzer dialysate pressure	mmHg
$t_1$	dialysis dose length	hours
$t_2$	time between dialysis doses	hours
$Q_F$	ultrafiltration flow rate	mL/min

## SUMMARY

Research to improve artificial renal replacement therapies is varied across the many different parts of a hemodialysis system. Work largely focuses on developing a better dialyzer – the component that is directly responsible for removing wastes from the blood – but less study is devoted to the entire hemodialysis system.

This work seeks to improve hemodialysis in two ways: by proposing a new renal replacement therapy that does not rely on traditional hemodialysis components, and by investigating the feasibility of adapting current hemodialysis practices to a portable format.

While an alternative renal replacement therapy may be the best solution to today's dialysis problems, this work further focuses on reducing hemodialysis to a portable format through systematic engineering design. In that process, a detailed system model is made in Simulink that can account for the large number of inputs of such a system – the blood flow rate, dialyzer size, treatment time, etc. – allowing for detailed exploration of the design space.

Once the model is completed, it is verified through *in vitro* experiments carried out with porcine blood. Additionally, the model is verified against published human hemodialysis data. After model verification, hemodialysis concepts are generated that allow for maximum portability under different patient conditions.

## CHAPTER ONE

### MOTIVATION FOR MODELING AND DESIGNING A HEMODIALYSIS SYSTEM

Research to improve artificial renal replacement therapies is varied across the many different parts of a hemodialysis system. Work largely focuses on developing a better dialyzer – the component that is directly responsible for removing wastes from the blood – but less study is devoted to the entire hemodialysis system.

This thesis serves as a thorough investigation of the hemodialysis process from a systematic engineering design perspective. This first chapter provides the motivation and context of this work. Chapter 2 provides a brief history of renal replacement and surveys current hemodialysis research. Chapter 3 provides a functional analysis of the human kidney and traditional hemodialysis, and then develops two concepts based on each examination. Chapter 4 documents the creation of a detailed system model of traditional hemodialysis, accounting for such things as urea generation rates and dialyzer size. Chapter 5 verifies the model created in Chapter 4 and then explores different system configurations through manipulation of the model. Chapter 6 concludes this thesis by providing analysis of the work provided, acknowledgements, and suggestions for future work.

#### **1.1 Renal replacement therapies**

The human kidney fills many life-sustaining roles; most importantly, it balances the solutes commonly found in the blood – like urea, creatinine, and sodium. It also plays an indirect role in many other important functions, like regulation of blood pressure and glucose metabolism.

The functional output of the kidney is measured by its glomerular filtration rate (GFR). End-Stage Renal Failure (ESRD) is a disease inflicting hundreds of thousands of patients worldwide that is

defined by a GFR below 15% of normal kidney function. Patients diagnosed with ESRD have two survival options: receive a donor kidney, or begin dialysis – a renal replacement therapy that relies on concentration gradients across a membrane to remove solutes from the blood.

While organ transplant is the best option, there are simply not enough donor kidneys available. Consequently, most patients begin peritoneal dialysis – a reasonable form of treatment that uses the body’s own peritoneum as a membrane – allowing users to retain many aspects of their normal pre-ESRD lifestyle. After a few years of peritoneal dialysis, the filtration ability of the peritoneum becomes inadequate for peritoneal dialysis and patients are usually forced to begin traditional hemodialysis.

Hemodialysis requires most patients to visit a clinic three times a week for three- to five-hour treatment sessions. Blood is circulated out of the body, cleansed through dialysis, and then returned to the body. Unfortunately, modern hemodialysis fails in two major ways: it is unable to clean the blood perfectly, and it is a very invasive process.

In this thesis, two primary methods of improving hemodialysis have been identified. Hemodialysis can be made more effective (by improving its ability to remove solutes from the blood), can have its experience improved (by developing a system that casts less restraint on a patient’s life), or both.

## **1.2 Research questions and hypothesis**

The goal of this thesis is to improve hemodialysis. First, the human kidney’s functionality will be analyzed to see if any of its waste-processing strategies can be leveraged in the development of an artificial kidney. Then an analysis of current hemodialysis from a systems-level perspective will attempt to reveal shortcomings of common practice that can be improved upon.

This thesis seeks to answer the following research questions:

**Research Question 1:**

*Can a renal replacement therapy be developed that provides an alternative filtration method while matching or exceeding current hemodialysis performance?*

**Hypothesis 1:**

*A renal replacement system that more closely mimics the behavior of a human kidney can provide a more effective treatment.*

There are many shortcomings of today's hemodialysis – it does not remove all solutes that need to be removed, and its intervallic nature disrupts homeostasis. Either a renal replacement system that can provide more exacting solute removal or one that can run continuously should improve patient health. Additionally, a treatment that is small enough to be portable will improve the patient's lifestyle – granting newfound mobility to a process that currently requires tethering to a machine several hours per week.

**Research Question 2:**

*Can a detailed hemodialysis system model be created that accurately takes into account different patient and dialysis variables?*

**Hypothesis 2:**

*By improving upon the work of Sargent & Gotch (1989), a detailed computer model can be created that offers optimization of the fundamental dialysis equations and considers patient variables.*

Hemodialysis can be performed on nearly any scale – but any system that is developed must remove enough solutes to maintain homeostasis. Therefore, while a portable system is easily developed, certain constraints must be placed on the system to make it effective.

**Research Question 3:**

*Is a portable hemodialysis system possible? What are the detailed system configurations that are possible?*

**Hypothesis 3:**

*By exploring the physics that govern hemodialysis, portable system configurations can be developed that meet the needs of chronic renal failure patients.*

Once a system model is built, a thorough investigation of the model is necessary. Because of the expected overwhelming number of inputs and outputs in such a model, the dominant factors must be determined. It is expected that a portable system will be possible with traditional hemodialysis equipment.

**Table 1-1. Organization of research questions.**

<b>Research Question</b>	<b>Corresponding Chapter</b>
<b>Question 1</b>	Chapter 3
<b>Question 2</b>	Chapter 4
<b>Question 3</b>	Chapter 5

**1.3 Validation and verification strategy**

The primary aspect of this thesis in need of verification is the system model created in Chapter 4. Because this system model is used to predict different system configurations and treatment schedules, its validity is paramount to the relevancy of this work.

The model is verified in two different ways: through *in vitro* experiments carried out at the Georgia Institute of Technology in Dr. David Ku’s laboratory and by comparing the model’s results to published hemodialysis data from actual patients receiving treatment.

Both methods of verification show the model is capable of predicting accurate results.

## CHAPTER TWO

### PAST AND PRESENT WORK IN RENAL REPLACEMENT

Chronic kidney disease (CKD) is a health disorder that will affect an estimated 660,000 Americans in 2010 (National Kidney Foundation, Inc., 2002). CKD is defined by five stages of decreasing renal function: from Stage 1, which is defined by a slightly reduced glomerular filtration rate; to Stage 5, which requires medical treatment. Unless receiving a donor kidney, these patients need an artificial renal replacement therapy (RRT) in order to avoid death.

Renal replacement therapy comes in several forms: peritoneal dialysis, hemodialysis, hemofiltration, or hemodiafiltration. Often patients begin treatment with peritoneal dialysis (a unique form of dialysis that uses the body's own peritoneum as a membrane) because it is the most convenient and requires the least lifestyle modification. As the body's peritoneum loses its ability to act as a membrane (details in Section 2.2), patients must switch to another form of treatment. In the United States, this is hemodialysis. In other countries, patients might begin treatment with hemodiafiltration. Hemofiltration is often used for treatment of acute renal failure.

#### **2.1 A brief history of renal replacement**

Kidneys fail for a variety of reasons, although most hemodialysis patients have a history of diabetes, high blood pressure, or a disease of the glomerulus (glomerulonephritis). For most of the history of humankind, renal failure was a death sentence – without properly functioning kidneys, a human would quickly succumb to the buildup of toxic solutes in his or her blood.

The following brief history of renal replacement is drawn largely from the excellent *Haemodialysis: A Historical Review* by William Drukker (Drukker, 1989).

### 2.1.1 The first dialyzer designed for human use

The first attempt to recreate the function of a renal system artificially was by a group of researchers at John Hopkins University, led by John J. Abel in 1913 (Abel, Rowntree, & Turner, 1913). His device (Figure 2-1) consisted of several 40 cm colloid tubes. Some success was had with dialyzing uremic dogs, but he was unable to try his device on humans due to lack of a suitable anticoagulant. The popular anticoagulant of the time, hirudin (made from ground leech heads), was not readily available (Drukker, 1989).

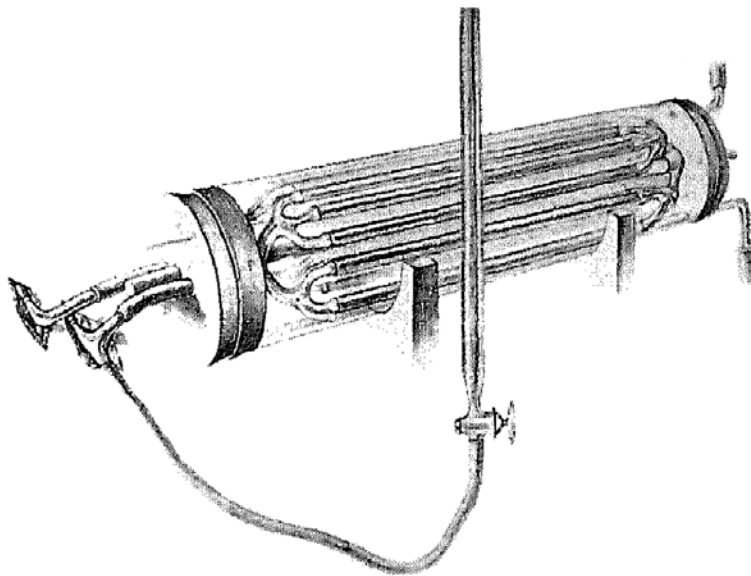


Figure 2-1. Abel's dialyzer (Abel, Rowntree, & Turner, 1913).

### 2.1.2 The first trial of dialysis on a human

Dr. Georg Hass, working without knowledge of Abel's work in Germany, performed the first successful human dialysis (Paskalev, 2001). His device (Figure 2-2) – similar to Abel's – was connected to a terminally ill renal failure patient for 15 minutes in 1924.

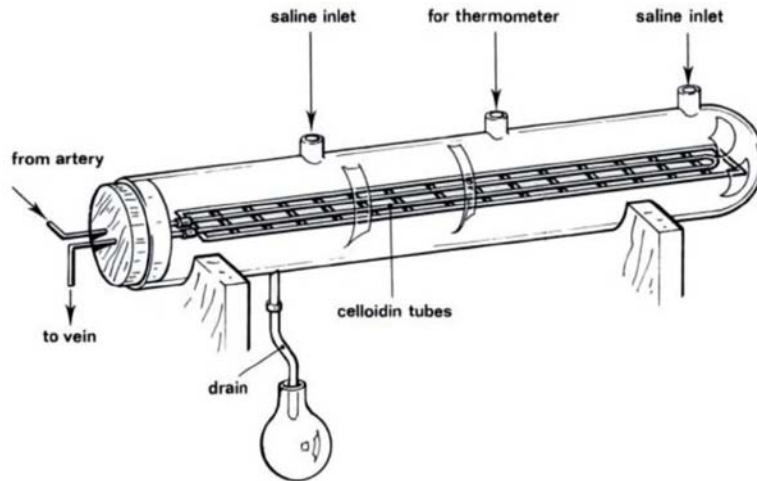


Figure 2-2. Haas' 1924 dialyzer (Gottschalk & Fellner, 1997).

While the results of this first dialysis are lost to history, Haas continued his human dialysis experiments. Like Abel, Haas had difficulty with blood coagulation. While he had access to ample hirudin, its toxic properties forced him to limit dialysis doses to no more than 60 minutes – too short to have any therapeutic effect (Drukker, 1989). By the end of his published work in the late 1920s, Haas had succeeded in removing some uremic toxins from patients, but had not been able to replace kidney function.

### 2.1.3 The drum dialyzer and the first successful renal replacement therapy

The next advancement in dialysis came by means of a Dutch doctor named Willem Kolff by combining two then-recent advances: heparin and cellophane. Heparin was a new, biocompatible anticoagulant that allowed for meaningful treatment times. Cellophane was also new at the time and proved to be well suited as a membrane material for dialysis.

In Kolff's dialysis machine (Figure 2-3), blood travels through cellophane tubing wrapped around a drum that was bathed in a dialysate solution (Kolff, 1965). Rotating the drum allowed for better concentration gradients. His first two attempts to dialyze unconscious uremic patients were unable

to revive them. The first patient, in February 1943, died following the dialysis. The second attempt was more successful, keeping the patient alive for twenty-six days (Drukker, 1989).

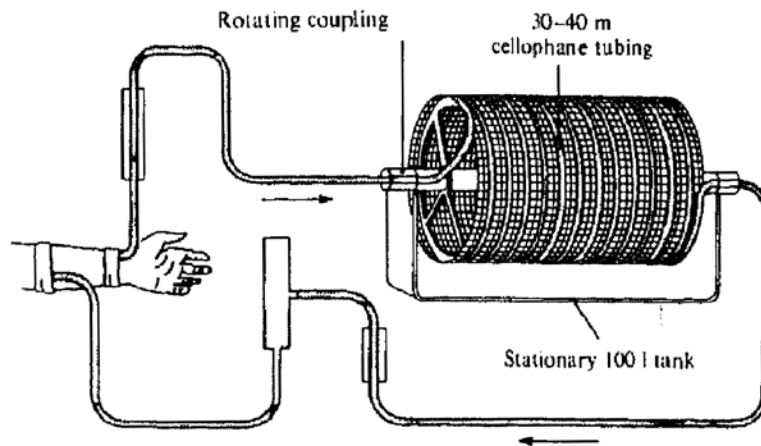


**Figure 2-3. The Kolff drum dialyzer (Gottschalk & Fellner, 1997).**

Kolff's first successful implementation of his dialyzer came in 1945. A 67-year-old unconscious patient suffering from end-stage uremia (from acute renal failure) regained consciousness after being dialyzed for eleven hours.

During his spare time during World War II, Kolff managed to build extra dialyzers that he sent around the world to various hospitals at the conclusion of the war (Figure 2-4). This exposed doctors all around the world to the science of dialysis, allowing for incremental advances of the Kolff dialyzer, like the Kolff-Brigham machine developed in Boston (Drukker, 1989).



**Figure 2-4. The first Kolff dialyzers ready to be sent around the world following the end of World War II, September 1944 (Kolff, 1965).**

#### **2.1.4 The coil and twin coil dialyzer**

The coil dialyzer was developed by Drs. Gordon Murray, Edmund Delorme, and Newell Thomas (Murray, Delorme, & Thomas, 1947) in Toronto, Canada. Their dialyzer wound cellophane tubing in a coil that sat in a bath of dialysate solution. Kolff improved their design and presented a “twin coil” dialyzer at the first meeting of the American Society for Artificial Internal Organs in 1955. A patient with prolonged acute renal failure was kept on twin coil dialysis for 181 days, but each time dialysis was performed (eleven times total), new arterial and venous blood lines had to be made (Drukker, 1989).

### **2.1.5 The development of reusable vein access**

The next leap in renal replacement came in the 1950s when Belding Scribner used Teflon to create a shunt (the Scribner Shunt, as it became known) that allowed regular access to a patient's arterial and venous blood streams. The Kolff dialyzer had proven successful in treating acute renal failure; the new shunts allowed a patient to dialyze regularly over a long period. Scribner combined his new shunt with a dialyzer designed by Frederik Kiil of Norway, to create the most effective and easiest to use dialyzer. The Kiil dialyzer had several incremental improvements, including a new membrane material (Cuprophane instead of cellophane), a pumpless design, and a flat-plate configuration of membrane tubules (Drukker, 1989).

### **2.1.6 Successful treatment of chronic renal failure**

The first successful treatment of a patient with chronic renal failure came in March of 1960 (Drukker, 1989). Dialysis was first performed weekly (without any improvements in technology), and then twice weekly. The patient survived eleven years. Treatment of chronic renal failure patients quickly spread throughout the world, thanks to the Scribner shunt.

Scribner, when he opened one of the first dialysis clinics, quickly ran into problems. Demand outpaced availability, a problem facing nearly all places offering dialysis to chronic kidney failure patients. In response to this ethical issue, he created what is now considered the first bioethics committee to determine which patients received dialysis – via an anonymous panel of regular citizens and doctors.

### **2.1.7 Single-pass dialysis and home hemodialysis**

Incremental improvements continued during the 1960s. Doctors began running dialysis machines in single-pass mode to increase dialysis efficiency. Previously, a large volume of dialysate was continuously cycled through the Kiil dialyzer. In order to prevent bacteria growth, the dialysate was

kept cold, and the blood was warmed before it was returned to the body. Using only fresh dialysate not only improved mass transport, but it also reduced infections.

Moving dialysis out of the clinic and into the home was also a focus of research. Home hemodialysis became popular during the 1970s, but declined in some parts of the world when peritoneal dialysis became available in the late 1970s. Today, where and how patients dialyze varies from continent to continent.

### 2.1.8 The hollow fiber dialyzer

In the late 1960s, the flat-plate Kiil dialyzer was replaced with the shell-and-tube hollow fiber dialyzer (Drukker, 1989). This configuration of the tubules allowed for greater effective surface area in a smaller package. Interestingly, Abel's 1913 dialyzer design (Figure 2-1) closely resembles modern dialyzers (Figure 2-5).

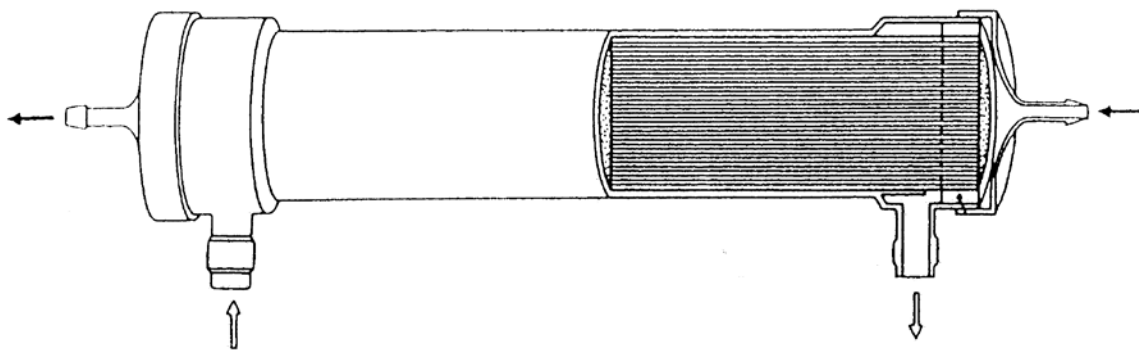


Figure 2-5. A shell-and-tube hollow fiber dialyzer.

## 2.2 Peritoneal dialysis

When patients are first diagnosed with Stage 5 chronic kidney disease, a first method of treatment is peritoneal dialysis. In 2001, 8.8% of dialysis patients were using some form of peritoneal dialysis for treatment, down from 10.5% in 1998. Peritoneal dialysis removes wastes from the blood much

like traditional dialysis, but uses the body's own peritoneal membrane surrounding the abdomen as a filter.

Dialysis fluid enters the abdominal cavity via a catheter. In a common form of peritoneal dialysis, continuous ambulatory peritoneal dialysis (CAPD), the patient's abdomen is filled with two to three liters dialysate, and dialysis occurs without the patient tethered to a machine. The dialysis process occurs via natural diffusion, and after a few hours, the dirty dialysate is drained. This process is performed four to five times per day, depending on the size of the patient.

An alternative form of peritoneal dialysis requires the patient to remain attached to a machine during dialysis. Continuous cycler-assisted peritoneal dialysis (CCPD) often occurs at night. The patient connects their catheter to a machine before sleeping that will automatically perform dialysate exchanges throughout the night. In the morning, a volume of dialysate is left in the abdominal cavity for a long exchange throughout the day.

Which form of peritoneal dialysis is used depends on the individual patient. Those with more residual kidney function might be more able to perform exchanges at night, while leaving their abdominal cavity empty throughout the day. As a patient's kidney functionality deteriorates, more frequent peritoneal dialysis can complement their dwindling renal function.

However, peritoneal dialysis has its limitations. Patients must be able to dialyze on a continuous schedule. While they are able to perform the procedure at home, they still must commit to it several times per day, every day of the week. Conversely, hemodialysis performed at a clinic requires only a few hours per day, but patients must rely on treatment schedules dictated by the clinic.

Peritoneal dialysis loses its effectiveness after several years of treatment because the dialysate used reduces the usability of the peritoneum as a membrane. The use of peritoneal dialysis has several

negative effects on the human body. Studies have found that after extended use of CAPD, the peritoneum membrane thickens, even to the point of complete occlusion (Di Paolo & Sacchi, 1989). This deterioration of the peritoneum is associated with the glucose in the dialysate.

Specifically, the glucose breaks down into glucose degradation products (GDPs) during the autoclaving process employed by dialysate manufacturers. These products, found primarily in dialysate that has been sterilized via heating (but can also develop during normal storage of the dialysate), have negligible short-term effects on human peritoneal mesothelial cells, but have been associated with the long-term degradation of the peritoneal membrane, ultimately reducing filtration rates (Witowski, et al., 2003).

Another issue of bioincompatibility of the dialysate fluid is its relatively low pH. Typical peritoneal dialysate fluid has a pH around 5.2; while the body's natural pH is 7.4. As the dialysate enters the body, the intracellular fluid rapidly drops in pH. This more acidic state has been associated with a negative impact on cell function. As the dialysate remains in the body, the pH is eventually raised to physiological levels after about two hours. However, even after the pH has normalized, cell function is still abnormal.

Current research is responding to these problems with new peritoneal dialysate formulae. Manufacturers of dialysate have developed multi-bag systems that keep the glucose separate from the buffer (Rippe, et al., 2001). The glucose, stored at a lower pH, is combined with the electrolyte-buffer prior to usage. This system helps inhibit the development of GDPs and provides a near pH-neutral system. Using two bags also allows bicarbonate to be used as a buffer (the body's natural buffer), instead of lactate (McIntyre, 2007). Both Fresenius and Baxter offer two bag solutions, while Gambro offers a three-bag system that also separates the hypertonic glucose (McIntyre, 2007).

Another way to address the development of GDPs is to replace glucose (the primary osmotic ingredient) with a more bio-friendly solution. Icodextrin-based dialysate, marketed by Baxter, has shown to be superior to traditional solutions (McIntyre, 2007). Icodextrin's high molecular weight makes it ideal for long dwells.

These newly available peritoneal dialysate solutions are awaiting the rigors of long-term trials, but short-term studies have verified their enhanced claims over traditional peritoneal dialysate fluids. Studies have reported improved peritoneal dialysis experiences and results due to the development of these new fluids and techniques.

### **2.3 Hemofiltration**

In 1977, an alternative form of renal replacement was developed in response to intensive care patients who suffered from severe hemodynamic instability (John & Eckhardt, 2006).

Hemofiltration, as it became known, acts in a very similar manner to the human kidneys: nearly all extra-cellular fluid is removed, and then desirable fluids are replaced in a second stage before the blood is returned to the body.

This method provides a distinct advantage over traditional hemodialysis. The molecules that the diffusion-based hemodialysis removes poorly – such as myoglobin and insulin – are easily cleared through hemofiltration (Forni & Hilton, 1997). Only the desired solutes are returned to the blood after filtration. Table 2-1 outlines a typical replacement fluid regimen.

**Table 2-1. Solute concentration in a typical hemofiltration fluid (Forni & Hilton, 1997).**

<b>Component</b>	<b>Quantity (mmol/L)</b>
<b>Sodium</b>	140
<b>Potassium</b>	0-4
<b>Calcium</b>	1.6
<b>Magnesium</b>	0.75
<b>Chloride</b>	101
<b>Lactate</b>	45
<b>Glucose</b>	11

However, there are serious limitations to widespread adoption of hemofiltration as an alternative to traditional hemodialysis. The large amounts of fluids lost during filtration must be replaced – amounting to large quantities of sterile fluid that must be provided during treatment. This has provided a serious barrier to market entry to prevent any commercialization of the technology for home use in the United States.

Recent research in hemofiltration has worked to apply this technique better in the intensive care setting. Many patients suffer renal failure while in the ICU, even if their primary affliction is not their renal system. Additionally, doctors must also provide for fluid losses, setting hemofiltration as an ideal solution: providing both renal replacement and a means to infuse fluids back into the blood at desired doses.

Studies published recently have recommended its use in place of isotonic-saline hydration in patients undergoing percutaneous coronary interventions (Marenzi, et al., 2003). Another study has shown the advantage of using high-volume continuous hemofiltration in acute pancreatitis patients (Jiang, et al., 2005).

In an attempt to draw on the benefits of hemodialysis (superior small-molecule removal) and hemofiltration (superior large-molecule removal), researchers have created a hybrid process. This

more recent renal replacement therapy – hemodiafiltration – works by using both a dialyzer and a hemofilter in series. Blood passes through both devices before it is returned to the body.

A recent study noted the effectiveness of hemodiafiltration (Saudan, et al., 2006). In that study, the three-month survival rate of patients with acute renal failure receiving hemodiafiltration was nearly twice that of patients receiving traditional hemofiltration. However, the study failed to show any improvement in recovering residual renal function of the patients' kidneys.

#### **2.4 Bioartificial kidneys**

Hemodialysis is effective at keeping a patient alive for several years after his or her progression to Stage 5 chronic kidney disease. However, physiological conditions slowly degrade after long-term treatment with hemodialysis. As the short-term problems associated with hemodialysis have been addressed and resolved in past decades, today's researchers are beginning to address the long-term consequences of artificial renal replacement.

Chief among these long-term concerns is replacing the tubular functions of the human kidney that provide metabolic, endocrine, and immune functions (Tiranathanagul, Eiam-Ong, & Humes, 2005). Aside from medical benefits of more kidney-like membranes, bioartificial membranes are not as susceptible to occlusion as traditional membranes, allowing dialyzers to last longer than just one treatment (Saito, et al., 2006).

The largest challenge facing the development of bioartificial membranes is growing proximal tubular cells in a lab. In order to meet the expected future demands of renal cells, a reliable source that can produce such cells is required. Researchers have begun using pig kidneys as cell donors (Humes, MacKay, Funke, & Buffington, 1999). Pig kidney cells were chosen because they closely resemble human kidney cells, and there is a plentiful supply of donor pigs. Cells are grown in the lab in Petri dishes, and implanted on high-flux dialyzers (Humes, MacKay, Funke, & Buffington,

1999). Traditional high-flux dialyzers are then used as scaffolds to hold the living cells on the membrane.

Hemodialysis systems that utilize bioartificial membranes do so by using two dialyzers simultaneously connected in series (Tiranathanagul, Eiam-Ong, & Humes, 2005). Like in traditional hemodialysis, the blood exits the body and is pumped through a traditional dialyzer. Instead of returning to the body, the blood leaves the dialyzer and enters the bioartificial tubule. The same dialysate used in the traditional dialyzer is reused after processing in the bioartificial tubule. After exiting the bioartificial tubule, the blood returns to the body. While in the tubule, the blood regains substances that would have otherwise been lost in traditional hemodialysis.

Initial testing of a bioartificial hemodialysis device began in 2001 on nephrectomized dogs (Tiranathanagul, Brodie, & Humes, 2006). Dogs were administered a dose of *Escherichia coli* (*E. coli*) proportional to their body weight, and then treated with either a bioartificial tubule or a placebo tubule. Among the many indications that the bioartificial tubule provided better treatment was that the dogs treated with the bioartificial tubule survived longer than the dogs receiving the placebo tubule. These promising results led to testing on pigs, which provided similar positive results (Tiranathanagul, Brodie, & Humes, 2006).

Buoyed by these results, the Food and Drug Administration approved human testing in 2003. Ten participants were selected at two U.S. hospitals that had predicted hospital mortalities ranging from 55% (ethylene glycol poisoning) to 97% (motor vehicle accident). Each patient was to be dialyzed with the bioartificial system for 24 hours, but five did not receive a complete dose for various medical reasons. While the study was conducted primarily to test the safety of the bioartificial tubule, some promising health results did emerge. Chief among these was the improved health of the patient for the three to seven days following bioartificial dialysis. While the study was too brief

and small to draw any conclusions, larger human trials were planned at the conclusion of the 2004 ten-patient study.

## **2.5 MEMS renal replacement research**

Polymer membranes have successfully been used for hemodialysis since the 1960s. Pores are created naturally through a curing process. Because the pores are created through the solidification of the polymer, the exact size of the pores cannot be exactly defined to meet needed specifications. Instead, polymer membranes have a pore size distribution that takes the form of a bell curve. Advances in membrane creation over the last half century have allowed scientists to sharpen its curve and shift it to a desired location, but the fact remains that pore size distribution is not ideal. Ideally, pore sizes would exactly correspond to the molecules desired to be removed. There would be little or no random distribution in pore size – the only variance in pore size would be to align intentionally with given molecules. While the shortcomings of polymer membranes have been known since their inception, researchers have been limited by the manufacturing technologies to realize an ideal membrane.

Microelectromechanical systems, or MEMS, are parts produced by a novel manufacturing process that can fabricate parts on scales that were unachievable when polymer membranes were first conceived for use on human patients.

The push for new membrane manufacturing processes is driven by the need for an implantable artificial kidney. While polymer membranes have their limitations, some of them can be addressed by frequently changing membranes. However, if an implantable system is developed, it must use a membrane that is sustainable for long periods inside the human body. For that reason, it must be resistant to occlusion and be biocompatible.

A MEMS membrane could address these problems and provide for an implantable renal replacement. Silicon is the primary material used in the manufacture of MEMS membranes, although the process used to create the pores is quite complex. The MEMS manufacturing process is able to create pores that can vary from 8 to 90 nm in size, with a resolution of 1 nm. Because of the pores' small size, novel tests have verified their size and distribution (Fissell, Fleischman, Humes, & Roy, 2007).

In an attempt to increase the effectiveness of the membranes, researchers have leveraged advances in bioartificial membranes. Proximal tubule cells from humans have been successfully implanted onto the silicon MEMS membrane, creating a membrane that has both ideal pore sizes and suitability for cell implantation.

An alternative approach has been taken by another research group at the Massachusetts Institute of Technology. Using mathematical models to predict the flow and mass transport inside small channels, they have designed a MEMS-based dialyzer that features hundreds of channels and layers.

Each layer of their dialyzer features countercurrent dialysate and blood flow through microchannels with a membrane separating the two flows. Plans for a renal replacement device call for 100 stacked layers to form one dialyzer. While this work has only produced a single layer device, tests from it indicate that it is twice as effective as traditional membranes (Kaazempur-Mofrad, Vacanti, Krebs, & Borenstein, 2004).

## **2.6 Computational efforts**

Researchers seeking to improve the performance of traditional hollow fiber dialyzers have long sought to leverage the power of computers to understand better the physical processes occurring inside the dialyzer during dialysis. Early computer models are primitive by today's standards, but provided a foundation for future research that has access to much more powerful computers.

Efforts in the 1970s attempted to account merely for two-dimensional mass transport in a single hollow fiber (Ross, 1974). The model created allowed researchers to explore the effects of varying the tubule diameter, flow rate, and tubule length quantitatively. While simple, this model provided relationships between key tubule characteristics and dialyzer physics.

With the rise of more powerful computers, more telling computer models could be developed. A dialyzer's sieving coefficient is the ratio of the volume flux to the mass flux, as shown in Equation 2-1.

$$S_D = \frac{K}{q} \quad (2.1)$$

A high sieving coefficient corresponds to relatively high mass crossing the membrane for a given flow rate. Fluid mechanists were unable to create an accurate model for the sieving coefficient in hollow fiber dialyzers until the 1990s. One-dimensional models in use predicted a steady decline in a dialyzer's sieving coefficient as the volume flux increased. However, experimental results showed that as the volume flux was increased, the sieving coefficient would fall and then subsequently rise.

A simple examination of the physics behind dialyzer performance would assume that as the volume flux increased, the sieving coefficient would decrease. While this holds true at lower flow rates, at high fluxes the sieving coefficient experiences a slight rise due to concentration polarization.

Models that are more accurate account for this thin boundary layer that develops on the inner surface of the membrane.

Three-dimensional computational efforts have been the focus of recent work. A model created at Ghent University in Belgium funded by Fresenius in 2002 accounted for flow, viscosity, hemocrit effects, and backfiltration (Eloot, De Wachter, Van Tricht, & Verdonck, 2002). Their work more closely examined the physics at distances very close to the membrane surface and within the

membrane itself, providing the most accurate model to date of the hydraulic permeability of the membrane.

## 2.7 Wearable renal replacement therapy

A prototype wearable renal replacement device has been developed by Gura et al. (2005). While their device does not introduce any significant advances in hemodialysis technology, its attempt to transform the hemodialysis experience is itself noteworthy.

In order to overcome issues surrounding the large amounts of dialysate used during a hemodialysis dose, the creators have employed modified REDY sorbent cartridges. Dialysate, after passing through the dialyzer and becoming dirty, is passed through the sorbent cartridge where activated carbon, urease, zirconium phosphate, and hydrous zirconium oxide absorb the wastes in the dialysate. The dialysate can then be returned to the dialyzer to remove more solutes from the blood. They claim to use less than 1 L of dialysate according to their 2007 patent filing of their best embodiments (Gura & Rambod, 2007).

**Table 2-2. Experimental results from Gura et al. (2007).**

	<b>Creatinine Clearance (mL/min)</b>	<b>Total Creatinine Removed (g)</b>	<b>Urea Clearance (mL/min)</b>	<b>Total Urea Removed (g)</b>
<b>Pig C</b>	20.10	0.91	29.40	7.61
<b>Pig D</b>	21.10	0.76	26.80	5.75
<b>Pig E</b>	23.50	1.14	27.30	5.37
<b>Pig F</b>	23.50	1.14	27.30	6.37
<b>Pig G</b>	22.30	0.95	25.70	6.46
<b>Pig H</b>	22.30	1.02	26.30	6.24
<b>Mean</b>	<b>22.13±1.34</b>	<b>0.99±0.15</b>	<b>27.13±1.27</b>	<b>6.13±0.85</b>

Preliminary tests of the device on six pigs (Table 2-2) had promising results without any complications.

Additionally, Gura et al. have developed a specialized pump for their prototype wearable artificial kidney. Special consideration has to be given to a pump's size and weight when designing a wearable device. For their device, they have developed a specialized dual-channel pulsatile pump controlled by microcontrollers.

## **2.8 Conclusion**

Most research conducted in the science of renal replacement focuses on improving the filtration method of the system. This is understandable – dialyzers and the peritoneum provide inadequate emulation of the human kidney. Many researchers are looking for a complete replacement of concentration gradient-based dialyzers with new technologies (like MEMS) or they are looking to augment biological functions through implanting of renal cells on a membrane.

This thesis will attempt to examine how all the parts of a hemodialysis system work together in order to develop a treatment concept. New technologies will be considered, but the primary focus will be on how systematic engineering design can improve hemodialysis.

## CHAPTER THREE

### CONCEPTUAL DEVELOPMENT

This chapter is devoted to the development of two renal replacement concepts: one that relies on established hemodialysis techniques, and one that is derived from the behavior of the human kidney. First, the functional performance of the human kidney is characterized, and then it is exploited to develop a concept that mimics its behavior. The functional analysis is also used to find alternative solution principles, which are used to develop a more traditional hemodialysis concept.

#### **3.1 Basic physiology of the human kidney**

All living organisms must constantly regulate their physiological condition in order to maintain life. The human kidneys play an important role in this process (called homeostasis) by providing several functions that help to maintain a healthy balance inside the body. While the primary function of the kidney is to balance solutes in the body, it is also responsible for secreting hormones that play an important role in other organs' regulation of homeostasis.

The basic functional unit of the human kidney is called a nephron. It is composed of five main parts: the renal corpuscle, the proximal tubule, the loop of Henele, the distal tubule, and the collecting ducts. In these parts, the kidney utilizes three main functions to regulate solutes in the blood: filtration, reabsorption, and secretion.

First, the kidney filters most substances across the glomerulus, a collection of capillaries surrounded by the Bowman's capsule, which together form the renal corpuscle as shown in Figure 3-1. There are many factors affecting glomerular filtration: size and charge of the molecules being filtered; size of the filtration slits of the glomerulus; charge of the glomerular basement membrane;

and several hemodynamic factors. Hemodynamic features include blood flow, convection, diffusion, the glomerular capillary pressure difference, and the Bowman's capsule pressure difference (Jennette, Hepinstall, Olson, Schwartz, & Silva, 2006).

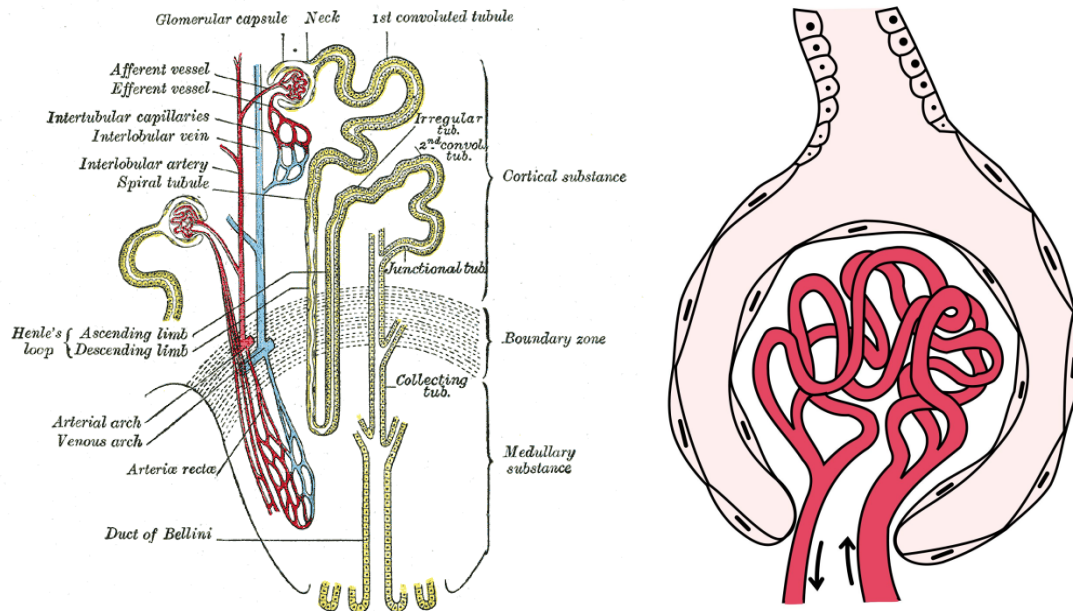


**Figure 3-1.** The figure on the left shows a complete nephron. In the figure on the right, the dark-red glomerulus is surrounded by the pink Bowman's capsule, forming the renal corpuscle.

After the substances have passed through the glomerulus, important substances are reabsorbed or excreted back into the blood stream in the proximal tubule, loop of Henele, the distal tubule, or collecting ducts. Lastly, substances that were not filtered across at the glomerulus can be excreted from the kidney at one of the later stages.

Approximately 625 mL of plasma flows through each kidney every minute. Of this 625 mL, each kidney filters approximately 20%, or 125 mL, across the glomerulus. However, only 1 mL/min of urine is excreted to the bladder. This discrepancy between the filtered and excreted amounts is

accounted for by reabsorption and secretion. After removing so much from the blood, the human kidney then works to reabsorb those substances that are beneficial for homeostasis.

As an example, all glucose found in the blood in the renal artery is filtered out of the blood in the renal corpuscle. However, glucose is vital for homeostasis, so it is immediately reabsorbed in the proximal tubule.

A hierarchical model of the kidney's waste removal process is displayed in Figure 3-2. The top figure shows how the basic functionality of the kidney – a filter – is used to separate the wastes out the blood. The bottom figure shows in detail how the five parts of the kidney use four different functional strategies to behave as a filter.

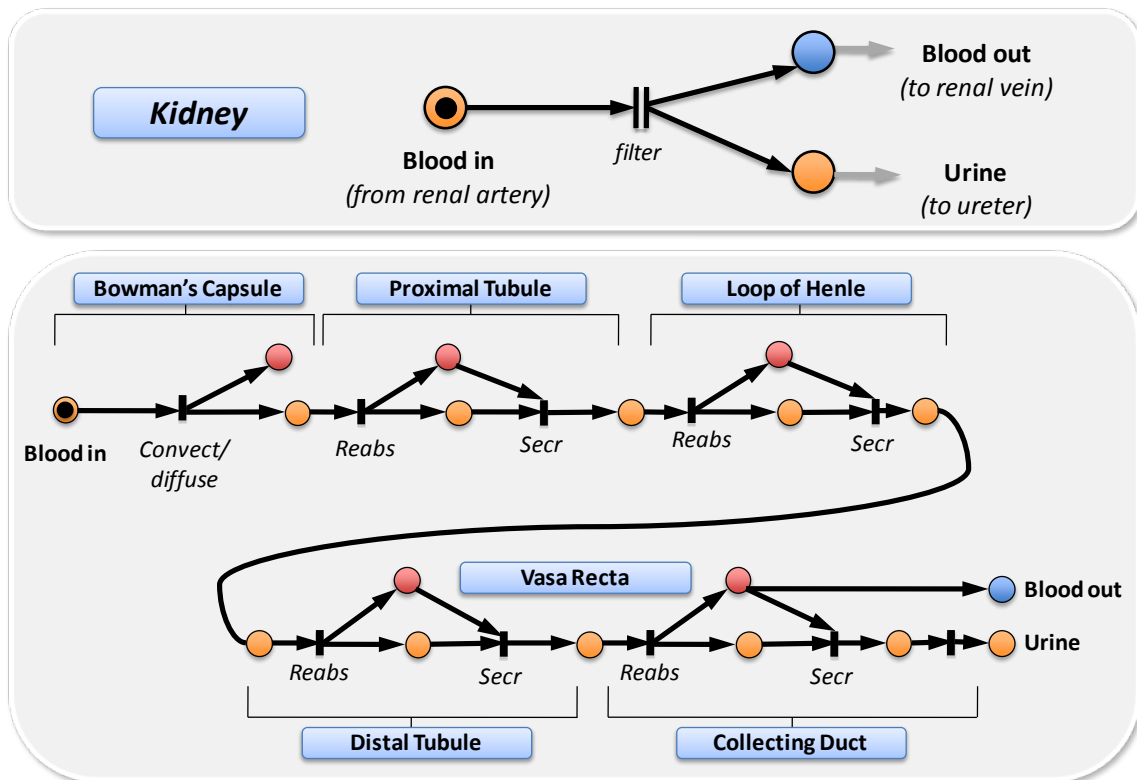


Figure 3-2. A functional model of waste removal in the kidney.

In Figure 3-2, at the kidney-level of abstraction, dirty blood comes in from the renal vein and wastes are filtered out into the urine, while the remaining clean blood returns to the body through the renal artery. The subsystem level of decomposition includes the Bowman's capsule, proximal tubule, loop of Henle, distal tubule, and the collecting duct. At this level, the blood plasma and its solutes are convected and diffused across the Bowman's capsule. The solutes in the plasma then go through several steps of reabsorption and secretion, finally being excreted through the collecting duct as urine.

There are two striking things to note about the function of the human kidney: that it uses thousands of small identical functional units (nephrons) instead of one large unit, and it uses a multi-step filtration process.

Its use of many small functional units instead of one large unit seems similar to many other biological systems. By dividing the function amongst many small units on a large scale, the kidney allows a small output item (the nephron) to produce big results. This idea is not only realized in biological realms, but also in industrial settings – like solar arrays. If there is a technology that works on a small scale, research can be dedicated not to making it larger, but rather to finding an effective way to replicate its functionality on a large scale.

The other interesting functional behavior of the human kidney is its filtration method. Instead of simply removing the undesirable molecules in the exact quantity in one pass, it clears both the desirable and undesirable solutes, and then reabsorbs those that it would like to retain. This interesting concept serves to create a multiphase filter, allowing for specialized molecule removal. Hemodiafiltration, an effective combination of hemodialysis and hemofiltration, relies on a similar principle. The primary drawback of this method is that large amounts of fluids are lost from the blood and must be replaced immediately – relegating this treatment to intensive-care settings.

## **3.2 Functional analysis of current renal replacement therapies**

This section will focus on the development of two key forms of renal replacement therapy: hemodialysis and hemodiafiltration, which were introduced in Chapter 2.

### **3.2.1 Review of current renal replacement therapies**

A summary of current research in the field of hemodialysis, hemofiltration, and hemodiafiltration was provided in Chapter 2. This section provides a further review of their function.

#### **3.2.1.1 Hemodialysis**

The first major innovation in treating kidney disease came in the 1940s. Williem Kolff is credited with constructing the first hemodialysis machine in 1943. His artificial kidney utilized blood flowing through cellophane tubing in a rotating drum assembly. This drum rotated in a tank of dialyzer medium (Davita, Inc., 2008). In the 1950s, Kolff's invention was advanced enough to solve the problem of acute renal failure.

It was not until the works of Belding Scribner that a solution for chronic end stage renal disease was envisioned. Scribner devised an idea of using Teflon tubes inserted into the artery and veins. After treatment, these tubes were connected using a U-shaped device, completing the circulatory circuit. This advancement allowed direct access to the circulatory system and ended the need for making incisions every time. Although several incremental advances have been made with traditional hemodialysis, the basic circuit and principle has remained the same.

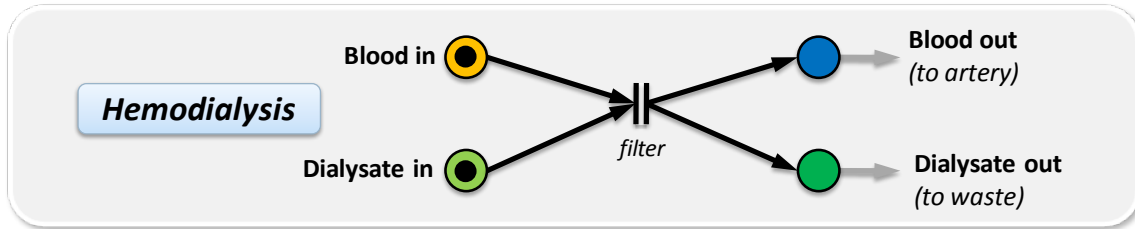


**Figure 3-3. Functional performance of hemodialysis.**

In hemodialysis, displayed in Figure 3-3 and Figure 3-4, solutes are filtered by diffusion across a semipermeable membrane. The primary component of modern hemodialysis is the dialyzer (labeled *filter* in Figure 3-3), which contains the semipermeable membrane. In the dialyzer, blood from the patient flows along one side of the membrane countercurrent to that of the dialysate, creating a concentration gradient across the membrane. Unlike the human renal system, the kidney has no deeper level of abstraction.

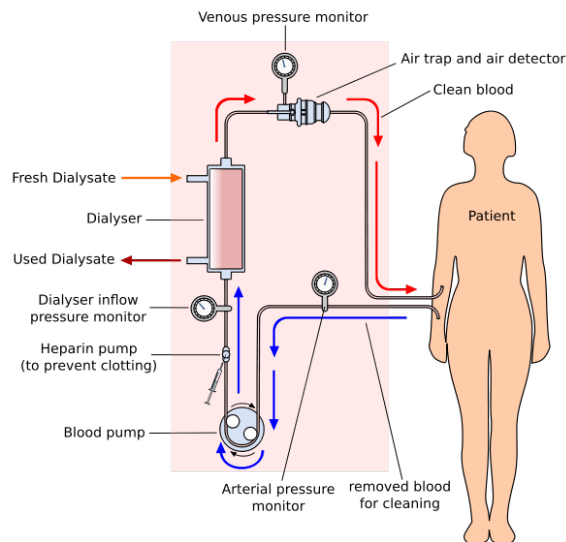


**Figure 3-4. A hemodialysis circuit (YassineMrabet, 2008).**

The general principle of hemodialysis is that small molecules will diffuse across the membrane to areas of lower concentration. The concentration of solutes to be filtered is zero, while

concentrations of those solutes to be kept in the blood is equal to that of the blood. Based on the laws of diffusion, the larger the molecule, the slower the rate of transfer across the membrane will be. Given that, molecules of small molecular weight, such as urea (60 Daltons), are filtered efficiently, while molecules with higher molecular weights, such as creatinine (113 Da), will be cleared less efficiently (Forni & Hilton, 1997). The waste, which is filtered across the membrane into the dialysate, is disposed of as dirty dialysate.

### 3.2.1.2 Hemodiafiltration

Another key innovation came by way of combining hemodialysis with a convective (filtration-based) renal replacement therapy known as hemofiltration. This hybrid process is called hemodiafiltration. In the 1960s, hemofiltration was introduced to enhance the removal of larger substances from the blood and improve hemodynamic tolerance (Forni & Hilton, 1997).

Building on benefits of hemofiltration, in the 1970s work began on creating a renal replacement therapy harnessing the benefits of hemodialysis (small molecular weight substance removal) and hemofiltration (middle molecular weight solute removal). Hemodiafiltration works in a similar fashion to the human kidney; a large amount of filtrate is filtered from the blood and then desirable components are replaced. In hemodiafiltration, blood and dialysate are pumped through the filter in a counter-current manner.

Similar to that of glomerular filtration, water and substances up to a molecular weight of 20,000 Da are convected and diffused across the membrane and into the dialysis fluid. Desirable substances are then replaced in the distal part of the hemodiafiltration circuit using a replacement fluid. The typical composition of the replacement fluid is displayed in Table 2-1. A typical hemodiafiltration circuit is displayed in Figure 3-5.

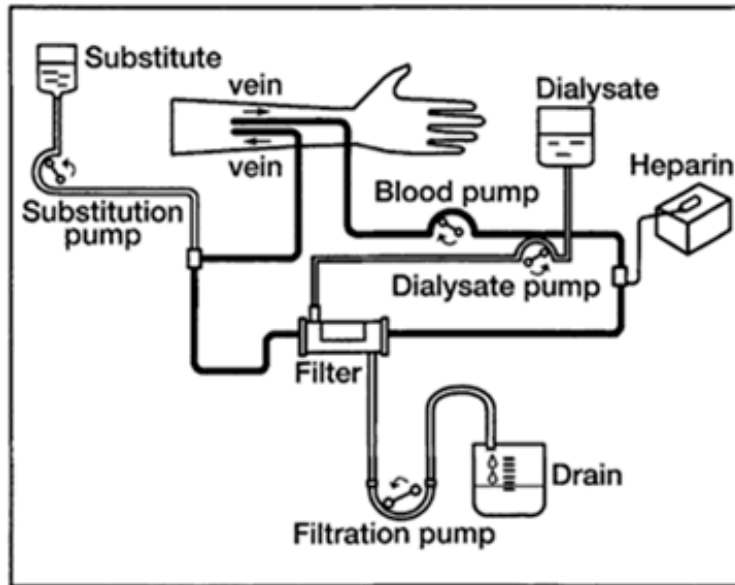


Figure 3-5. A typical hemodiafiltration circuit (Asahi Kasei Medical Company).

As displayed in Figure 3-5, blood and dialysate are pumped through the filter and the filtrate is drained. The substitution fluid containing the desired substances is then infused into the blood in the distal part of the circuit.

### 3.2.2 Performance assessment of hemodialysis and hemofiltration

In this study, these renal replacement techniques are compared based on solute removal and mortality rate. A summary of results from recent studies is as follows:

#### *Studies on small molecular weight solute removal:*

- Clearance of small solutes (< 500 Da) such as urea (60 Da) and creatinine (113 Da) is largely dependent on diffusion processes. Hemodialysis and hemodiafiltration both showed effective removal of these small solutes, while hemofiltration did not. There was little difference between hemodialysis and hemodiafiltration in clearance of these small solutes (Maduell, 2005).

- Studies by Ward, et al. (2000) showed small improvements (10 to 15%) of urea and creatinine removal for hemodiafiltration and high-flux hemodialysis.

*Studies on medium molecular weight solute removal:*

- In a study by Ahrenholz, et al. (1997), the experimenters showed a 123% improvement in clearance of inulin (5200 Da) in hemodiafiltration versus high-flux hemodialysis (Maduell, 2005).
- $\beta_2$ -microglobulin (11,800 Da) is not removed at all by hemodialysis because it is larger than the typical hemodialysis membrane pore. Kerr et al. (1992) reported 54.8% reduction of  $\beta_2$ -microglobulin of high-flux hemodialysis and 62.7% reduction in hemofiltration after a 3 hour session. Lorney et al. (1998) reported a 49.7% reduction using high-flux hemodialysis, compared to 72.7% with hemodiafiltration, in a 4 hour session. In a 245-minute session, Maduell et al. (2005) reported -0.2, 60, and 75% reductions with hemodialysis, high-flux hemodialysis, and hemodiafiltration, respectively.
- In a study by Ward et al. (2000), hemodiafiltration resulted in greater removal of  $\beta_2$ -microglobulin than high-flux hemodialysis, as indicated by a significantly higher pre- to post-treatment change in concentration ( $73 \pm 1\%$  versus  $58 \pm 1\%$ , respectively).
- In renal failure,  $\beta_2$ -microglobulin accumulates in the body and can be deposited in bone and joints in the form of amyloid. In the HEMO study (Cheung, et al., 2006), a significant relationship was found in pre-dialysis  $\beta_2$ -microglobulin and all causes of mortality; mortality increased by 11% for every 10 mg/L rise in  $\beta_2$ -microglobulin concentration (Petrie, Ng, & Hawley, 2008).
- Dember and Jaber (2006) estimated yearly accumulation of 111, 97, and 51 g for hemodialysis (4 hours, 3 times per week), high-flux hemodialysis (4 hours, 3 times per

week), and hemofiltration (2 hours, 6 times per week), respectively. Hemodiafiltration should show results similar to that of hemofiltration (Petrie, Ng, & Hawley, 2008).

*Recent studies on mortality:*

- In the Dialysis Outcomes and Practice Patterns (DOPPS) study (Canaud, et al., 2006), after adjusting for demographic and other contributors to mortality, experimenters reported a 35% better survival rate with hemodiafiltration (11.9 deaths/100 patient years) versus hemodialysis (14.2 deaths/100 patient years).
- In analysis of data from The European Clinical Database, Jirka et al. (2006) reported a 35.3% better survival rate with hemodiafiltration versus hemodialysis. This study was also adjusted for other contributors to mortality.

Studies of small molecular weight solute removal such as urea and creatinine showed efficient removal in both hemodiafiltration and hemodialysis, with hemodiafiltration showing slight improvement. In studies of middle molecular weight solute removal, hemodiafiltration was shown to improve the removal of  $\beta_2$ -microglobulin significantly.  $\beta_2$ -microglobulin amounts were shown to correlate to increased mortality. In specific large-scale studies on mortality, hemodiafiltration was shown to have a nearly 35% improvement in survival rate.

A summary of the use of kidney filtration strategies in renal replacement systems is displayed in Table 3-1. Two assessments of the human kidney function are given: *High Level* (a basic description of kidney function) and *Detailed Level* (a more detailed description of kidney performance). Table 3-1 shows that hemodialysis matches kidney functionality at a higher level than hemodiafiltration. Similarly, a concept will be developed that more closely mimics the functional performance of the human renal system.

**Table 3-1. Summary matching functional relationship between hemodialysis and hemodiafiltration against the human kidney.**

Level of Decomposition	Hemodialysis	Hemodiafiltration
<p><b>High Level:</b>                      “The composition of blood in the kidney is modified through filtration.”</p>	<p>Removal of waste from the blood through one-step filtration process.  <b>Shows only good small solute removal.</b></p>	
<p><b>Detailed Level:</b>                      “Filtration in the kidney is performed by removing mostly all substances from the blood through convection/diffusion in the Bowman’s capsule and reabsorbing and secreting needed substances in the proximal tubule, loop of Henle, and distal tubule, and collecting duct. The remaining solutes are excreted through the collecting duct.”</p>		<p>Removal of waste through a two-step filtration and reabsorption process.  <b>Shows good small, medium, and large solute removal.</b></p>

In the early development of renal replacement therapies, engineers developed hemodialysis as a means to replace the function of the kidney and treat kidney disease. Hemodialysis mimics the general behavioral strategy of the kidney in filtering the blood of waste; however, it is not very efficient at removing harmful middle molecular weight solutes from the blood and does not have a particularly high survival performance on a long span of time.

Scientists developed hemodiafiltration as a means of improving on the performance of renal replacement therapy. Hemodiafiltration functions in a similar fashion as that of the human kidney; hemodiafiltration filters large amounts of water and substances from the blood through convection and diffusion, and then replaces the substances needed for bodily function. This setup has shown improved performance in removal of small and middle molecular weight solutes, as well as significant improvements in the survival rates of patients receiving this form of treatment.

### 3.3 Functional analysis of the human kidney

The goal of this section is to derive a superior renal replacement treatment by analyzing the performance of the human kidney. The failures of current RRTs have already been outlined; the goal now is to explore how the human kidney functions from a systems perspective to see if any strategies can be exploited in the design on a new RRT.

#### 3.3.1 Decomposition of human kidney function

First, a simple model of the human renal function is modeled in Figure 3-6. The kidney inputs dirty blood and outputs urine and clean blood. There is also a control signal dictating kidney operation.

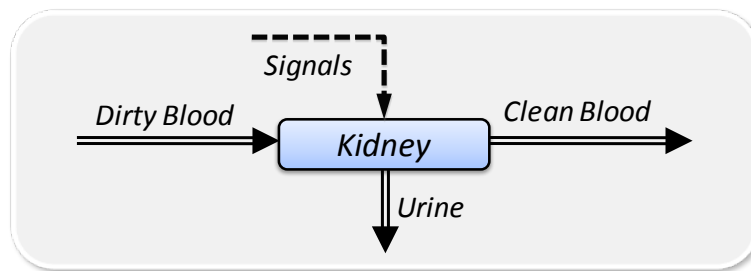


Figure 3-6. Simple system model of the human kidney.

#### 3.3.2 Behavioral assessment of kidney

The behavior of a kidney is displayed in Figure 3-7. The human kidney is modeled as a continuous system with the state of the system dictated by the composition of solutes at different places. The behavior of the kidney (*filter*) is represented by a two parallel lines. *Blood in* passes through the kidney (*filter*) and then is separated into two flows: *Blood out* (to the renal vein) and *Urine* (to the ureter).

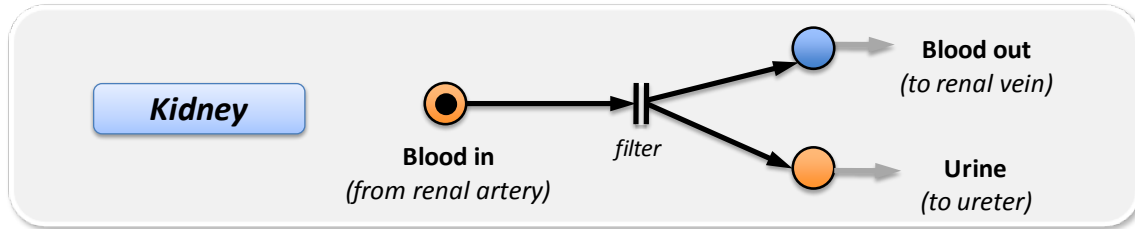


Figure 3-7. Model of the overall behavior of the human kidney.

### 3.3.3 Decomposition of the kidney into subsystems

The system is decomposed into its subsystems, as shown in Figure 3-8. The functional unit of the kidney is the nephron. The nephron can be further decomposed into its different subsystems, including the Bowman's capsule, proximal tubule, loop of Henle, distal tubule, and the collecting duct.

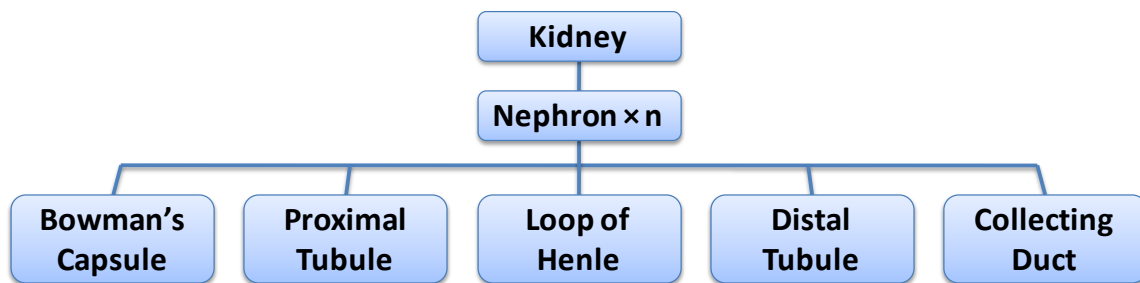


Figure 3-8. Structural decomposition of the human kidney.

Next, the interactions between the components are modeled and displayed in Figure 3-9. As seen in the figure, blood solutes from the Bowman's capsule flow through the proximal tubule, loop of Henle, and the distal tubule, before exiting at the collecting duct as urine. Solute are also exchanged with the vasa recta before leaving the kidney in the clean blood.

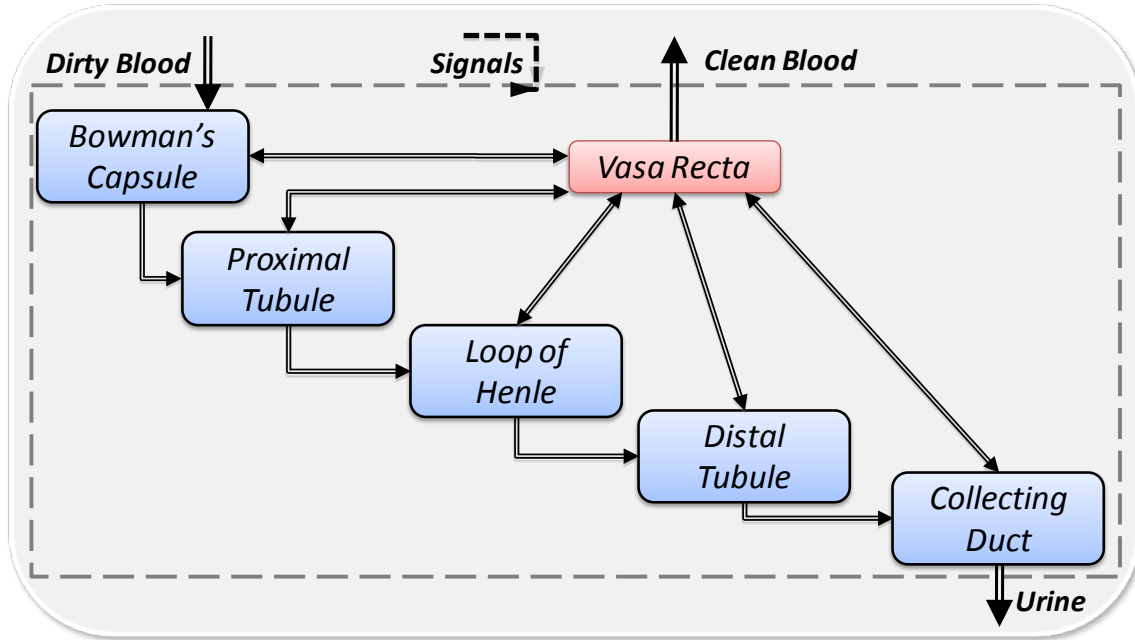


Figure 3-9. Kidney subsystem interactions.

### 3.3.4 Functional assessment of the behavior of subsystems

The standalone behaviors of the subcomponents (Bowman's capsule, proximal tubule, loop of Henle, distal tubule, and the collecting duct) are now identified. The individual behaviors of the kidney subsystems displayed in Figure 3-8 are defined in Figure 3-10. In Figure 3-10, the behaviors of three solutes ( $\text{Ca}^{2+}$ , glucose, and urea) are represented.

Consider the behavior of the proximal tubule. The mass flux of  $\text{Ca}^{2+}$ , glucose, and urea at entry to the proximal tubule is 540, 800, and 933 mmol, respectively. In this tubule 70% of  $\text{Ca}^{2+}$ , 100% of glucose, and 50% of urea are reabsorbed into the blood. The composition of the blood (in the vasa recta) after reabsorption is then 378, 800, and 467 mmol, respectively. The composition of the blood leaving the proximal tubule is 162, 0, and 467 mmol, respectively. These figures are repeated at the entry of the loop of Henle.

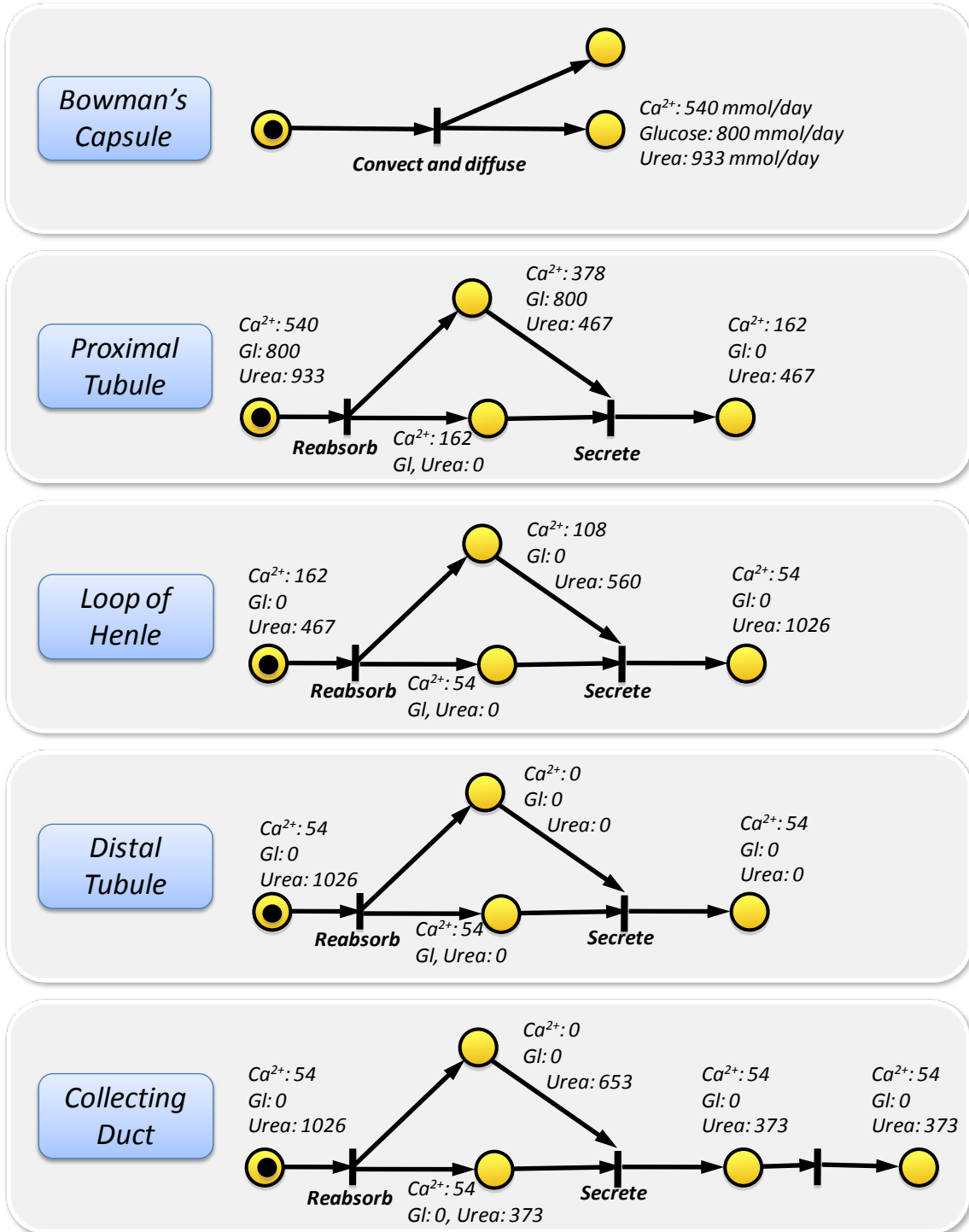


Figure 3-10. Standalone behaviors of each of the kidney subsystems. All figures are in mmol/day.

### 3.3.5 Compiled functional analysis

Figure 3-11 displays the completed model for the human kidney. In the figure, the transition *filter* (shown in the top half of Figure 3-11) is defined using a dashed line in the lower model.

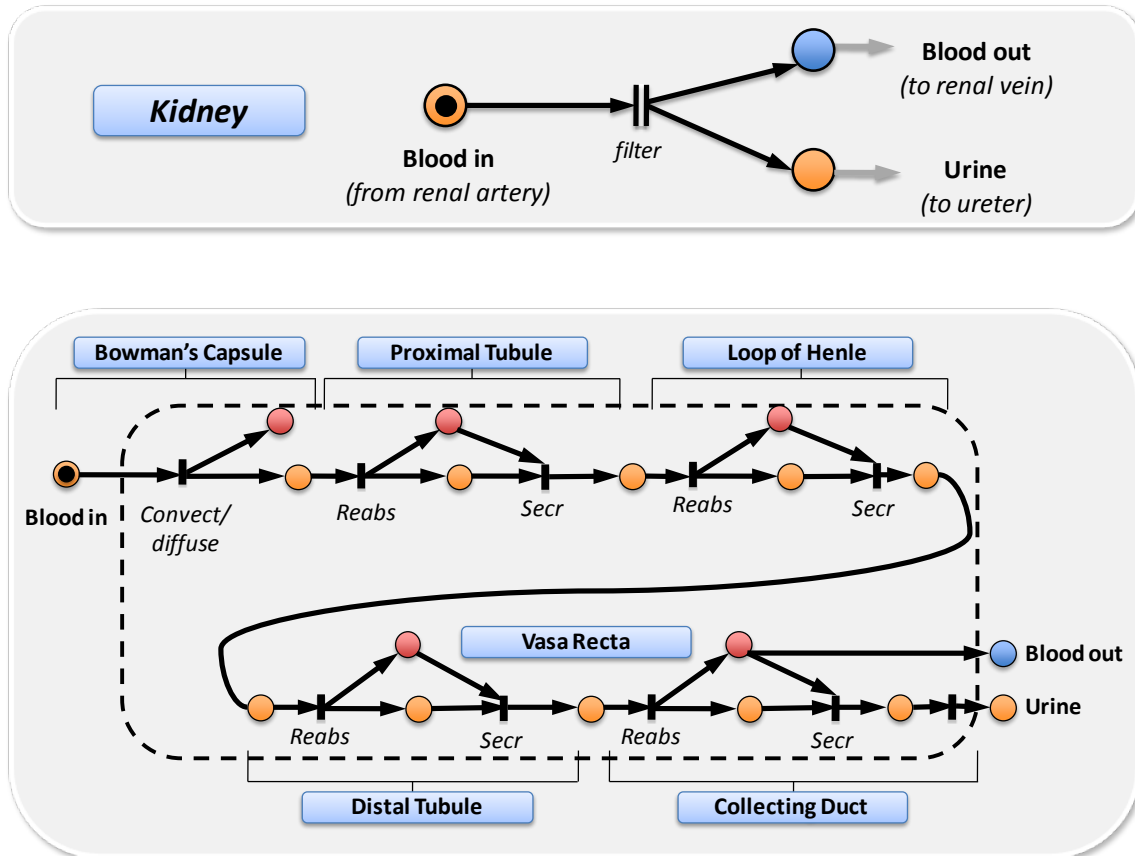
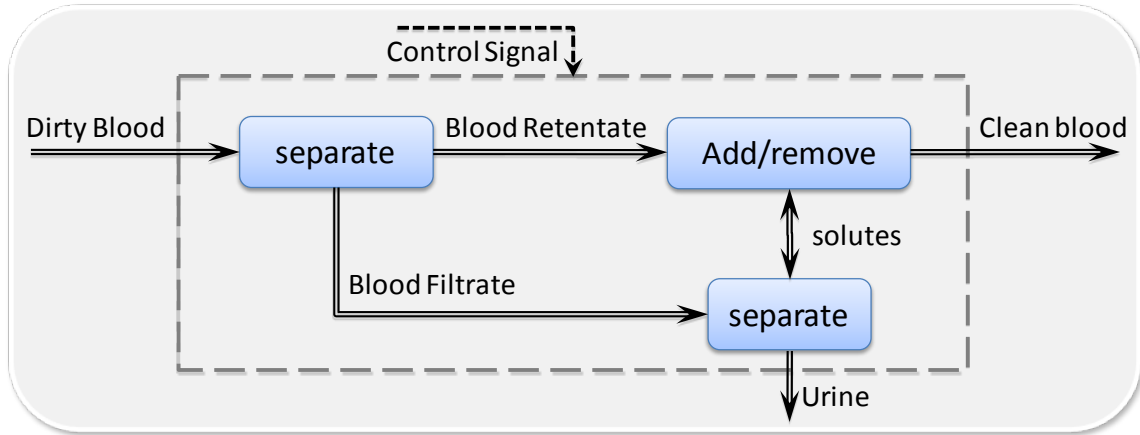


Figure 3-11. Hierarchical function representation of the human kidney.

### 3.3.6 High-level functional results

The biological strategies modeled in the previous section are used to stimulate the generation of working principles. Based on the strategy extracted for waste removal in the kidney in Section 3.3, the following high-level function structure, displayed in Figure 3-12, is generated. This model will help guide the conceptual design process.



**Figure 3-12. High-level function of the human kidney.**

In this model (Figure 3-13) the dirty blood is first separated into blood filtrate and retentate. After reabsorbing the needed substances and secreting the unneeded ones, the now clean blood is circulated back into the body. The rate of reabsorption and secretion of the substances is regulated by the body.

### 3.4 Requirements list for a renal replacement device

The first step towards the development of a concept is to create a requirements list for the final design. In the case of an artificial kidney, the most obvious requirements set standards on solute clearance. Beyond solute clearance, the device must be biocompatible and practical for everyday use.

A requirements list is presented below:

#### Operational Properties

1. Conform to target excretion rates(Guyton 1986):

Na<sup>+</sup>            0.128 mEq/min

K<sup>+</sup>             0.06 mEq/min

Ca <sup>2+</sup>	0.0048	mEq/min
Mg <sup>2+</sup>	0.015	mEq/min
Cl <sup>-</sup>	0.134	mEq/min
HCO <sub>3</sub> <sup>-</sup>	0.014	mEq/min
H <sub>2</sub> PO <sub>4</sub> <sup>-</sup>	0.05	mEq/min
HPO <sub>4</sub> <sup>2-</sup>	0.05	mEq/min
SO <sub>4</sub> <sup>2-</sup>	0.033	mEq/min
Glucose	0.0	mg/min
Urea	18.2	mg/min
Uric acid	0.42	mg/min
Creatinine	1.96	mg/min

2. Does not coagulate the blood.
3. Maintains blood pressure by regulating plasma output.
4. Filtered blood is returned to the bloodstream.
5. Waste is excreted from the system in a sanitary manner.

#### **Physical Properties**

1. Materials and processes that are in contact with body and blood must be biocompatible.
2. Materials must comply with government regulation.
3. Provides a superior experience to today's hemodialysis

Important care was given to this list to ensure it was free from a specific design or technology. It can therefore be used at later stages of the design process to help make decisions and evaluate alternatives.

### **3.5 Functional analysis of renal replacement**

In its most basic sense an artificial kidney must access the blood in the body, clean the blood, return the blood to the body, and properly manage the waste extracted. The human kidney is able to complete all these tasks completely inside the body, utilizing the human metabolism as a source of energy and the bladder to excrete wastes. The kidney is also able to decode hormonal signals to adjust its filtration process.

The human kidney does an excellent job filtering wastes because it has an excellent hormonal feedback system tied to an exacting filtration process that is entirely biocompatible. Today's dialysis machines rely on a few lumped parameters and weekly readings to determine dialysate dose. Worse, the dose of dialysis is not specific to individual solutes, but just to a general treatment of all solutes in the blood. While the human kidney can instantly respond to a condition – like dehydration – by decreasing the amount of water removed from the blood, hemodialysis takes out the same amount with each treatment. Patients attempt to account for their own homeostasis through dietary changes, but no artificial system adequately replaces the renal functions.

Ideally, engineers could leverage some of the body's natural solutions in designing a renal replacement device. However, the complex biological nature of the human kidney makes this unfeasible with today's technology. A close examination of the basic functions might reveal a method alternative to both the kidney and today's dialysis that is functionally similar.

### 3.5.1 Development of function structures and working principles

In designing a new hemodialysis device, one must first break the process down to its most basic functions. Once the most basic functions are known, solutions can be derived. This method attempts to remove designer bias by treating every possible solution as equals. Table 3-2 compares the functional difference between the human kidney and clinical hemodialysis.

**Table 3-2. The functional difference between the human kidney and clinical dialysis.**

Functions	Human Kidney Solution	Clinical Hemodialysis Solution
Filtration	Cells	Membrane
Energy	Human metabolism	AC power
Pressure	Natural blood pressure	Pump
Waste output	Human bladder	External bladder (drain)
Feedback loop	Hormones	Artificial sensors

The five basic functions of the renal system are filtration, energy, pressure, waste output, and feedback. While the solutions to each of these functions are known for both the human kidney and traditional hemodialysis, it is best to expand the table to include every possible solution. Figure 3-13 expands the basic solutions to each function, including methods used by the kidneys, current dialysis machines, and new solutions.

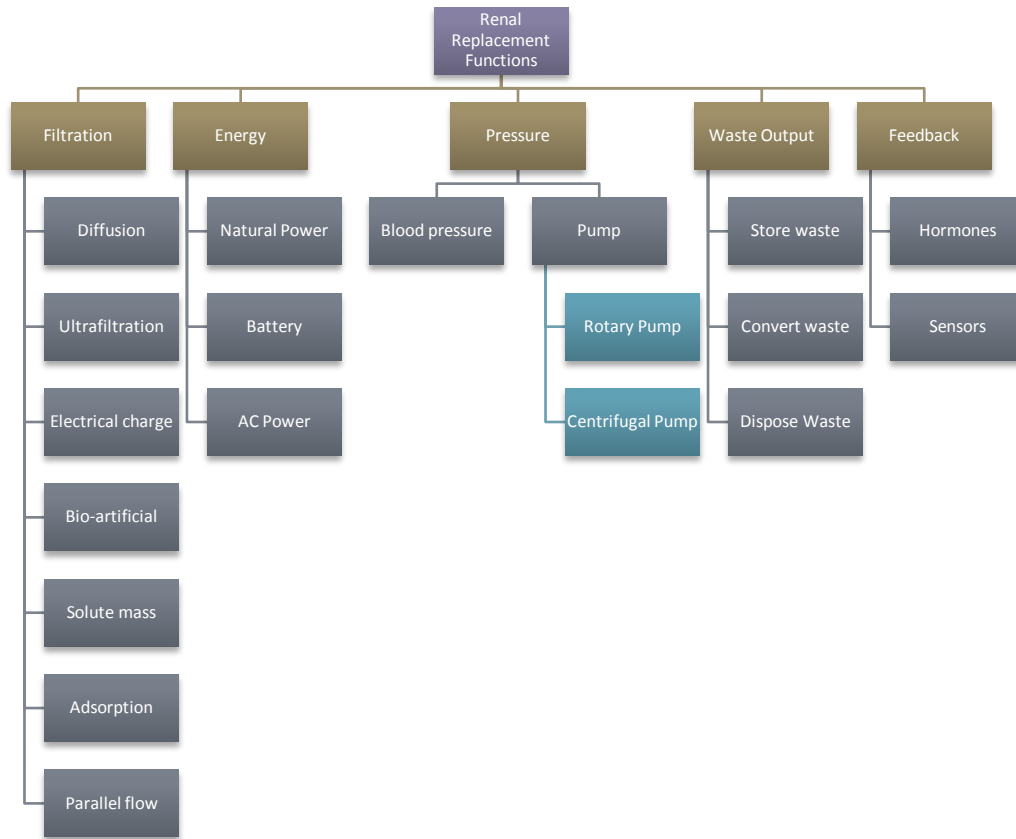


**Figure 3-13. Function structures and solution principles of an RRT.**

### 3.5.2 Analysis of working principles

In order to develop a renal replacement concept, the functional space outlined in the previous section must be explored and evaluated. This means all options must be examined to determine what principles meet the functional needs, and then evaluate these working principles based upon design metrics.

#### 3.5.2.1 Filtration working principles

There are seven separate functional methods to filter wastes from the blood. For each of these functional methods, there are working principles – manifestations of these functions in the form of

actual technologies. For example, diffusion has several working principles, including hollow-fiber membranes (used in current dialysis machines) and other membrane configurations.

#### *3.5.2.1.1 Diffusion*

Diffusion is the primary form of mass transport in membrane-based filtration. Two fluids flow on opposite sides of a hollow-fiber membrane (either counter- or parallel-flow), and molecules and solutes are transported via a concentration gradient through the pores of the membrane. Those molecules and solutes whose concentration is equal on both sides of the membrane lack a strong driving force to traverse the membrane.

Control over which solutes cross the membrane barrier is primarily done by modifying the relative concentration of the fluid on the dialysate side of the membrane. For example, the fluid travelling countercurrent to blood, dialysate, contains no urea, driving the urea in the blood across the membrane. Alternatively, blood contains glucose, which needs to remain in the blood. Dialysate contains glucose, deterring the glucose in the blood from diffusing across the membrane.

The other primary factor affecting diffusion rates is the physical properties of the membrane itself. Specifically, the size and shape of the holes plays a large role in the mass transport properties of the membrane. Because solutes can only pass through holes larger than themselves, the holes of a semi-permeable membrane must correspond to the various solutes that need to diffuse out of the blood.

Unfortunately, membranes cannot be made with specific hole sizes due to their manufacturing processes. Membranes are formed from a cured polymer that naturally creates tiny pores for the solutes to move across during dialysis. Because the pores are created through the curing of the polymer, there is a relatively uncontrollable size distribution. While some control can be exerted over the pore sizes, a bell curve distribution is inevitable.

One solution to this pore-size distribution problem is to create the pores manually of the exact size needed. But because of the pore's extremely small size (around  $20 \times 10^{-6}$  in diameter), no existing manufacturing technology can create individual pores in the needed size range. If pores could be created that corresponded to the exact size of solutes, artificial kidneys could behave in a superior fashion: filtering out only the exact molecules needed in a stage like fashion.

#### *3.5.2.1.2 Filtration*

Ultrafiltration is a membrane-based separation strategy in which hydrostatic pressure forces particles in a mixture across a semi-permeable membrane. Large solutes in the mixture are retained, while smaller solutes and the liquid pass through the membrane.

Ultrafiltration already has some use, but it has some serious drawbacks. First, the blood must be pressurized far beyond normal human blood pressure to force molecules across a membrane – a membrane that already lacks the exacting pore sizes, as explained before. Worse, this solution principle results in considerable water loss from the blood. In order to implement this method with today's technology, an artificial kidney would have to account for large amount of water loss and raised blood pressures, creating two major obstacles to using ultrafiltration as a primary method of solute removal.

#### *3.5.2.1.3 Electrical charge*

Another separation strategy is driven by the electric charge of the solutes in a mixture. This process – termed electrophoresis – is commonly used to sort ions in a fluid. A fluid, full of ions to be sorted, is mixed with a buffer solution and run between two oppositely charged plates. As the fluid and buffer flow parallel along the plates, the charged ions are pulled towards the plates based upon their electric charge.

While this system works quite well in a lab for non-biological fluids, using electrophoresis to remove solutes from the blood is not as easy. First, not all waste solutes have a distinguishable charge. More importantly, the need for a buffer solution to be mixed with the blood makes electrophoresis nearly impossible to implement. Another considerable factor is the biocompatibility and associated heat generation of electric fields needed to sort the solutes.

Therefore, while electrophoresis holds some promise as a way to remove wastes from the blood in a precise manner, it has some serious technological hurdles that have not yet been overcome by today's science. In addition, while electrophoresis holds promise as a better way to filter wastes, it seems that implementing it as part of an implantable device seems extremely difficult because of the electric fields and currents generated during its use.

#### *3.5.2.1.4 Bio-artificial*

Bio-artificial separation uses actual mammalian renal cells as part of a membrane-based filtering system. Living renal cells are suspended onto a polymer membrane scaffold, and behave as actual renal cells in the kidney: pumping solutes in and out of the blood (details in Section 2.4). A limit to using bio-artificial membranes is that as an emerging technology they are not ready for implementation yet. Only small-scale clinical trials have been run, meaning the technology is years away from any sort of application.

#### *3.5.2.1.5 Solute mass*

Centrifugation is a separation strategy involving the use of centrifugal force for the separation of substances in a mixture. In this case, the heavier components of the mixture move away from the axis of the centrifuge, while lighter components move towards the axis.

The feasibility of using differences in solutes' mass as a sorting principle is doubtful. The throughput and resolution associated with centrifugal sorting is orders of magnitudes smaller than what would

be required for any sort of renal replacement. While the idea works in theory, its application in a renal replacement device is limited.

#### *3.5.2.1.6 Adsorption*

Adsorption is a separation strategy that uses chemical affinity to separate specific substances from a mixture. In this case, a sorbent is used to adsorb the unwanted substances from the mixture.

As discussed earlier in this chapter, sorbent cartridges have already been applied directly to the blood with unsuccessful results. Current sorbent technology is not capable of fulfilling this functional need.

#### *3.5.2.1.7 Parallel flow*

At very specific flow conditions, two fluids can flow parallel to one another without mixing.

Considered a form of a membrane-less dialysis, the solutes in the two fluids can diffuse across the fluid boundary without the transport of fluid molecules. This concept has been studied for use in hemodialysis by Leonard and coauthors (2005).

#### *3.5.2.2 Energy solution principles*

There are two obvious ways to power an artificial renal replacement device: use the body's natural power, or an external power source. In order to use a natural (human) power source, an artificial kidney would somehow have to convert heat (at a relatively cool 37 °C), translate motion, or rely on normal blood pressure as a source of energy. Alternatively, the artificial device could use an external electrical power source.

If electricity is supplied to the kidney from an external (non-natural) source, there are two options: store the energy, within a battery in the system; or bring it to the system, via a cord, from an external source. Using a traditional wall socket is the only feasible method to bring power into the

system if it is not stored in a battery. A battery that stored the energy in the system could be of a variety of sizes, weights, and power.

While a human-powered solution would be ideal, there is no feasible way to convert enough power that would be needed for the electrical components of a hemodialysis system. The powered parts – the pump and sensors – do not require remarkable amounts of energy, but enough to consider not using the body as a power source.

Of the two other options, the best solution depends on the final concept. A device that depends on its size, weight, or portability as its competitive advantage would likely require a battery in its final design. Alternatively, a device that provided superior filtration capability – without regard to size or portability – could reasonably use a wall socket as its source of power.

#### 3.5.2.3 Pressure working principles

In order to achieve mass transport across a semi-permeable membrane, there must be a transmembrane pressure (TMP). Other methods of filtration considered also require some sort of pressure to work properly. There are two obvious methods to create the needed pressure for proper filtration: use a pump to raise the natural human blood pressure, or adapt the renal replacement system to the normal human blood pressure.

While using the body's natural pressure would be ideal, there are limitations. For one, the use of a pump is already needed to move the dialysate (save for a potential energy-based pumping system), and the blood flow rate needs to be controlled for optimal dialysis. For these reasons, the use of a pump in a renal replacement system is nearly unavoidable.

However, the inclusion of a pump into the system is not a considerable issue. The pressures and flow rates involved in dialysis are relatively slow and low enough that the size, weight, and power

requirements of the pump should be straight-forward to achieve. As outlined in later chapters, reducing the size and weight of a hemodialysis system is focused largely on other system components. Including a small pump to achieve desired TMP and blood flow rate is a reasonable solution principle.

#### 3.5.2.4 Waste output solution principles

Two types of wastes are associated with hemodialysis: the waste removed from the blood that must be disposed (urine, in human kidneys), and any wastes created by the choice of cleaning method. For example, when diffusion is used as the primary method of waste removal with a semi-permeable membrane, the counter-flow liquid (dialysate) is dirtied and must be disposed.

While the wastes collected from the blood account for about 1 mL/min in the human kidney, dirty dialysate can accumulate at rates from 100-500 mL/min, depending on the hemodialysis system configuration. At the extreme, a 500 mL/min treatment for four hours creates 120 L of dirty dialysate. This is a major obstacle if a hemodialysis system is to be reduced in size or made portable; however, if the system is focused on merely improving clearance rates while remaining plugged into the wall, expending dialysate at 500 mL/min is not a serious issue. Current dialysis machines tend to follow this principle: they are designed for clinical use, and the price of dialysate has been reduced enough that it is economical to design a system that operates at such high flow rates.

An alternative solution principle is to find a way to regenerate the dirtied dialysate. Dirty dialysate is similar to clean dialysate, but contains enough wastes from the blood that if it were to run through the dialyzer for additional passes, there would be an insufficient concentration gradient to drive diffusion. Ultimately, a subsystem would have to be created that filtered the wastes from the dialysate, and then returned the cleansed dialysate to the dialyzer.

While it seems obvious, creating a sorbent system that cleans the blood directly – instead of the dialysate – is not possible. Cleaning the blood with dialysate, and then cleaning the dialysate seems wasteful from an overall systems perspective, especially if cleaning the dialysate creates more liquid that must be cleaned. However, all these issues have been addressed by past research.

Dialysate cleaning methods have been developed that use absorbent cartridges. Dirty dialysate passes through a cartridge where the wastes are absorbed by various dry powders, all while the base dialysate solution is able to pass through. This system creates very little new volumes of wastes. Dialysate cleaning sorbents fell into disuse in the 1980s because the price of clean dialysate reached levels that are more economical.

#### 3.5.2.5 Feedback working principles

One of the great discrepancies between artificial renal replacement and human kidneys is the way the human kidney can fine-tune its filtration to meet the body's needs. In fact, the kidneys do much more than simply remove wastes from the blood – the kidneys work in concert with many other organs to maintain homeostasis. For example, while the human heart has primary control over blood pressure, the kidney also plays a role by controlling how much water is retained in the blood. The more water left in the blood, the higher the blood pressure.

Several hormonal cycles give the kidney feedback. While hemodialysis systems do not have the ability to decode these hormonal signals, the real problem is that artificial filtration methods are not precise enough to respond to such signals. Semi-permeable membranes cannot adjust the diffusion rate of particular solutes instantly – only through methods previously discussed.

An obvious alternative is to use electronic sensors to provide feedback. However, while more advanced sensors may be available (perhaps to measure urea concentration in real-time) there is

little a system with a semi-permeable membrane can do with such information. If the system uses an alternative form of filtering, however, sensor complexity could become a relevant issue.

### 3.6 Concept formation

These strategies can now be used to develop working principles for an artificial human kidney. Two solutions are devised from two different strategies: a bio-inspired design that leverages strategies from the human kidney; and a traditional (yet portable) hemodialysis system is conceptualized.

#### 3.6.1 A bio-inspired renal replacement therapy

The two primary solution principles chosen for use in the bio-inspired renal replacement system are ultrafiltration-based separation followed by electrophoresis-based separation. Thus, the functions in the kidney function structure from Figure 3-12 can be replaced by specific working principles (from Section 3.5.2), as displayed in Figure 3-14.

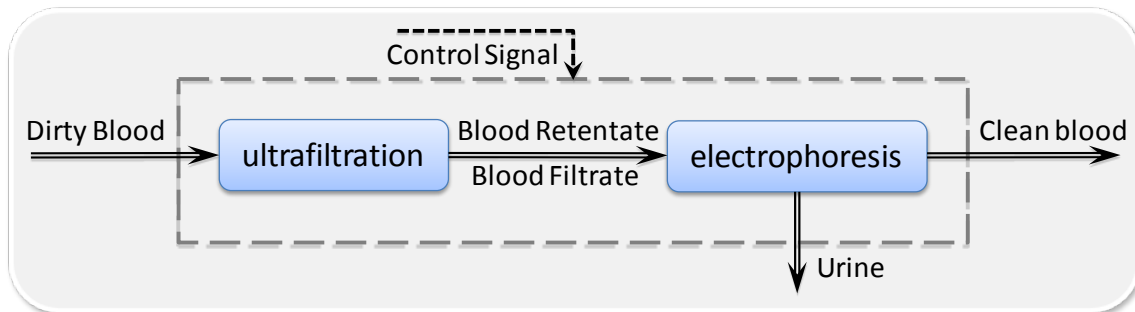


**Figure 3-14. Specific working principles for a renal replacement therapy concept.**

Of the five different functions of a renal replacement therapy identified in Section 3.5.1, this concept will use electrophoresis and ultrafiltration as its filtration method, AC power as its power input (although further improvements could certainly allow it to be battery powered), a rotary pump to increase the fluid pressures, waste will be disposed of, and sensors will be used to control signals.

Two different filtration methods are used because this concept mimics the behavior of the kidney, which uses a multistage filtration method. Table 3-3 summarizes the working principles used in this concept.

**Table 3-3. Morphological chart for bioinspired concept.**

	<b>Filtration</b>	<b>Power</b>	<b>Pressure</b>	<b>Waste</b>	<b>Signals</b>
<b>Bioinspired Device</b>	electrophoresis and ultra-filtration	AC power	rotary pump	disposed of	electronic sensors

The work done in Section 3.3 is leveraged to develop a system-level design of an RRT that mimics the behavior of a human kidney, as shown in Figure 3-15. Blood is removed from the body and then the plasma is separated from the blood via ultrafiltration. Electrophoresis-based separation principles are applied to the plasma to remove the unwanted solutes, while the remaining plasma is recombined with the retentate. Waste is collected in a reservoir, while power is supplied from a wall socket and a rotary pump provides the needed pressure increase.

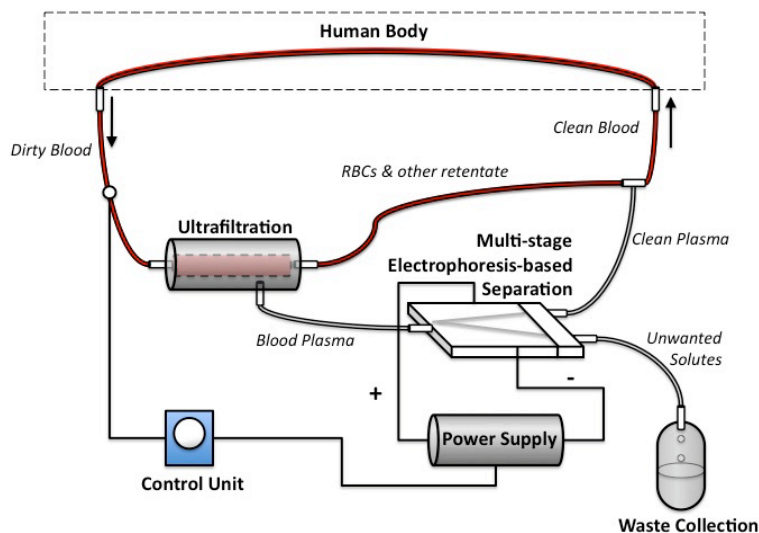


**Figure 3-15. A bio-inspired renal replacement therapy (RRT) concept.**

This system behaves in a similar manner to the human kidney. Just as the glomerulus separates all solutes – good and bad – from the blood, the filter in this setup acts in the same manner. And just as the proximal tubule, distal tubule, loop of Henle, and collecting duct absorb, excrete and secrete solutes; the stage-based electrophoresis correctly adjusts the solute concentrations in the blood.

Based on the working principles in Figure 3-14, the concept displayed in Figure 3-15 is developed.

### 3.6.2 A portable traditional hemodialysis system

A more technologically safe path can be followed by attempting to modify a current hemodialysis system to make it more portable. This would use traditional solution principles (diffusion via a semi-permeable membrane) but would focus on how the system could be optimized with respect to portability. Table 3-4 summarizes the different working principles (examined in Section 3.5.2) used in this concept.

**Table 3-4. Morphological chart for portable hemodialysis system.**

	<b>Filtration</b>	<b>Power</b>	<b>Pressure</b>	<b>Waste</b>	<b>Signals</b>
<b>Bioinspired Device</b>	membrane	battery	rotary pump	stored	electronic sensors

As has been previously explained, any dialysis treatment that is more regular in nature is a more healthy treatment for the patient. Clinical hemodialysis dialyzes a patient every other day, allowing for extreme urea and solute build-up in the blood – which eventually causes long-term health problems. If traditional hemodialysis could be modified to be more portable (and could therefore be used more regularly), a patient’s health could be improved without the need for the development of far-reaching new technologies.

This concept will only modify traditional dialysis as necessary to make it more portable. While many exciting advances in membranes and hemodialysis are being developed around the world, a

stable technology is best suited for the rigors of the transformation to a wearable configuration. The traditional idea of a membrane, pumps, and sensors will be retained while their size and weight is reduced to allow for the most portable configuration.

A requirements list for a renal replacement device has already been formulated in Section 3.4.

However, this list was not specific to a portable hemodialysis device. The previous requirements list should be augmented with additional requirements to satisfy the need for a portable system.

#### 3.6.2.1 Augmented requirements list for a portable hemodialysis device

In addition to the requirements listed in Section 3.4, the following requirements are added to aid in the design of a portable renal replacement system:

1. The device should be light.

*Defining a threshold for portability is difficult. Ten kilograms (22 lbs.) is chosen as a reference value for initial consideration. As concepts are explored in Chapter 4, the ratio of their performance to their weight will give a more accurate assessment of a concept.*

2. The device remains independent during dialysis.

*The previous requirement set the weight limit of this device, which is strongly tied to patient mobility, but this requirement seeks to address another issue of mobility – connectivity. Even if a device is developed that is very light, if it requires that the patient remain tethered to a wall outlet or another machine, than portability has been lost.*

3. The device is of a reasonable size.

*Now that the device is light and independent, it needs to be small enough to be portable. Like weight, this requirement does not have an exact value, but consideration needs to be given to its size if the device is either wearable or portable.*

This augmented requirements list will be used as a reference in Section 3.7.2 to help shape a concept when considering the working principles of Section 3.5.2.

### **3.7 Comparison and discussion of performance**

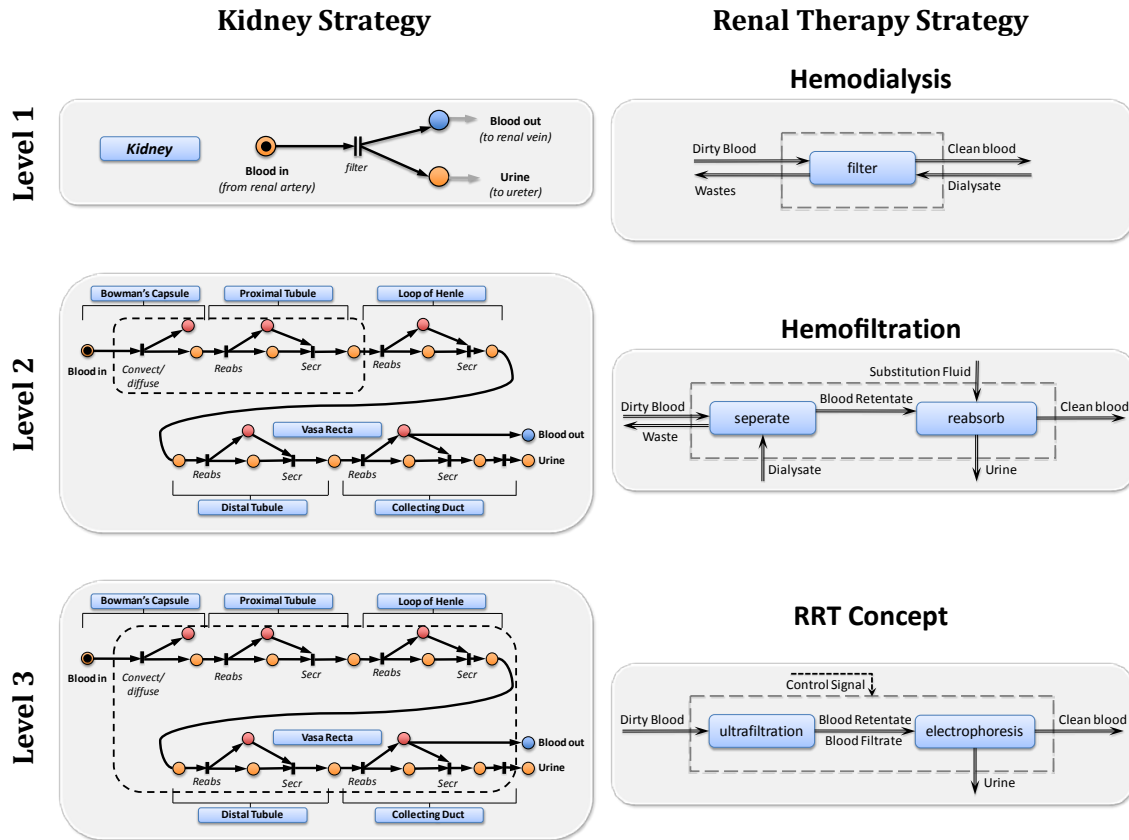
After the analysis presented in this chapter, two primary concepts have been developed: a more portable hemodialysis system, and a bio-inspired renal replacement therapy.

#### **3.7.1 A bio-inspired hemodialysis system**

One goal of this exploration was to design a renal replacement therapy that more closely mimics the waste removal strategy of the kidney. This comparison is summarized in Table 3-5 (referencing Figure 3-11). In Section 3.3, hemodialysis and hemodiafiltration were compared based on their behavioral similarity to the kidney. Hemodialysis can be seen as similar to the first level of behavior of the human kidney, which is simply filtration of the blood.

Hemodiafiltration, on the other hand, possesses a deeper level of behavioral similarity by first filtering most of the substances from the blood, and then replacing the needed substances using a substitution fluid. Although this method is more similar to the actual behavior of the kidney than hemodialysis, it still lacks in allowing regulation of the reabsorbed solutes. In the kidney, needed substances are regulated through multiple steps of secretion and reabsorption throughout the nephron. The RRT concept developed in Section 3.6.1 allows for continuous regulation of the needed solutes using a multi-stage electrophoresis system.

Table 3-5. Renal replacement therapy comparison.



The question now becomes, “What type of advantage would this RRT concept have over existing renal therapies?” As this is just a research concept, the performance of the system can only be theorized. To get a true estimate of performance, many years of development and trials are needed. However, the RRT concept presented in Figure 3-15 has several theorized advantages over the current renal therapies, including:

1. selectivity in filtration,
2. two-stage processing, and
3. continuous solute regulation.

One of the key advantages of the RRT concept is its ability to reabsorb selectively molecules. There are two obvious ways to filter out individual molecules: by size or by charge. Size selectivity is limited by the manufacturing capabilities of current membrane technologies. In order to filter selectively by charge, a membrane must be made with the exact pore size of the selected molecule. Today's technology is currently not capable of such precision manufacturing (pore sizes are around 15  $\mu\text{m}$  in size). Even if this were possible, the membrane would still allow any molecule smaller than this cutoff point through the membrane. Charge selectivity, on the other hand, allows filtration of molecules by charge. The strength of the filter is defined by the electric field and the resolution of the charges of the molecules. Thus, the electrophoresis-based reabsorption strategy allows individual molecules to be selectively reabsorbed, which is not currently feasible with current membrane-based technologies.

Another key advantage of the RRT concept is the two-stage solute processing. In the RRT concept, ultrafiltration is used to separate all of the substances from the blood and multi-stage electrophoresis is used to reabsorb selectively the needed substances. It is believed that it is much more efficient to remove all the substances from the blood and selectively reabsorb the needed substances than to try to remove only selected waste from the blood in a "one shot" fashion, as is done in current dialysis technologies.

In addition, the electrophoresis-based separation process in the RRT concept allows for continuous solute regulation. In the RRT concept, solute regulation can be performed on a continuous basis, as opposed to intermittently when using a replacement fluid in hemodiafiltration. A continuous-based therapy will help to increase the hemodynamic stability and biocompatibility of the treatment.

### **3.7.2 A portable traditional hemodialysis system**

There are many ways that traditional hemodialysis can be improved. Improvements can be categorized into two main categories: effectiveness and experience. Today's hemodialysis is reasonably effective but with a poor experience. The survival rate for patients on hemodialysis is approximately 35% after five years of treatment (Dijk & Jager, 2001). In those five years, patients are tethered to a machine twelve hours per week. Improvements in hemodialysis can seek to increase life expectancy or to make the dialysis experience less demanding.

However, these seemingly independent goals actually converge: it has been shown that one of the reasons for patient mortality on hemodialysis is its intervallic nature (Francisco, 2006). By simply performing hemodialysis more often, many of the negative symptoms associated with hemodialysis improve (Locatelli & Buoncristiani, 2005). However, there is a realistic limitation to daily or perhaps continuous dialysis: patients cannot be expected to remain attached to a hemodialysis machine so often.

While there are many novel ways to filter blood and achieve artificial renal behavior (Section 3.5.2), current hemodialysis technology might be best suited for portability. The augmented requirements list of Section 3.6.2.1 outlines the expectations of a portable system. These requirements could be met, but a more thorough investigation of current hemodialysis technology is needed. Chapter 4 serves as a thorough investigation of the behavior of a hemodialysis system in an attempt to determine hemodialysis's feasibility as a portable system.

Developing a more portable hemodialysis process will lead towards the realization of continuous hemodialysis. Unlike developments in dialyzer technology (like bio-artificial membranes), developing a more portable artificial kidney has the advantage to improve both effectiveness and

experience. Further, individual advances in hemodialysis technologies can be incorporated into a working portable design.

Developing a more portable artificial kidney also brings hemodialysis patients closer to the realization of an implanted artificial kidney. Currently, all system processes associated with hemodialysis are performed external to the body inside a hemodialysis machine. By incrementally bringing the hemodialysis process away from external machines and towards the human body, we are opening doors to implantable research. Once items are adapted from their large, machine-based manifestations to wearable sizes, further research can bring them inside the body.

### **3.8 Conclusion**

Two concepts were developed in this chapter – one that mimics the functionality of the human kidney, and one that seeks to shrink traditional components. While it would be ideal to pursue both concepts, a more realistic approach is to successfully develop the traditional concept first and then work on a more radical renal replacement concept.

The research question this chapter focused on was:

*Can a renal replacement therapy be developed that provides an alternative filtration method while matching or exceeding current hemodialysis performance?*

This chapter has seen the development of two concepts – one derived from the function of the kidney, and one that seeks to shrink current hemodialysis. The bio-inspired design does provide an alternative filtration method (electrophoresis), but can only provide better hemodialysis performance in theory.

The theoretical performance increase of the bio-inspired concept can be attributed not to its exact separation method – electrophoresis – but rather to its exacting filtration specifications. The novelty of this concept lies in how it is designed to mimic the functionality of the human kidney and not in its implementation.

By pulling everything out of the blood and then returning only the needed solutes, it guarantees that harmful solutes will not build up in the blood over time – the primary problem associated with long-term hemodialysis.

However, because the bio-inspired concept requires clearing a technological hurdle that is beyond the scope of this thesis, further work will focus on improving traditional hemodialysis. Work towards improving traditional hemodialysis will give insight to renal replacement that will be invaluable if the bio-inspired concept is pursued in the future.

To that end, Chapter 4 will focus on the systematic modeling of a traditional hemodialysis system. The complex relationship between the flow rates and dialysis components will be examined in detail, and a Simulink model will be created to simulate all functions of a hemodialysis system.

## CHAPTER FOUR

### CREATION OF A SYSTEM MODEL

The challenge of designing a portable hemodialysis system is to modify a traditional system's components so that they are small enough to be a part of a portable system. As discussed in the previous chapter, the largest hurdle towards this goal is managing the large volume of dialysate involved with the use of a counter-flow dialyzer. In order to create the most portable system, the volume of dialysate must be minimized – effectively creating a system with the slowest possible dialysate flow rate.

Creating an effective system with the slowest possible dialysate flow rate leads to important design considerations throughout the entire system. Variables such as blood flow rate, clearance, and dialysate flow rate are all related – one cannot simply slow the dialysate and maintain an optimum clearance of undesirable solutes. This chapter will explore all the design considerations of a slowed dialysate flow rate, among other considerations.

#### **4.1 System model objectives**

While two concepts were developed in Chapter 3, it would be more realistic to pursue the traditional hemodialysis-based concept first to develop competency in the field, and then pursue a more advanced concept in the future. Because pursuing both concepts would be well beyond the expectations of a thesis, this work is devoted to the design of a portable hemodialysis system.

Specifically, a system model will first be created that thoroughly covers all aspects of traditional hemodialysis, in order to determine how best it can be minimized for portability. The following subsections describe the exact objectives of this system model.

#### **4.1.1 Identify parameters that have the largest impact on system weight**

As has already been discussed in Chapter 3, the volume of dialysate is the largest obstacle towards the development of a portable hemodialysis device. Chapter 3 discussed different ideas towards limiting the use of dialysate, but a system model is needed to test each concept thoroughly. For example, if dialysate is recirculated through the dialyzer (as discussed in Section 3.2.2), how much longer would the dialyzer need to run in order to adequately treat the patient? Is it even possible to develop a feasible system that relies on dialysate recirculation? Different combinations of dialysate flow rates and treatment schedules can be examined.

#### **4.1.2 Determine the relationship between blood and dialysate flow rate**

Solutes are removed from the blood via a concentration gradient in a counterflow dialyzer. The equations that govern this solute transport (Section 4.3) are complex and do not produce a clear relationship between the two flow rates. Modern published literature explains the rule-of-thumb among designers is that the dialysate flow rate should be twice the blood flow rate (Ward & Leypoldt, 2001), but a portable hemodialysis system uses blood flow rates far below clinical rates. A system model should be able to determine which dialysate flow rates are best for a portable hemodialysis system.

#### **4.1.3 Determine feasible treatment schedules of a portable system**

Once the dialysis process is accurately modeled, the model should then account for the day-to-day changes in a patient's urea levels to see if the proposed concept is dialyzing enough to maintain homeostasis. For example, if a concept requires dialysis to run for an inadequate amount of time, the patient's average daily urea levels will rise, presumably to an unhealthy level. When the patient's natural urea generation rate matches the amount of urea removed each day via hemodialysis, their condition is considered steady state. This concept is explored in Section 5.3.

## 4.2 Hemodialysis components

In a typical hemodialysis system (Figure 4-1), blood leaves the body through an implanted port, flows through medical tubing, is passed through a pump to raise its pressure, enters the blood compartment of the dialyzer, and then is returned to the body at approximately the same pressure at which it was drawn from the body. Heparin is added as an anti-coagulant.

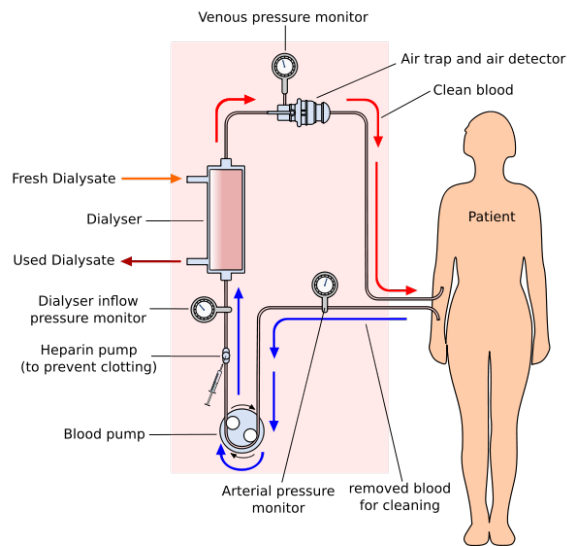


Figure 4-1. A typical hemodialysis circuit (YassineMrabet, 2008).

This entire process is listed as a flow chart in Figure 4-2. The blood loop is kept as simple and clean as possible to minimize infections and complications.

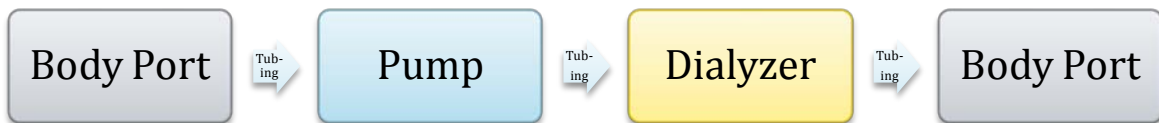


Figure 4-2. The flow path of the blood during hemodialysis.

The dialysate loop is similar. Dialysate is drawn from a reservoir via a pump, and is then pumped through a dialyzer counter to the flow of the blood. After the dialysate has run through the dialyzer, it is disposed.

A more detailed look at the primary components in a traditional hemodialysis system is provided next.

#### 4.2.1 Dialyzer

Dialyzers take the shape of long cylinders, typically 16 to 25 cm in length and 3 to 5 cm in diameter. They house a collection (typically 10,000 to 15,000) of porous hollow tubules, with spacing between the tubules, as shown in Figure 4-3. The blood flows through the tubules, while the dialysate flows countercurrent in the spacing between the tubules. Solutes are driven by a concentration gradient through the pores of the membrane from one fluid to another.

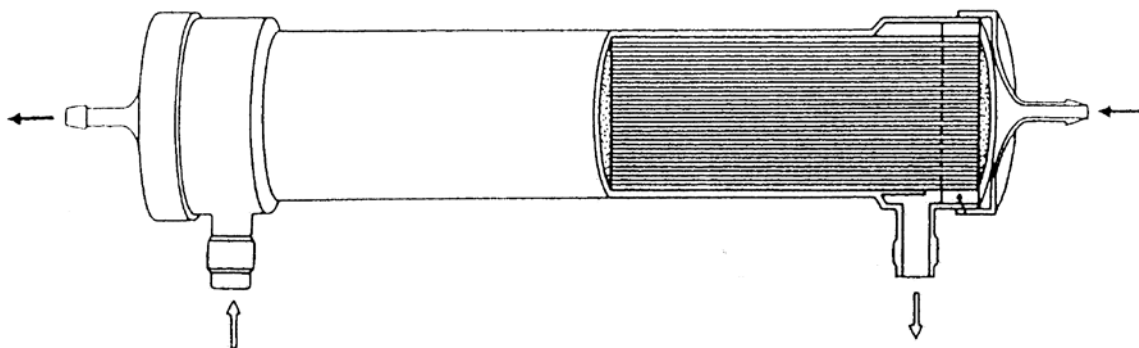


**Figure 4-3. A typical dialyzer. The blood enters on the right and travels through thousands of tiny tubules before exiting on the left. The dialysate enters on the bottom left, fills the spacing around the tubules and exits on the bottom right.**

The most important characteristic of dialyzers is their overall mass transfer coefficient ( $K_0$ ), a measure of how effective a dialyzer is at transporting a particular solute across a fixed area of its membrane. In turn,  $K_0$  (in conjunction with the surface area ( $A$ ) and the flow rates) can be used to calculate the clearance ( $K$ ), the rate at which blood is cleaned.

Typically, dialyzers are fixed in diameter, so the longer the dialyzer, the more surface area it has and therefore higher clearance rate. Membrane material typically does not vary between individual models from the same product line from a manufacturer, so increasing the dialyzer length from 16 to 20 to 24 cm brings about a linear increase in surface area.

#### **4.2.2 Dialysate**

Dialysate is the fluid that runs counter to the blood through the dialyzer. Because mass transport is based on a concentration gradient, the composition of the dialysate is very important in the removal of solutes from the blood.

Substances that are to be removed have little presence in the dialysate, while substances that are to be left in the blood are present in dialysate. In between those two extremes are the substances that must be carefully balanced – the blood is not to be entirely cleaned of their presence, so the dialysate still contains a quantity of that particular substance. The substances that commonly appear in commercial dialysate solutions are sodium, potassium, calcium, magnesium, chloride, acetate, bicarbonate, and glucose (Ronco, Fabris, & Feriani, 1996).

#### **4.3 Fundamentals of dialyzer physics**

Perhaps the most important element of any hemodialysis system is the dialyzer. The dialyzer has the most direct impact on the overall solute clearance of the system, while other components can only affect clearance rates indirectly.

Understanding the physics behind membrane clearance will allow the primary dialyzer characteristics – size, flow rates – to be integrated into a system model. First, the basics of membrane physics must be explored.

### 4.3.1 Fick's Law

The transportation of solutes across a semi-permeable membrane is measured by their flux ( $J$ ), which is a function of the concentration difference ( $dc$ ), separation distance, ( $dx$ ), area of diffusion ( $A$ ), and the diffusion coefficient ( $D$ ). The diffusion coefficient is a constant value for an individual solute, is dependent only on temperature, and is measured in  $\text{cm}^2/\text{s}$ . In 1855, Adolf Fick, a German physiologist who created the first working contact lens, derived an equation that described the diffusion of a gas across a membrane:

$$J = -DA \frac{dc}{dx} \quad (4-1)$$

Fick's Law describes one-dimensional concentration flux. In order to develop the parameters for the semi permeable membrane inside a dialyzer, it is necessary to make simplifications and assumptions regarding Fick's Law with regard to common properties of semi permeable membranes.

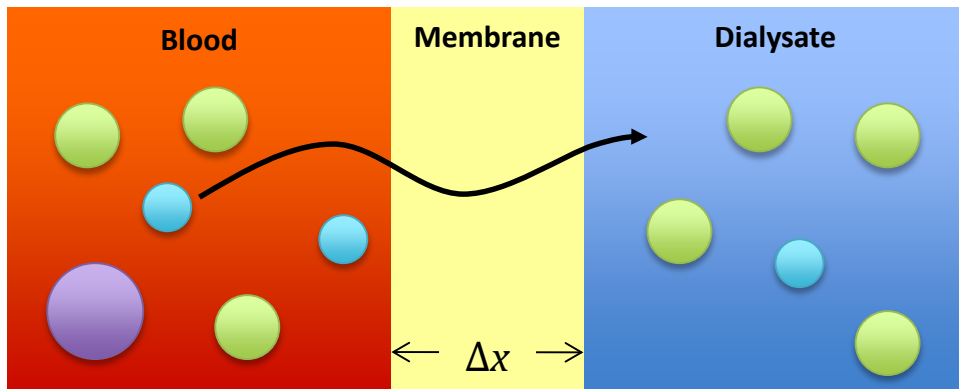


**Figure 4-4.** The number of solutes passing through the membrane depends on the thickness of the membrane ( $\Delta x$ ), the ratio of the number of solutes on each side ( $\Delta C$ ), the size of the membrane ( $A$ ), and the diffusivity constant ( $D$ ).

First one assumes that the membrane thickness is constant the entire length of the membrane, and from tubule to tubule. This simplification highlights the primary factors of mass transport in

membrane diffusion: the total concentration difference of the two fluids ( $\Delta C$ ), and the total contact area ( $A$ ). Because the diffusion coefficient ( $D$ ) only varies with temperature for a given solute, it can safely be left out (Sargent & Gotch, 1989).

#### 4.3.2 Overall mass transfer coefficient

The next consideration to be made is how well a particular semi-permeable membrane can transport solutes for a given concentration difference. To compare two membranes, one might subject equal-sized (same area) samples of each to the same concentration difference. The amount of solutes that passed through each membrane in a given time could then be compared.

The membrane that passed more solutes would have a higher overall mass transfer coefficient ( $K_0$ ). The overall mass transfer coefficient is the ratio of the unit mass flux (mass flux per unit of area) to the concentration gradient, stated in Equation 4-2. While  $K_0$  is a function of the concentration gradient, it can be considered a constant for the gradients experienced in dialysis (Sargent & Gotch, 1989).

$$K_0 = \frac{\text{flux per unit area}}{\text{concentration difference}} = \frac{J/A}{-\Delta C} \quad (4-2)$$

Individual membranes have a fixed  $K_0$  value for each solute. A membrane with a higher  $K_0$  value is capable of moving a larger number of that particular solute through its pores at a given concentration. The concentration difference can be equated as the driving force in diffusion and is measured in units of cm/min.

The mass transfer coefficient ( $K_0$ ) is a common measure of a membrane's effectiveness. When multiplied by the membrane's total area ( $A$ ) and the concentration difference ( $\Delta C$ ), the mass transfer rate is known:

$$K_0 \times A \times -\Delta C = J \quad (4-3)$$

A unit balance for this equation can be shown:

$$\frac{\text{cm}}{\text{min}} \times \text{cm}^2 \times \frac{\text{g}}{\text{cm}^3} = \frac{\text{g}}{\text{min}}$$

Because both the mass transfer coefficient ( $K_0$ ) and the effective surface area ( $A$ ) are fixed for a particular dialyzer, manufacturers often lump  $K_0A$  together and publish the  $K_0A$  specifically for urea (a primary target of dialysis) as a part of the membrane specifications.

#### 4.3.3 The concentration difference

In a dialyzer, four concentrations are important for each substance of interest: the input blood concentration ( $C_{Bi}$ ), the input dialysate concentration ( $C_{Di}$ ), the output blood concentration ( $C_{Bo}$ ) and the output dialysate concentration ( $C_{Do}$ ). In a counter-flow dialyzer, the input concentration difference ( $\Delta C_i$ ) is the difference between the input blood concentration and the output dialysate concentration:

$$\Delta C_i = C_{Bi} - C_{Do} \quad (4-4)$$

Alternatively, the output concentration difference ( $\Delta C_o$ ) is the difference between the output blood concentration and the input dialysate concentration:

$$\Delta C_o = C_{Bo} - C_{Di} \quad (4-5)$$

The best way to determine a single overall concentration difference from the input and output concentrations is to use a log-mean concentration difference:

$$\Delta C_{\log\text{-mean}} = \frac{\Delta C_i - \Delta C_o}{\ln[\Delta C_i / \Delta C_o]} = \frac{(C_{Bi} - C_{Do}) - (C_{Bo} - C_{Di})}{\ln [(C_{Bi} - C_{Do}) / (C_{Bo} - C_{Di})]} \quad (4-6)$$

The problem with this definition is that it requires the output concentrations of the blood and dialysate – the exact variables that need to be estimated in a system model. Fortunately, the concentration difference between the input blood and dialysate streams ( $C_{Bi}$  and  $C_{Di}$ ) may be used instead of the log-mean concentration difference without any significant loss in accuracy (Sargent & Gotch, 1989):

$$\Delta C \approx C_{Bi} - C_{Di} \quad (4-7)$$

#### 4.3.4 Dialysance

While the overall mass transfer coefficient ( $K_0$ ) was derived from the concept of comparing two different membranes, the dialysance ( $D$ ) can be derived from the need to compare different blood and dialysate flow configurations on the same membrane. The diffusive dialysance is the magnitude of flux to be expected per unit of concentration driving force (Sargent & Gotch, 1989). Diffusive dialysance is defined as:

$$D = \frac{\text{concentration change of blood}}{\text{concentration gradient between blood and dialysate}} \quad (4-8)$$

The dialysance ( $D$ ) will remain constant throughout a hemodialysis session, even as the concentration difference between the blood and dialysate decreases (as the blood becomes “cleaner” and the dialysate remains at a lower concentration), the amount of solutes leaving the blood will decrease. In terms of system variables, the dialysance can be defined as:

$$D = \frac{Q_B(C_{Bi} - C_{Bo})}{C_{Bi} - C_{Di}} = \frac{Q_D(C_{Do} - C_{Di})}{C_{Bi} - C_{Di}} \quad (4-9)$$

It should be noted that this definition of dialysance uses the simplified concentration gradient ( $C_{Bi} - C_{Di}$ ) instead of the log-mean concentration difference.

Most significantly, a value for a hemodialysis configuration’s dialysance ( $D$ ) can be derived without the need for concentration values. Just the blood flow rate ( $Q_B$ ), the dialysate flow rate ( $Q_D$ ), and the membrane properties ( $K_0A$ ) are needed to determine the dialysance ( $D$ ). This can be shown in the following equations.

First, the mass flowing in and out of a dialyzer must be equal:

$$Q_B(C_{Bi} - C_{Bo}) = Q_D(C_{Do} - C_{Di}) \quad (4-10)$$

Dividing both sides of Equation 4-10 by the simplified concentration gradient ( $C_{Bi} - C_{Di}$ ):

$$\frac{Q_B(C_{Bi} - C_{Bo})}{C_{Bi} - C_{Di}} = \frac{Q_D(C_{Do} - C_{Di})}{C_{Bi} - C_{Di}} \quad (4-11)$$

Defining the flux as the product of the blood flow rate and the concentration change of the blood through the dialyzer:

$$J = Q_B(C_{Bi} - C_{Bo}) \quad (4-12)$$

The unit balance for this is shown:

$$\frac{\text{mg}}{\text{min}} = \frac{\text{mL}}{\text{min}} \times \frac{\text{mg}}{\text{mL}}$$

Substituting Equation 4-9 and 4-12 into Equation 4-11:

$$\frac{J}{C_{Bi} - C_{Di}} = D \quad (4-13)$$

Therefore:

$$J = D(C_{Bi} - C_{Di}) \quad (4-14)$$

Substituting the log-mean concentration difference (Equation 4-6) into Equation 4-3:

$$J = K_0 A \left[ \frac{(C_{Bi} - C_{Do}) - (C_{Bo} - C_{Di})}{\ln[(C_{Bi} - C_{Do}) / (C_{Bo} - C_{Di})]} \right] \quad (4-15)$$

Setting Equation 4-14 and 4-15 equal to each other:

$$D(C_{Bi} - C_{Di}) = K_0 A \left[ \frac{(C_{Bi} - C_{Do}) - (C_{Bo} - C_{Di})}{\ln[(C_{Bi} - C_{Do}) / (C_{Bo} - C_{Di})]} \right] \quad (4-16)$$

Rearranging the previous definitions for dialysance (Equation 4-9):

$$C_{Bi} - C_{Do} = (C_{Bi} - C_{Di}) \left( 1 - \frac{D}{Q_D} \right) \quad (4-17)$$

$$C_{Bo} - C_{Di} = (C_{Bi} - C_{Di}) \left( 1 - \frac{D}{Q_B} \right) \quad (4-18)$$

Substituting these values into values into Equation 4-16 yields:

$$\begin{aligned}
 & D(C_{Bi} - C_{Di}) \\
 &= K_0A \left[ \frac{\left( (C_{Bi} - C_{Di}) \left(1 - \frac{D}{Q_D}\right) \right) - \left( (C_{Bi} - C_{Di}) \left(1 - \frac{D}{Q_B}\right) \right)}{\ln \left[ \frac{\left( (C_{Bi} - C_{Di}) \left(1 - \frac{D}{Q_D}\right) \right)}{\left( (C_{Bi} - C_{Di}) \left(1 - \frac{D}{Q_B}\right) \right)} \right]} \right] \quad (4-19)
 \end{aligned}$$

Simplifying:

$$\frac{K_0A(1 - Q_B/Q_D)}{Q_B} = \ln \frac{1 - D/Q_D}{1 - D/Q_B} \quad (4-20)$$

Solving for the dialysance ( $D$ ):

$$D = \frac{e^{\frac{K_0A(1 - \frac{Q_B}{Q_D})}{Q_B}} - 1}{\frac{K_0A(1 - \frac{Q_B}{Q_D})}{Q_B} - \frac{1}{Q_D}} \quad (4-21)$$

The power of this equation is it allows the output blood and dialysate concentrations ( $C_{Bo}$  and  $C_{Do}$ ) to be calculated knowing only the blood flow rate ( $Q_B$ ), the dialysate flow rate ( $Q_D$ ), the membrane properties ( $K_0A$ ), and the input concentrations ( $C_{Bi}$  and  $C_{Di}$ ). This will be fully explored in Section 4.7 as an overall system model is developed.

In the special case when the input dialysate concentration is zero (as it is for most hemodialysis scenarios, this assumes that the dialyzer is run in “single-pass” mode), the previous equation can be restated as the Michaels equation (Ward & Leyboldt, 2001), where the overall clearance is solved:

$$K = Q_B \left[ \frac{e^{\frac{K_0 A (1 - \frac{Q_B}{Q_D})}{Q_B}} - 1}{e^{\frac{K_0 A (1 - \frac{Q_B}{Q_D})}{Q_B}} - \frac{Q_B}{Q_D}} \right] \quad (4-22)$$

#### 4.4 Dialyzer design

The membrane can be viewed as providing a resistance to solute diffusion, similar to how wires provide electrical resistance in current flow. Recalling the equation for the total flux across the dialyzer:

$$J = -K_0 A \Delta C \quad (4-23)$$

Rearranging (Sargent & Gotch, 1989):

$$\text{unit flux} = \frac{J}{A} = \frac{-\Delta C}{1/K_0} \quad (4-24)$$

The inverse of the mass transfer coefficient ( $K_0$ ) can therefore be seen as resistance to mass flux:

$$R_0 = \frac{1}{K_0} \quad (4-25)$$

The more resistance the membrane provides solute diffusion, the less solutes will be able to pass in a given area.

Specifically, there are three resistances in membrane dialysis (Sargent & Gotch, 1989): resistance at the blood-membrane barrier ( $R_B$ ), the resistance of traveling through the membrane ( $R_M$ ), and the

resistance at the membrane-dialysate barrier ( $R_D$ ). Because the solutes traverse each of these resistances sequentially, the total resistance ( $R_0$ ) is the sum of all three:

$$R_0 = R_B + R_M + R_D \quad (4-26)$$

The only way to increase mass transfer is to decrease the resistances the solutes are subjected to, or increase the driving force. Because the driving force is the concentration difference between the blood and dialysate, there is little room for improvement: one is not free to increase the concentration of solutes already in the blood. This leaves decreasing the membrane-resistance as the primary focus.

Knowing how these resistances are accounted for in mass transfer, one can evaluate different forms of membrane configurations for dialysis. While  $R_M$  is a function of the physical properties of the membrane (thickness, material, pore geometry), both  $R_B$  and  $R_D$  will depend on the fluid flow at the surface of the membrane – which can vary greatly with the different physical configurations of membranes.

There are two primary shapes dialyzers could come in: flat-plate designs, where membrane layers are sandwiched between counter-current fluid layers, or shell-and-tube designs where the blood flows through thousands of tiny tubes in a counter-flow of dialysate fluid. Studies in the 1970s showed that the membrane in flat-plate membranes accounted for 40–70% of the total resistance, while the membranes in shell-and-tube dialyzers accounted for around 90% of the total resistance (Sargent & Gotch, 1989). By reducing the resistance of the fluid flows to near-negligible levels in shell-and-tube designs, the flat-plate design was abandoned in favor of researching better membranes – to reduce the membrane resistance, now the primary resistance in dialyzers.

## **4.5 Modeling pump power requirements**

In the case of designing a hemodialysis system, there are more important factors than the flow characteristics. The most important concern is to maintain a sterile flow path for the blood and dialysate. Any pump used in the system must not allow harmful agents contact with the blood or dialysate, and it must maintain its sterility throughout its life.

### **4.5.1 Overview of different types of pumps**

There are two primary types of pumps: centrifugal pumps and positive displacement pumps. Centrifugal pumps are the most common, because many feel they provide the best mechanical reliability. However, positive displacement pumps are preferred over centrifugal pumps under certain circumstances. Positive displacement pumps are traditionally preferred in industry when high pressure is coupled with low flow.

In the case of designing a hemodialysis system, there are more important factors than the flow characteristics: the most important concern is to maintain a sterile flow path for the blood. Any pump used in the system must not expose harmful agents (such as bacteria or viruses) to the blood or dialysate, and it must maintain this sterility. Only one type of pump can easily provide this, and performs adequately at the system's flow characteristics: a peristaltic pump.

Peristaltic pumps are a special kind of rotary positive-displacement pumps. Moving rollers squeeze a flexible tube, providing for a pressure and velocity increase. Because the fluid only is exposed to the flexible tubing, and not the moving parts of the pump, it is very easy to maintain sterility. The pump life is also adequate – only the flexible tubing needs to be replaced on a regular interval. Additionally, peristaltic pumps are noted for their superior metering abilities.

#### 4.5.2 Estimating the pressure drop across the dialyzer

In the interest of designing a wearable artificial kidney, the two most important variables in pump selection and design are its size and its needed voltage. Unfortunately, there is no clear-cut way to relate pump size, power, and output. However, there are two very different ways to analyze peristaltic pumps to aid in the design of a wearable artificial kidney: an analysis of the fluid physics can provide a rough estimate to the power requirements (but cannot account for losses), or a survey of currently available peristaltic pumps could provide an average correlation between power, size, and weight.

The first thing that must be calculated regarding the pump is the pressure rise it must provide in the hemodialysis circuit. In traditional hemodialysis, blood enters the circuit at about 120 mmHg (15.999 kPa) from the arterial side (systolic pressure), and reenters the blood stream at the venous side (diastolic pressure) around 80 mmHg (10.666 kPa) (Moffett, Moffett, & Schauf, 1993). If a hemodialysis system is designed for regular home use, the blood will most likely be drawn from the venous side for safety reasons.

In order to calculate the pressure drop across the blood circuit, one must account for the three primary resistances: the resistance of the tubing from the vein to the dialyzer, the resistance of the dialyzer itself, and the resistance of the tubing from the dialyzer back into the vein. First, the resistances located inside the dialyzer will be examined.

As discussed in previous chapters, a hollow fiber dialyzer consists of thousands of small, hollow tubes. Blood enters the dialyzer; its flow is split by a baffle into thousands of tubules, and then rejoined by an exit baffle before leaving the dialyzer. To calculate the pressure drop across the dialyzer, the pressure drop across just one tubule can be analyzed.

First, it is necessary to collect the known parameters of the system. There are typically 10,000 tubules in a dialyzer, each with an inner diameter of about 300 microns (0.0003 m). A large dialyzer has a length of about 20 cm (0.20 m). The blood is thinned before entering the dialyzer, creating a relative blood viscosity of approximately four times that of water, at 37 °C (Moffett, Moffett, & Schauf, 1993).

Knowing these parameters, one can begin to apply them to the Navier-Stokes equations: specifically, the Hagen-Poiseuille equation dictating pressure driven flow through a circular cross-section:

$$Q = \frac{\pi R^4}{8\eta L} \Delta P \quad (4-27)$$

First we will test this equation at a typical hemodialysis flow rate of 300 mL/min ( $5 \times 10^{-6} \text{ m}^3/\text{s}$ ), which is  $5 \times 10^{-10} \text{ m}^3/\text{s}$  per tubule, if there are 10,000 tubules. Solving for the pressure drop:

$$5 \times 10^{-10} = \frac{3.1416 \times 0.0004^4}{8 \times 0.04 \times 0.20} \Delta P$$

This equation predicts a 15.1 mmHg pressure drop across a dialyzer under typical hemodialysis conditions. However, it is known that the pressure drop is closer to 20 mmHg in a shorter (0.16 m) dialyzer, leaving the model presented here off by about 33%.

This discrepancy can be accounted for by:

1. The resistance in the baffles used to divert the flow into the tubules, located at both ends of the dialyzer;
2. The non-uniform shape of the tubules; and

3. The Fahraeus-Lindquist effect (Polaschegg & Levin, 1996), which modifies the viscosity of the blood in small diameter pathways.

The Hagen-Poiseuille equation can be solved for various flow rates, dialyzer lengths, and tubule diameters in order to examine the effects various parameters have on the pressure drop of the dialyzer. Knowing the pressure drop of the dialyzer is an important step towards selecting a pump. Figure 4-5 shows the relationship between tubule size, flow rate, and pressure drop. Figure 4-6 shows the relationship between dialyzer size, flow rate, and pressure drop.

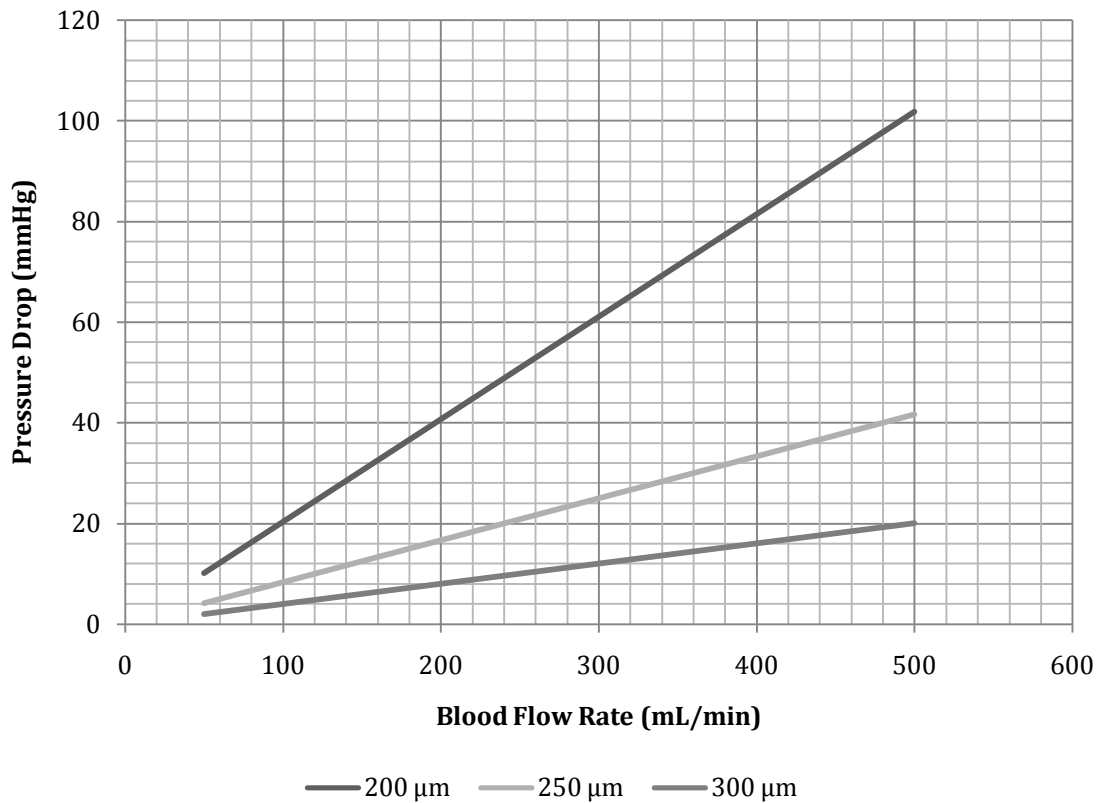
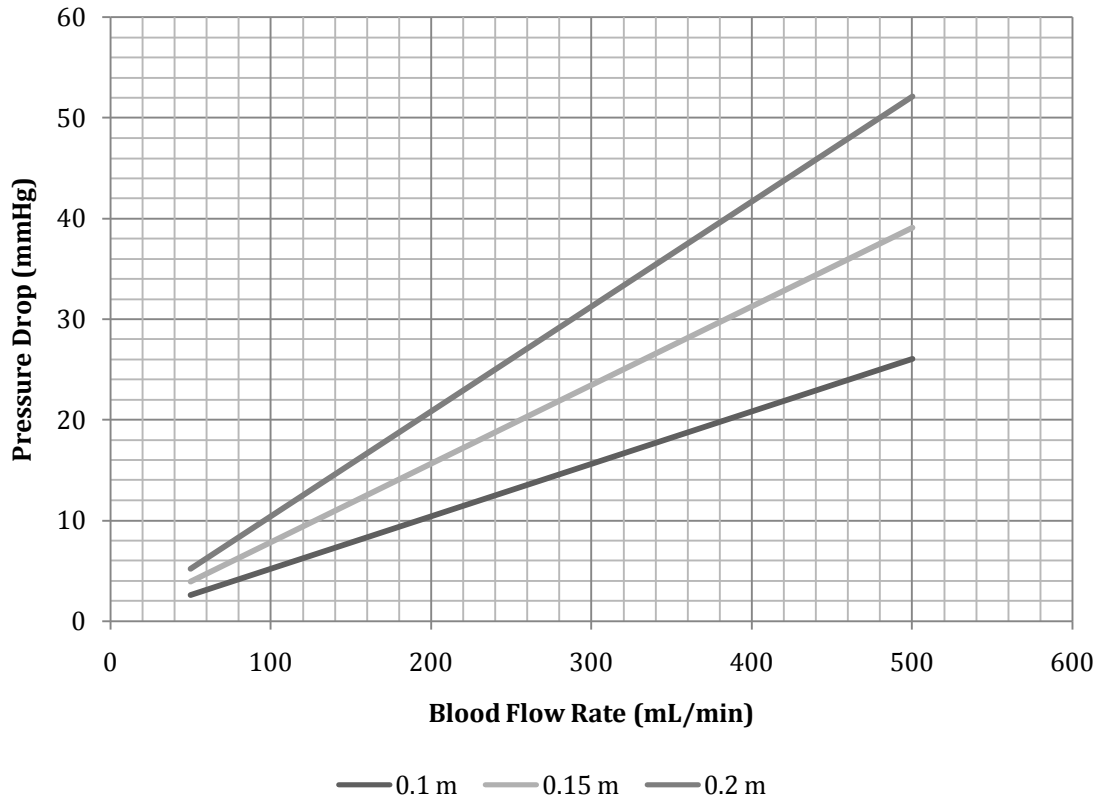


Figure 4-5. The expected pressure drop according to the Hagen-Poiseuille equation in 0.16 m length dialyzers of various tubule inner diameters.



**Figure 4-6. The expected pressure drop according to the Hagen-Poiseuille equation in tubules of 250  $\mu\text{m}$  in dialyzer of lengths of 0.1 m, 0.15 m, and 0.2 m at various flow rates.**

While a more detailed analysis could remedy the shortcomings of simply using the Hagen-Poiseuille equation to calculate the pressure drop in the dialyzer, it would only achieve results that confirm already-available data. Suzuki et al. (2001) already provides data for the pressure drop of a hollow fiber dialyzer at a variety of blood flow rates; this data can be used as a baseline for future considerations.

The Hagen-Poiseuille equation can also be solved for the flexible tubing connecting the dialyzer to the human vein. Assuming 1.0 m of tubing length, a 0.005 m inner diameter, a flow rate of 300 mL/min ( $5 \times 10^{-10} \text{ m}^3/\text{s}$ ), and a viscosity of 0.04 cp, the equation looks as follows:

$$5 \times 10^{-10} = \frac{3.1416 \times 0.0005^4}{8 \times 0.04 \times 1.0} \Delta P$$

This yields a pressure drop of 3.2 mmHg, a small value compared to the pressure drop associated with the dialyzer.

#### **4.5.3 Relating the pressure drop to pump power requirements**

The goal of this section is to integrate the pump variables into a larger system model. Already it has been shown how increasing dialyzer size (tubule inner diameter and length) increases the pressure that must be supplied by the pump. This is important because changing the dialyzer is a simple way to modify the clearance-performance of the system directly.

However, there are certain negative ramifications of a larger dialyzer, aside from the simple fact of increased physical size. A more powerful pump (and perhaps heavier) might be required to provide the needed pressure change if a larger dialyzer was selected. At this point, the flow rate, pressure change, and the specific gravity of the fluid are known. Hopefully this is enough information to relate those system variables to the power required by the pump. If the power required is known, the weight of the associated power source (batteries) can be integrated into the system model.

There are two types of power variables associated with positive displacement pumps. The fluid power is the power transmitted from the pump to the fluid. The brake power is the power transmitted to the pump, regardless of how much is imparted to the fluid. The differences between these two variables are the losses associated with the pump:

$$\text{Losses} = \text{Brake Power} - \text{Fluid Power} \quad (4-28)$$

Since the ultimate goal is to estimate the weight of the associated pump and batteries, we are interested primarily in brake power and not fluid power. However, the power imparted to the fluid is easily calculated by multiplying the flow rate and the output pressure:

$$\text{Fluid Power} = \text{Flow Rate} \times \text{Flow Pressure} \quad (4-29)$$

In a scenario we might expect to encounter in the development of a small portable hemodialysis system (100 mL/min flow rate and 100 mmHg output pressure), the fluid power is 0.0222 W:

$$\frac{1.667 \times 10^{-6} \text{ m}^3}{1 \text{ s}} \times \frac{13222 \text{ N}}{\text{m}^2} = \frac{0.0222 \text{ N} \cdot \text{m}}{1 \text{ s}} = 0.0222 \text{ W}$$

The losses associated with the positive displacement pump are manifested in the equation for its brake power:

$$\text{Brake Power} = \frac{\text{Flow Rate} \times \text{Pressure}}{\text{Pump Efficiency}} \quad (4-30)$$

At this point, this equation leaves us with two knowns and two unknowns. While the flow rate and pressure have already been calculated, the input power and the efficiency are both unknown. Usually one is known (for example, calculating the efficiency of a pump already in use), but if both are unknown, then significant modeling or estimation must be used to calculate the other. As a way to determine the input power required, specifications from currently available pumps could be

analyzed. While there are many different types of pumps available, only pumps with the following characteristics were analyzed:

1. Peristaltic positive-displacement pumps
2. Powered by a direct current
3. Operates in the 1–1000 mL/min flow rates
4. Single roller head
5. Less than 5 kg in weight

The goal is to select pumps that fall within the expected operating range of a portable hemodialysis system. Pumps that require alternating current are often not only too powerful and too large, but they operate at a very high voltage and current – making their brake power too high. Some pumps have multiple roller heads, which would obscure the relationship between the brake power and the fluid power.

One particular manufacturer, Omega, not only has a large selection of peristaltic pumps available in specifications already outlined, but they also provide detailed specifications of all their pumps. This allows for the calculation of the efficiency of their entire line of pumps. Table 4-1 lists select pumps available, and from the voltage, amperage, and flow rates provided by the manufacturer the calculated the power and efficiency of the individual pump.

**Table 4-1. Selected pump data (Omega).**

Model	Voltage (V)	Amperage (A)	Power (W)	Flow Rate (m <sup>3</sup> /s)	Efficiency
<b>FPU101</b>	12	0.37	4.44	$5 \times 10^{-8}$	0.02%
<b>FPU110</b>	12	0.75	9.00	$9.167 \times 10^{-7}$	0.14%
<b>FPU119</b>	12	1.20	14.4	$3.25 \times 10^{-6}$	0.30%
<b>FPU124</b>	12	2.20	26.4	$1.25 \times 10^{-5}$	0.63%

Every pump available from this manufacturer has an input voltage of 12 V. However, the amperage varies, so calculating the brake power is simple. Here is a sample calculation for the FPU110 pump:

$$12 \text{ V} \times 0.75 \text{ A} = 9.00 \text{ W}$$

Calculating the associated efficiency of the pump is also shown:

$$\frac{9.167 \times 10^{-7} \text{ m}^3/\text{s} \times 13332 \text{ Pa}}{9.00 \text{ W}} = 0.001358$$

This pump has a remarkably low efficiency. All pumps from this manufacturer have an input voltage of 12 V, while the amperage varies between 0.37 and 2.2 A. Together, these account for a considerable power requirement of 9 W. On the other hand, the output flow rate and pressure (13,332 Pa is equivalent to 100 mmHg, an estimate of the maximum pressure inside the dialysis circuit) translate to a mere 0.01222 W imparted to the fluid.

Typical peristaltic pump efficiencies are near 50%, but typical pumps also move much more than 55 mL/min of fluid. A brushless direct-current peristaltic pump used in a ventricular assist device had a measured efficiency between 31% and 34% – but it also had a flow rate of 5 L/min (Baker, Gardner, Gaumont, Geselowitz, & Snyder, 1998).

The entire selection of pumps is graphed in Figure 4-7. While the line is smooth above 400 mL/min, below 200 mL/min the line becomes quite chaotic. The goal of this exploration of commercially available pumps is to relate flow rate and pressure to input power via efficiency. While this graph cannot provide a relationship that differentiates between individual flow rates for the system model, it clearly shows a very poor efficiency in the range of flow rates associated with a portable hemodialysis system– well below 0.30%.

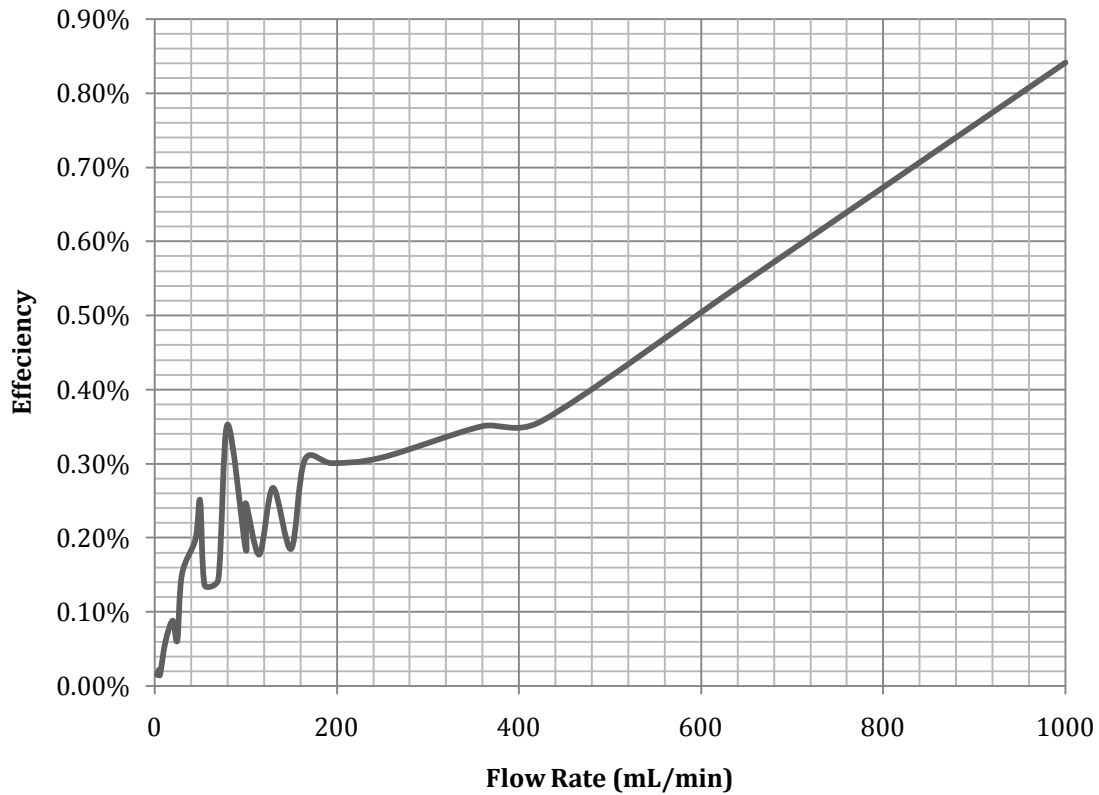


Figure 4-7. The efficiency of various peristaltic pumps from the same manufacturer.

Because no clear relationship between pump size and output can be drawn from either theoretical analysis or examination of commercially available pumps, pump size effects will not be integrated into the system model.

#### 4.6 Exploring the primary equations of a hemodialysis system

Now that various aspects of a hemodialysis system have been analyzed, a unified system model can be constructed. The goal of this system model is to predict how different system configurations will influence the treatment schedule of a patient. The model should examine different combinations of flow rates, dialyzer sizes, treatment times, and patient conditions. Because we are interested in a portable system, the model should be optimized for portable use.

#### 4.6.1 System parameters

The individual solute clearance,  $K_0$ , is the measure of clearance of an individual solute. It is a function of the membrane material and the physics of the individual solute. Often this variable is lumped with the surface area to create a new parameter,  $K_0A$ . When manufacturers provide specifications for their dialyzers, the lumped parameter is usually provided only with regard to urea. This is the  $K_0A$  that is used in Equation 4-22 for calculation of the overall dialyzer clearance. Because  $K_0$  is a function of the solute and the membrane material, it is constant for dialyzers of the same material but different lengths. As the size (length) of the dialyzer increases, the  $K_0A$  increases in proportion to the increasing area. If the number of tubules and their diameter remains constant as the length is increased (which is common), then the  $K_0A$  increases linearly with the length.

**Table 4-2. Various dialyzers and their clearance rates (Baxter Healthcare Corporation).**

Dialyzer Name	$K_0A$ (mL/min)	Area (m <sup>2</sup> )
<b>Baxter Xenium 110</b>	824	1.1
<b>Baxter Xenium 130</b>	993	1.3
<b>Baxter Xenium 150</b>	1123	1.5
<b>Baxter Xenium 170</b>	1239	1.7
<b>Baxter Xenium 190</b>	1487	1.9
<b>Baxter Xenium 210</b>	1614	2.1

The blood flow rate and dialysate flow rate can be chosen to maximize the overall system clearance according to Equation 4-22. However, changing those flow rates has ramifications on the amount of dialysate used and treatment time. Additionally, there is a link between the dialysate flow rate and the blood flow rate: they work together to change the overall dialyzer clearance. Only through careful manipulation of the system model can the best flow rates be chosen.

#### 4.6.2 Precursory analysis of the Michaels equation

The most basic analysis of hemodialysis can be provided by examining the Michaels equation. As explained in Section 4.3, the Michaels equation (Equation 4-22) provides a relationship between blood flow rate, dialysate flow rate, dialyzer size, membrane material, and overall dialyzer clearance. Again, this equation only holds for the common hollow fiber dialyzer design in counter-current flow.

As a first test of this equation, the blood flow rate ( $Q_B$ ) will be increased as all other variables are left constant. The  $K_0A$  parameter will be set at 100 mL/min and the dialysate flow rate ( $Q_D$ ) will be fixed at 250 mL/min. This analysis will show the basic relationship between blood and dialysate flows for this specific case.

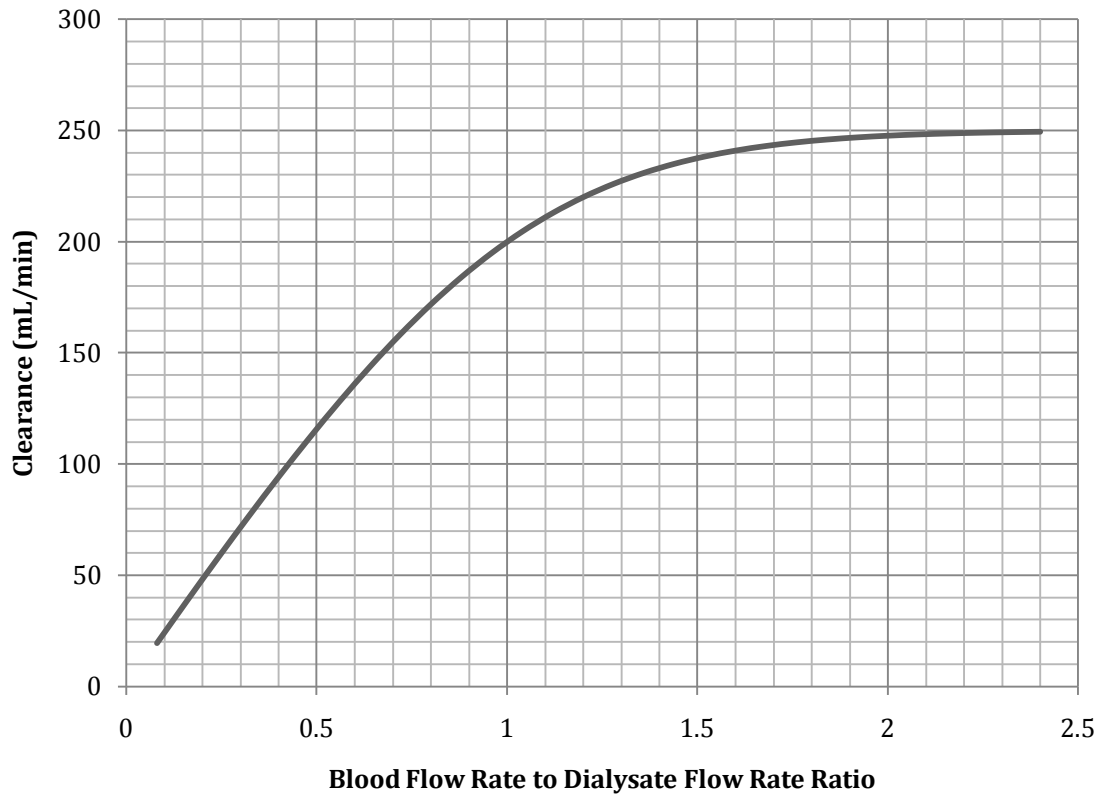


**Figure 4-8. The relationship between the blood and dialysate flow rates with respect to overall dialyzer clearance. The  $K_0A$  was 1000 mL/min and the dialysate flow rate ( $Q_D$ ) was 250 mL/min.**

Keeping all other variables the same, the relationship between the dialysate and blood flow rates becomes clear in the simple case of Figure 4-8. There is a steep increase in overall dialyzer clearance at a 0.5 ratio (125 mL/min), and after a 1.5 ratio (375 mL/min) the clearance steadies. From this analysis, it seems as if selecting a ratio of at least 1.5 for this blood flow rate would be ideal. However, a more detailed analysis is needed. Since the dialysate flow rate needs to be minimized, tradeoffs between treatment time and dialysate flow rate should be considered.

#### **4.6.3 Effect of dialyzer size in the Michaels equation**

Another important variable that can be considered with the Michaels equation is the effect the dialyzer size has on overall clearance. The size of the dialyzer is generally changed only by

lengthening it – the number of tubules remains unchanged. With the dialysate flow rate kept at 250 mL/min, the  $K_0A$  was examined in ranges from 500 to 2000 mL/min at four different blood and dialysate flow ratios. From Figure 4-9, it seems that the largest factor is not the size of the membrane, but the ratio of the flow rates.

The overall dialyzer clearance varied little between flow ratios of 1.5 and 2.0. There seemed to be little gain from increasing the dialyzer size in any case. While Figure 4-9 does not explore it, the largest dialyzers benefit from faster dialysate flow rates (Baxter Healthcare Corporation) – this data was plotted at a constant dialysate flow rate of just 250 mL/min. Clinical hemodialysis can have dialysate flow rates much higher.

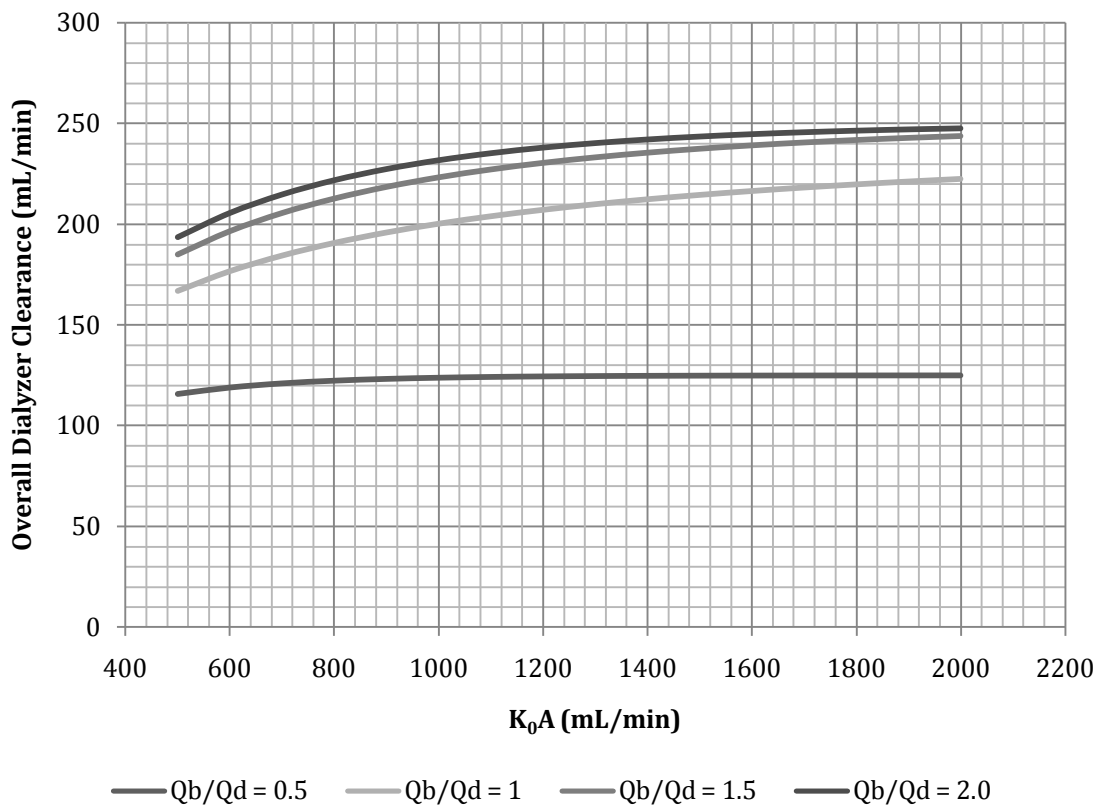


**Figure 4-9. The relationship between the size of the dialyzer and overall dialyzer clearance at various blood and dialysate flow ratios.**

One of the limiting factors in a portable hemodialysis system is the blood flow rate. Because blood is drawn from the veins (and not the arteries) in a portable system, the blood flow rate is limited to below 100 mL/min. This unique situation calls for special analysis of the Michaels equation. Most commercially available dialyzers are designed for much higher flow rates than what might be encountered in a wearable system, but the Michaels equation can calculate how they will respond to a slower blood flow rate. Figure 4-10 shows the clearance of different-sized dialyzers at a range of dialysate flow rates and a blood flow rate of 80 mL/min.

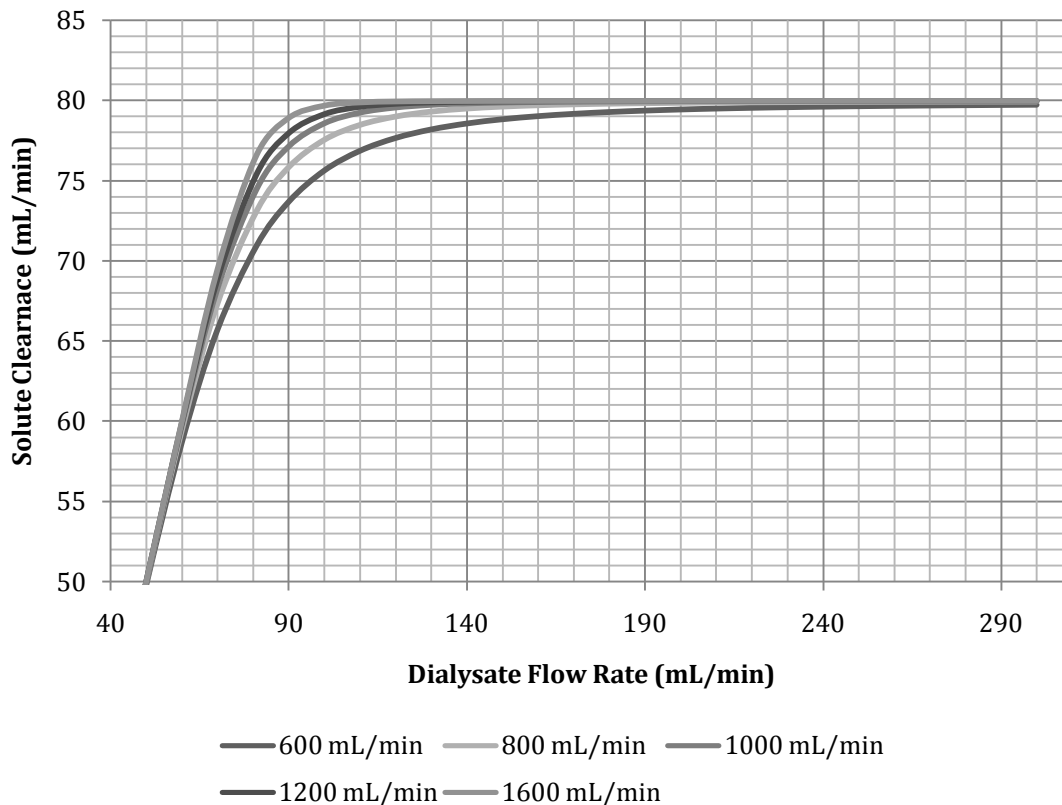


**Figure 4-10. Various dialyzer sizes are compared at an 80 mL/min blood flow rate.**

It can be reasoned from Figure 4-10 that the size of the dialyzer has little impact at the slow flow rates encountered in a portable hemodialysis system. Interestingly, all five hypothetical dialyzers have a peak around an 80 mL/min dialysate flow rate – a ratio of 1.0 (the blood flow rate was also

80 mL/min). Previous manipulation of the Michaels equation (Figure 4-8) had implied that the best ratio was above 1.5.

The unusual ratio is a product of the unusually slow dialysate flow rate. It was previously discussed that there were two primary factors of the Michaels equation – the blood flow rate and the large lumped parameter that accounts for the flow ratios and dialyzer size. However, by plotting several different curves of different fixed dialysate flow rates (Figure 4-11), it becomes clear that the best ratio also changes with the dialysate flow rate. At high clinical-level dialysate flow rates, it is best to have a ratio of about 2.0. When the dialysate flow rate is reduced, the ideal ratio is reduced along with it.

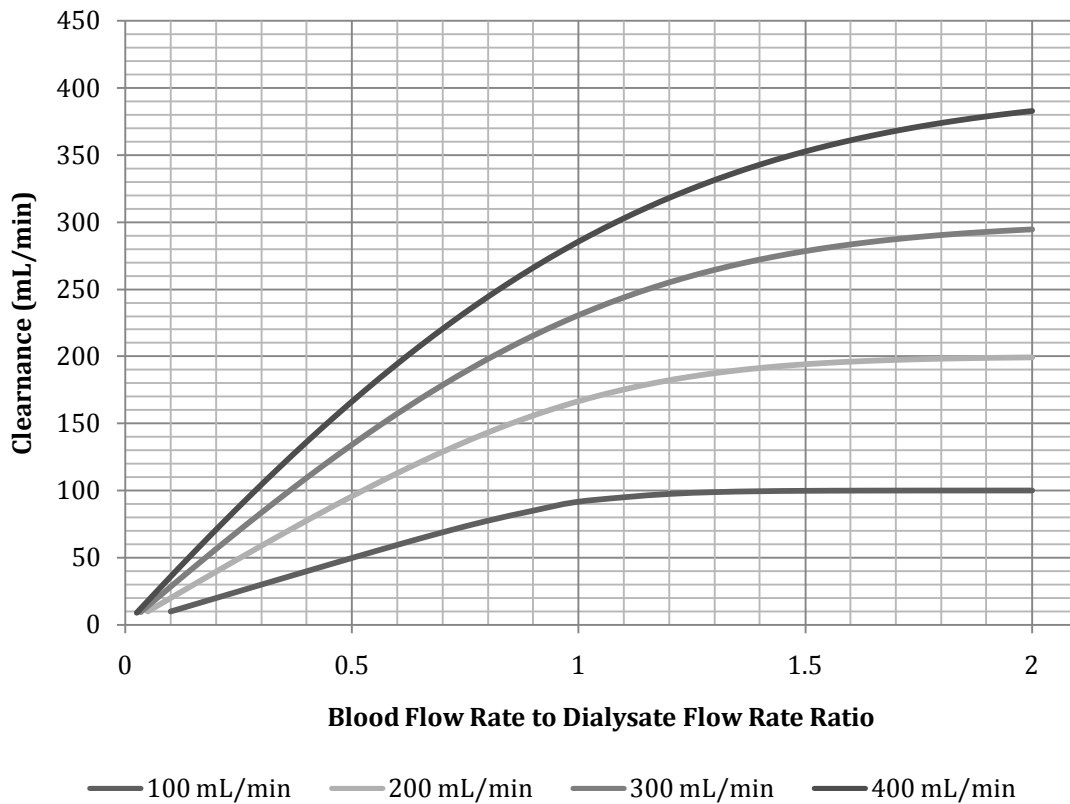


Figure 4-11. The overall dialyzer clearance at four different dialysate flow rates.

Because venous-side ports are limited to a blood flow rate of 80 mL/min, choosing a higher dialysate flow rate is unreasonable. From this analysis, it is clear that choosing a ratio of 1.0 will not only provide the highest overall clearance rates, but it will also reduce the need for dialysate.

#### **4.7 Modeling Hemodialysis in Simulink**

Because of the complex nature of a hemodialysis system, it is easiest to use a program such as Matlab Simulink to model its performance beyond simple manipulation of the Michaels equation.

The only variable that is optimized by the simulation is the dialysate flow rate. Many of the variables in the simulation are dependent on patient specifics. For example, a patient's urea generation rate and total blood volume are functions of his or her size and diet. Before the simulation can be run, values for these variables must be selected that correspond to a realistic scenario. In the examples in this thesis that contain urea generation, the assumed value was 17.3611 mg/min (unless otherwise noted), which corresponds to 25 g/day, a typical value (Moffett, Moffett, & Schauf, 1993).

Similarly, the blood flow rate ( $Q_B$ ) is limited by which method the blood is extracted from the body, and is therefore not subjected to optimization. It has already been shown through Equation 4-22 that a higher blood flow rate is the best way to increase solute clearance, so it is known that the port that provides the highest blood flow rate is the best choice. However, due to varying patient conditions, a port with a less-than-optimal flow rate might have to be selected.

The total volume of dialysate can be defined by the system. There are two ways to determine the total amount of dialysate used by the system: if it is single-pass (no dialysate reuse), then the amount of dialysate used is the dialysate flow rate ( $Q_D$ ) times the treatment length. However, if the dialysate is to be recirculated, then the total dialysate volume is independent of the dialysate flow

rate. The Simulink model accounts for both these scenarios by calculating both volumes and outputting only the lower value.

This works because the model always recirculates dialysate. If a single-pass system is tested, the dialysate volume is simply set to a very large number (generally over a billion gallons of dialysate), so that the system is effectively always drawing from a reservoir of clean dialysate. However, when the system outputs how much dialysate is required, it reads both the input volume (again, in the billions) and the dialysate flow rate times treatment length volume. The lesser of these two values is the actual dialysate volume ( $V_D$ ). In the case where the amount of dialysate is limited, it will be less than volume based on the dialysate flow rate.

The other two important variables are the initial concentrations of the blood and dialysate. In every case, the initial dialysate urea concentration is set to 0 mg/mL. Regardless of whether a system is single-pass or uses recirculation, its initial concentration should be zero (although the user has control over this parameter). The blood, however, depends on the individual patient's BUN (blood urea nitrogen, the amount of nitrogen in the blood in the form of urea) reading, and is therefore dependent on how often they dialyze (among other factors). For example, patients who dialyze less frequently would have a higher initial BUN. So if the model were to test a system that dialyzed only a few times per week, a higher initial BUN should be selected for the input value. If a daily system is to be tested, a lower initial BUN should be selected to reflect the probable level of urea in their blood before dialysis began.

The dialysis schedule is modeled as a pulse input; if the patient is dialyzing then the output is one and if they are in between treatments the output is zero. This value is then multiplied with the milligrams of urea removed from the blood.

#### 4.7.1 Step-by-step procedure used in the model

The model predicts the urea concentration of blood every minute. Figure 4-12 is a screenshot of the model in Simulink.

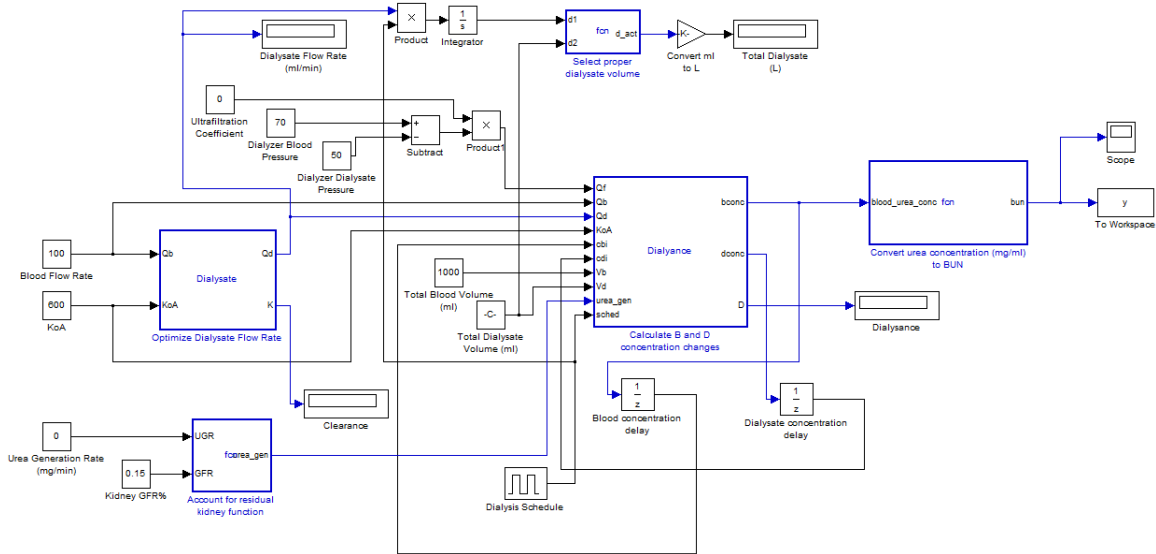


Figure 4-12. A screenshot of the Matlab Simulink model.

##### 4.7.1.1 Step one: define inputs

At a minimum, the blood flow rate ( $Q_B$ ), dialyzer properties ( $K_0A$ ), initial blood volume ( $V_B$ ), initial dialysate volume ( $V_D$ ), urea generation rate ( $\dot{G}$ ), trade-off coefficient ( $\alpha$ ), residual kidney function ( $GFR\%$ ), initial blood concentration ( $C_{Bi}$ ), initial dialysate concentration ( $C_{Di}$ ), ultrafiltration coefficient ( $K_{UF}$ ), dialyzer blood pressure ( $p_B$ ), dialyzer dialysate pressure ( $p_D$ ), and treatment schedule ( $t_1$  and  $t_2$ ) must be defined. A summary of these inputs, with their associated units, is available in Table 4-3.

**Table 4-3. The inputs of the system model.**

Parameter Name	Variable	Units
Blood flow rate	$Q_B$	mL/min
Dialysate flow rate	$Q_D$	mL/min
Dialyzer properties	$K_0A$	mL/min
Trade-off coefficient	$\alpha$	-
Urea generation rate	$\dot{G}$	mg/min
Residual kidney function	$GFR\%$	-
Total blood volume	$V_B$	mL
Total dialysate volume	$V_D$	mL
Incoming blood urea concentration	$C_{Bi}$	mg/mL
Incoming dialysate urea concentration	$C_{Di}$	mg/mL
Dose length	$t_1$	min or hours
Time between doses	$t_2$	min or hours
Ultrafiltration coefficient	$K_{UF}$	mL/min/mmHg
Dialyzer blood pressure	$p_B$	mmHg
Dialyzer dialysate pressure	$p_D$	mmHg

**Table 4-4. The parameters calculated by the system model.**

Parameter Name	Variable	Units
Dialysate flow rate	$Q_D$	mL/min
Dialysance	$D$	mL/min
Dialyzer clearance	$K$	mL/min
Total dialysate volume	$V_D$	mL
Outgoing blood concentration	$C_{Bo}$	mg/mL
Outgoing dialysate concentration	$C_{Do}$	mg/mL

#### 4.7.1.2 Step two: calculate a trade-off dialysate flow rate

The next step is to calculate the best dialysate flow rate ( $Q_D$ ) from the blood flow rate ( $Q_B$ ) and the dialyzer properties ( $K_0A$ ). The model tests every dialysate flow rate between 1–1000 mL/min, in 1 mL/min intervals, recording the highest possible clearance in accordance with Equation 4-22. While this is generally the clearance corresponding to a dialysate flow rate of 1000 mL/min, this

value is then used to find the slowest possible dialysate flow rate that corresponds to a clearance that is 95% of the maximum.

The model then tests every dialysate flow rate again, starting at 1 mL/min at 1 mL/min intervals until it achieves the desired 95% clearance. The 95% value was chosen arbitrarily; choosing 90% also works well, but percentages below that begin to select dialysate flow rates with insufficient clearances. From Figure 4-11, the 95% value attempts to find the best dialysate flow rate. In the following simulations, the 95% value is termed the *trade-off coefficient* and is symbolized by  $\alpha$ .

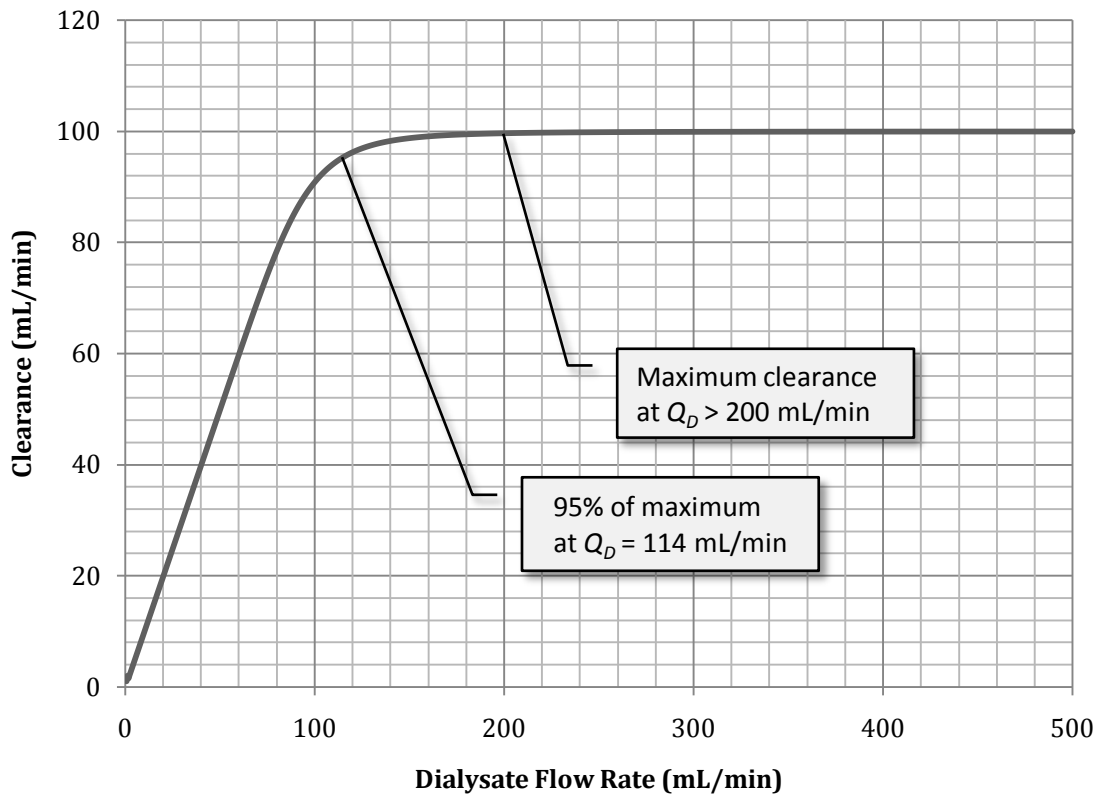


**Figure 4-13. The trade-off dialysate flow rate. The maximum clearance is 100 mL/min (at  $Q_D > 200$  mL/min), and the trade-off clearance is 95 mL/min (at  $Q_D = 114$  mL/min).**

An example of this is shown in Figure 4-13. For a dialyzer of  $K_0A = 1000$  mL/min and  $Q_B = 100$  mL/min, the clearance ( $K$ ) is plotted against dialysate flow rates ( $Q_D$ ) from 1–500 mL/min

(the model calculates from 1–1000, but the plot was truncated to better show the trade-off curve). The maximum possible clearance of 99 mL/min is shown to be at a dialysate flow rate ( $Q_D$ ) of greater than 200 mL/min. Multiplying the maximum possible clearance by 95% yields a clearance of 95 mL/min. The model starts its search at 1 mL/min, gradually increases the dialysate flow rate, and then stops once 95% value is found. In this case, the model would stop its search after testing the clearance corresponding to a dialysate flow rate of 114 mL/min.

#### 4.7.1.3 Step three: calculate the urea concentration of the blood leaving the dialyzer

The time-dependency of the model begins at this step. The model works in one-minute increments, so this step begins the iterative nature of the model. The dialysance ( $D$ ) was already calculated in Step 2, this value is used with the initial blood and dialysate concentrations ( $C_{Bi}$  and  $C_{Di}$ ) and the dialysate flow rate ( $Q_D$ , calculated in Step 1) to determine the amount of urea removed in the first minute. Recalling Equation 4-9:

$$D = \frac{Q_B(C_{Bi} - C_{Bo})}{C_{Bi} - C_{Di}} = \frac{Q_D(C_{Do} - C_{Di})}{C_{Bi} - C_{Di}}$$

In the case when the blood flow rate ( $Q_B$ ) is 100 mL/min, the dialysate flow rate ( $D$ ) is 114 mL/min, and the  $K_0A$  is 1000 mL/min, the calculation for the dialysance ( $D$ ) is 95.16 mL/min:

$$D = \frac{e^{\frac{1000\left(1-\frac{100}{114}\right)}{100}} - 1}{\frac{e^{\frac{1000\left(1-\frac{100}{114}\right)}{100}}}{100} - \frac{1}{114}}$$

$$D = 95.16 \text{ mL/min}$$

Continuing, if the initial blood concentration ( $C_{Bi}$ ) is 6.43 mg/mL, the initial dialysate concentration ( $C_{Di}$ ) is 0.0 mg/mL, then the concentration of the blood out ( $C_{Bo}$ ) is:

$$95.16 = \frac{100 \times (6.43 - C_{Bo})}{6.43 - 0.0}$$

$$C_{Bo} = 0.31 \text{ mg/mL}$$

The dialyzer has significantly reduced the urea concentration of the blood leaving the dialyzer after one minute.

Calculating the output dialysate concentration provides an easy way to calculate the mass of urea transported, and is needed if dialysate is recirculated:

$$95.16 = \frac{114 \times (C_{Do} - 0.0)}{6.43 - 0.0}$$

$$C_{Do} = 5.37 \text{ mg/mL}$$

A simple mass balance can be performed to verify the results:

Incoming Mass = Outgoing Mass

$$(Q_B \times C_{Bi}) \times (Q_D \times C_{Di}) = (Q_B \times C_{Bo}) \times (Q_D \times C_{Do})$$

$$(100 \times 6.43) \times (114 \times 0.0) = (100 \times 0.31) \times (114 \times 5.37)$$

$$643 = 31 + 609$$

$$643 \approx 640$$

The discrepancy can be accounted for by rounding.

4.7.1.4 Step four: calculate the new concentrations of the blood and dialysate volumes

After the fluids (blood and dialysate) leave the dialyzer, they are mixed with the remaining volumes. In the case of this example, this is 5 L of blood. Dialysate is often disposed of, but its total volume can be arbitrarily set by the user.

Once the cleaned blood mixes with the remaining blood, the concentration of the total blood volume has decreased. The new urea concentration in the blood is calculated by first calculating the previous total mass of urea in the blood volume:

$$\text{mg}_{total} = C_{Bi} \times V_B \quad (4-31)$$

Following the example in Step 3:

$$\text{mg}_{total} = \frac{6.43 \text{ mg}}{\text{mL}} \times 5\,000 \text{ mL}$$

$$\text{mg}_{total} = 32\,150 \text{ mg}$$

The patient started with 32 g of urea in their blood.

Next, the mass of urea removed in the first minute can be determined by multiplying the concentration of the dialysate leaving the dialyzer ( $C_{Do}$ ) and the dialysate flow rate ( $Q_D$ ):

$$\text{mg}_{removed} = C_{Do} \times Q_D \times t \quad (4-32)$$

In the example:

$$\begin{aligned} \text{mg}_{removed} &= \frac{5.37 \text{ mg}}{\text{mL}} \times \frac{114 \text{ mL}}{\text{min}} \times 1 \text{ min} \\ \text{mg}_{removed} &= 612.18 \text{ mg} \end{aligned}$$

In this case, 612.18 mg of urea has been removed from the blood. At this point, the generation of urea and residual kidney function must be accounted for. Because many dialysis patients still have some kidney function (generally a glomerular filtration rate [GFR] less than 15%), their residual kidney function ( $GFR\%$ ) can be considered by lessening the urea generation rate ( $\dot{G}$ ). A typical human generates 25 g of urea per day, which is 17.361 mg/min.

$$\text{mg}_{generated} = (1 - GFR\%) \times \dot{G} \times t \quad (4-33)$$

In this example, a urea generation rate ( $\dot{G}$ ) of 17.261 mg/min has been assumed, but no residual kidney function:

$$\begin{aligned} \text{mg}_{generated} &= (1 - 0) \times \frac{17.361 \text{ mg}}{\text{min}} \times 1 \text{ min} \\ \text{mg}_{generated} &= 17.361 \text{ mg} \end{aligned}$$

The new total mass of urea in the blood can be calculated by subtracting this value from the previously determined total mass of urea and adding the amount of urea generated:

$$\text{mg}_{total}' = \text{mg}_{total} - \text{mg}_{removed} + \text{mg}_{generated} \quad (4-34)$$

In the case of the example presented:

$$\text{mg}_{total}' = 32\,150 \text{ mg} - 612.18 \text{ mg} + 17.361 \text{ mg}$$

$$\text{mg}_{total}' = 31\,555.18 \text{ mg}$$

Now that the new total mass of urea in the blood is known, the new blood concentration can be determined by dividing the new total mass by the total blood volume ( $V_B$ ):

$$C_{Bi}' = \frac{\text{mg}_{total}'}{V_B} \quad (4-35)$$

In the example, this results in a new urea concentration of 6.311 mg/mL:

$$C_{Bi}' = \frac{31\,555.18 \text{ mg}}{5\,000 \text{ mL}} = 6.311 \text{ mg/mL}$$

These calculations are also performed on the dialysate. When the dialysate is run in single-pass mode, the volume of the dialysate is set to an arbitrarily high value (above  $1 \times 10^9$  mL). While the dirty dialysate is still “mixed” with the total volume of dialysate, the extremely high dialysate volume ensures that it does not affect the results. If dialysate is to be recirculated, its value can be set by the user.

#### 4.7.1.5 Step five: iterate

The previous step is performed at one-minute intervals. The new blood concentration ( $C_{Bi}'$  in the previous step) is now the incoming blood concentration ( $C_{Bi}$ ) of the dialyzer. While the dialysance ( $D$ ) and total volumes ( $V_B$  and  $V_D$ ) do not change between iterations, the blood and dialysate concentrations are constantly updated.

#### 4.7.1.6 Outputs of the model

The model's primary output is a matrix of the urea blood concentration ( $C_B$ ) and the time. An example of actual output from the model is in Table 4-5. The same parameters were used as the example of this section, so the validity of the model can be confirmed. Section 4.7.1.4 predicted the urea concentration in the blood would be 6.311 mg/mL after the first minute; the model predicts 6.309 mg/mL. The discrepancy can be attributed to rounding (the model does not round; the example did).

**Table 4-5. The output from the model of the first four minutes from a simulation.**

Time (minutes)	Blood Urea Concentration ( $C_B$ , mg/mL)
0	6.428571
1	6.309173
2	6.192048
3	6.077152
4	5.964442

How long the simulation runs depends on the dose length ( $t_1$ ) and the time between doses ( $t_2$ ). To simulate clinical dialysis (2-hour treatment, every-other day),  $t_1$  and  $t_2$  could be set to 2 and 46 hours, respectively.

#### 4.7.2 Other considerations of the model

Aside from what was detailed in Section 4.7.1, the model makes other considerations.

The primary factor not already mentioned is the role of ultrafiltration in dialysis. Ultrafiltration ( $Q_F$ , mL/min) accounts for a small amount of mass transport due to the pressure gradient between the blood and dialysate flows in the dialyzer. It is accounted for by the pressure difference ( $p_B - p_D$ )

and a new parameter, the ultrafiltration coefficient ( $K_{UF}$ , mL/min/mmHg) (Sargent & Gotch, 1989):

$$Q_F = K_{UF} \times (p_B - p_D) \quad (4-36)$$

The mass flux associated with ultrafiltration is the product of the ultrafiltration coefficient ( $Q_F$ ) and the urea blood concentration leaving the dialyzer ( $C_{Bo}$ ):

$$J_{UF} = K_{UF} \times (p_B - p_D) \times C_{Bo} \quad (4-37)$$
$$J_{UF} = Q_F \times C_{Bo}$$

The model has the ability to account for this mass transport, but in the cases presented in this thesis it is not accounted for. It was left out because there is no easy estimation of either the pressure gradient ( $p_B - p_D$ ) or the ultrafiltration coefficient ( $K_{UF}$ ). While accounting for ultrafiltration would have ostensibly provided greater accuracy, using poorly estimated values would negate any benefit. Additionally, the role of ultrafiltration is minor (Sargent & Gotch, 1989), so not accounting for it is reasonable.

#### **4.7.3 Assumptions in the model**

The model makes several assumptions. The equations used to calculate the changing concentrations do not use the actual concentration gradient between the dialysate and the blood, but rather the simplified concentration difference between the blood inlet and the dialysate inlet. As explained before, this is not expected to have a serious impact on the results.

Another assumption made by the model is perfect mixing. When the dirty dialysate and blood leave the dialyzer, they are returned to a hypothetical vat (or body), and then perfectly mixed with the existing blood or dialysate to create a new concentration level. A real-world hemodialysis experiment would probably have imperfect mixing. For example, blood returned from the body would be returned on the venous side of the bloodstream, while the blood drawn into the dialyzer

would come from the arterial side. The blood drawn into the dialyzer would not be diluted by the clean blood, and would actually have a higher concentration of urea, resulting in model that predicts slightly lower clearances. On the dialysate side, dialysate is usually not recirculated, but if it was, the dialysate drawn would be a little cleaner than predicted by the model, also resulting in clearances higher than predicted.

This is considered a one-compartment model, in reference to the how the model treats the body's fluid volume. In a one-compartment model, the dialyzer interacts with a hypothetical reservoir of all the fluid in the body. In a two-compartment model, the body's fluid volume is divided into fluids: extracellular and intracellular. In two-compartment hemodialysis models, the dialyzer interacts directly with the extracellular fluid, and the extracellular fluid in turn interacts with the intracellular fluid.

Two-compartment models were developed to reflect a sudden rise of solutes in the patient's blood after dialysis ends. Once dialysis ends, the extra- and intercellular fluids equalize, and the extracellular fluid gains solutes from the intercellular fluid, which was not as well dialyzed. Ziólko and coauthors (2000) studied the accuracy of both one- and two-compartment models, and noted that they both have similar accuracy. They concluded that two-compartment models should only be used when "explaining a steep increase of toxin concentration immediately after the end of dialysis" (p. 1163). Because this model will be used to determine day-to-day changes in patient BUN, and not intricate BUN changes, a one-compartment model will suffice.

Constant flow rates are assumed, which would probably not be the case during a typical hemodialysis session. As the dialyzer is primed, and during its use, the blood flow rate can easily fluctuate. Because these fluctuations are expected to be minor, this oversight in the model is not of concern.

Further, the equations used in this model also assume there is no blood- or dialysate-side resistance to diffusion – that all resistance lies in the transport across the membrane. Because the membrane accounts for 90% of the resistance (Sargent & Gotch, 1989), this is a reasonable assumption.

#### **4.8 Conclusion**

The creation of a detailed system model has allowed for an exploration of all the different parameters associated with hemodialysis. The final goal is to put together a system configuration that best meets the goals stated in Chapter 3 of a portable system.

A summary of what has been learned in this chapter:

1. Blood flow rate is one of the most important variables in hemodialysis. Because of the large volume of blood in the body, the only way to sufficiently remove urea in a satisfactory time scale is to increase the blood flow rate. Unfortunately, a home-based system is limited to blood flow rates below 100 mL/min due to the types of blood ports that must be used in a non-clinical setting. Any system that is embodied must work around this limiting flow rate.
2. Optimal dialysate flow rate is closely tied to the blood flow rate. At slower blood flow rates, the dialysate flow rate does not need to exceed about a one-to-one ratio. This actually works in the favor of a home hemodialysis system. At high blood flow rates, the best dialysate flow rate can be double the blood flow rate, vastly increasing the volume of dialysate needed. Since one of the goals of this chapter was to devise a system that uses less dialysate, having a system with a slower blood flow rate is advantageous.
3. Peristaltic pump efficiency is terrible for pumps in the flow rate range needed for dialysis. For machines that are plugged into the wall, this is inconsequential. However, if a battery-powered system were developed, designing a pump that is more efficient would be

important. The effect of pump power on the system was not integrated into the Simulink model, but its importance is noted.

4. The size of the dialyzer has a marginal impact on the clearance of urea during hemodialysis. Because the physical size of a large dialyzer (with a  $K_0A$  of 1600 mL/min) is not limiting, at this point in the design process there is no reason not to use the largest available dialyzer. Portable systems that rely on slow blood flow rates need all the help in urea clearance available.

With this knowledge, Chapter 5 verifies the model and creates proposed treatment scenarios.

## CHAPTER FIVE

### MODEL VERIFICATION AND PROPOSED SCENARIOS

In Chapter 3, a concept was developed that could provide better hemodialysis for patients. A model was developed in Chapter 4 that can thoroughly test different arrangements of the concept developed in Chapter 3.

Before concepts can be generated with the model, it must first be verified. Verification of the model is found in Section 5.1. After verification, Section 5.2 models very basic dialyzer configurations and tests different dialysate-reducing ideas (recirculation, regeneration, etc.). Finally, Section 5.3 uses information gathered in Section 5.2 to create reasonable system concepts.

#### 5.1 Validation of the hemodialysis system model

This one-compartment model can be verified in two ways: comparing its results to published hemodialysis patient data, and against an *in vitro* laboratory setup involving hemodialysis components.

##### 5.1.1 Laboratory setup

Porcine blood was obtained during desanguination at a local abattoir and heparin (APP Pharmaceuticals) was added to the blood immediately after collection at a dose of 3.5–7.0 USP/mL blood. The heparinized porcine blood was then transferred to the laboratory in a thermally insulated container and left to separate until the erythrocytes settled to the bottom and the plasma formed a distinct layer on the top. Dialysate was prepared by mixing concentrates with deionized water at a ratio of 1: 1.72: 42.28 (acid concentrate: bicarbonate concentrate: deionized water).

Two modes of dialysis were experimentally tested:

1. passing only fresh dialysate through the dialyzer (“single-pass”), and
2. recirculating dialysate (“recirculation”).

Recirculation uses less dialysate, but lessens the mass transfer rate from the blood due to a smaller concentration gradient.

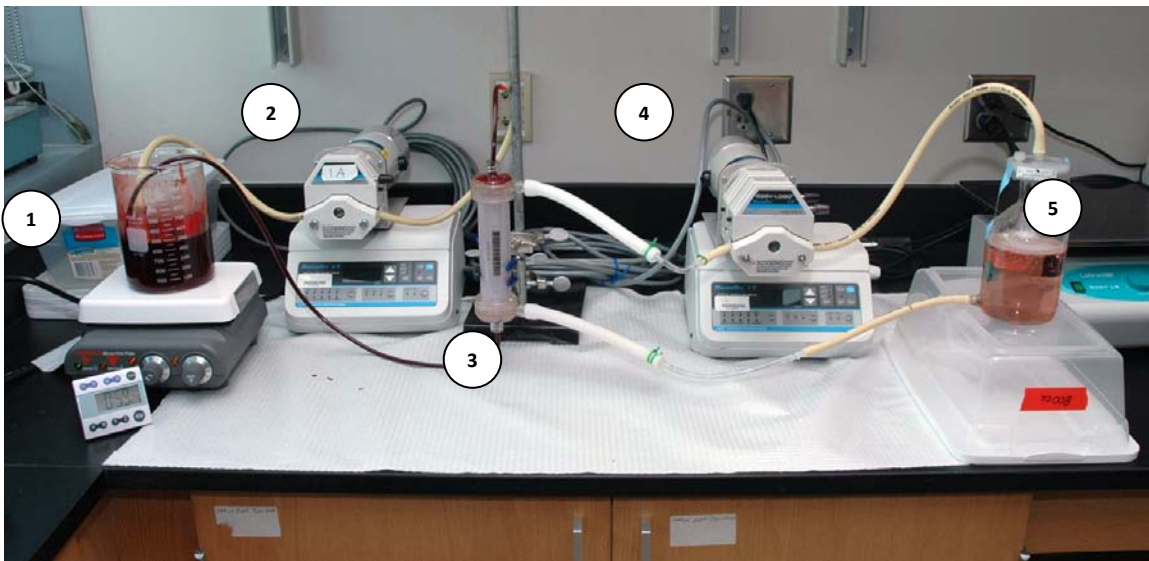


**Figure 5-1. The laboratory setup. From left to right: the blood reservoir (1), the blood pump (2), the dialyzer (3), the dialysate pump (4), and the dialysate reservoir (5).**

The plasma and dialysate flowed through the circuit shown in Figure 5-1 at flow rates of 100 mL/min and 150 mL/min, respectively. For single-pass mode, the dialysate flowed out of the dialyzer into a waste container. A Polyflux dialyzer (Gambro) was used to perform the dialysis. Small volume samples (less than 1 mL) were removed from the blood reservoir during the experiments at specified time points and the blood urea nitrogen (BUN) was measured with an iSTAT analyzer (Abbott).



**Figure 5-2. The dialysate reservoir seen early in (left) and later in (right) dialysis when the dialysate is recirculated through the dialyzer.**

As dialysate is recirculated through the dialyzer, some of the plasma is transferred into the dialysate. This is not desirable – only the unwanted solutes are supposed to cross – and is due largely to a pressure gradient (TMP) across the membrane walls. In Figure 5-2, the dialysate reservoir is shown early (left) and late (right) in dialysis. At the start of the experiment, the dialysate was clear.

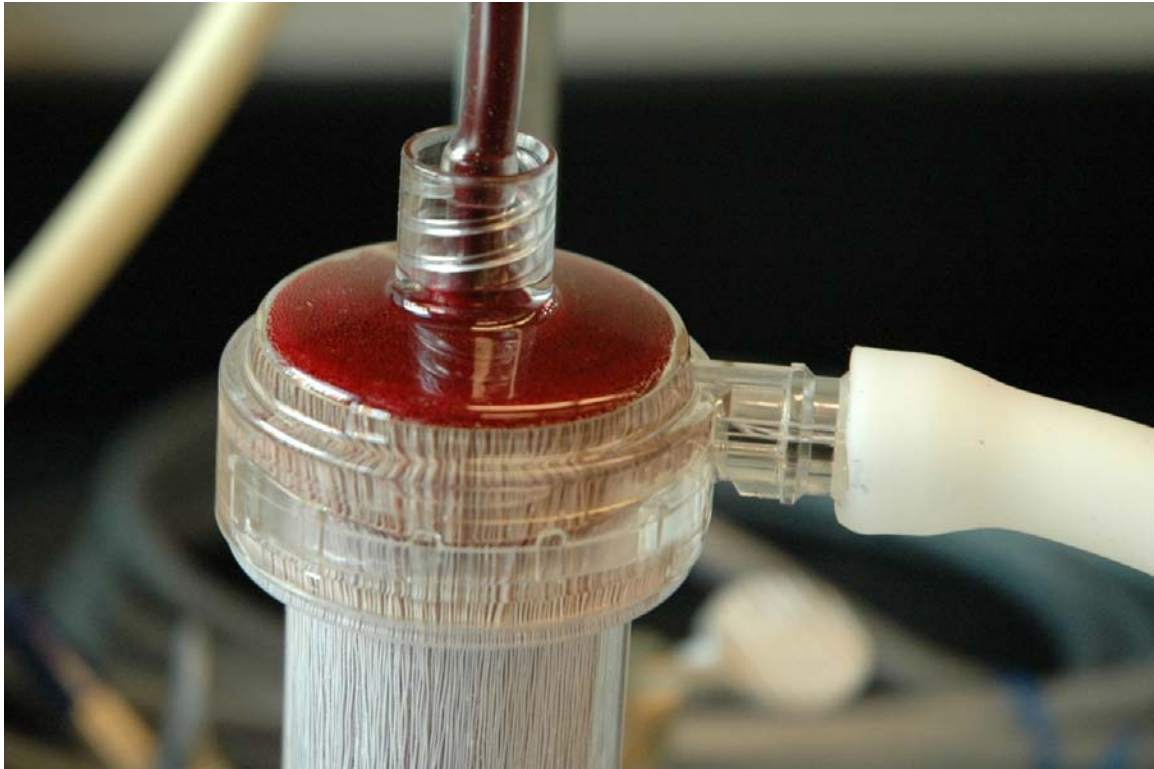


**Figure 5-3. A close-up of the dialyzer after dialysis. Porcine blood has filled the baffle at the entrance of the dialyzer and the thousands of tubules that run the length of the dialyzer. Dialysate flows counter to the blood and exits in the tube on the right.**

Most dialyzers are designed for single-use. After dialysis, their narrow tubules are still filled with blood and much more likely to clot if used more than once. Figure 5-3 shows a dialyzer after dialysis. The area where the blood has pooled is a baffle that is designed to evenly distribute the blood to each of the thousands of tubules seen at the bottom of the picture. However, despite the baffle, blood flows most readily through the inner tubules and the least through the outer tubules.

### **5.1.2 Validation via laboratory tests**

The results of the BUN versus time for the *in vitro* experiments had good results. Figure 5-4 (single-pass) and Figure 5-5 (recirculation) compare experimental results to the model. The model agrees well with the experimental data as can be seen in the figures.

It should be noted that there is some error associated with the iStat Analyzer. According to the manufacturer-provided specifications, measurements in the BUN ranges provided have a standard deviation of 0.76 mg/dL.

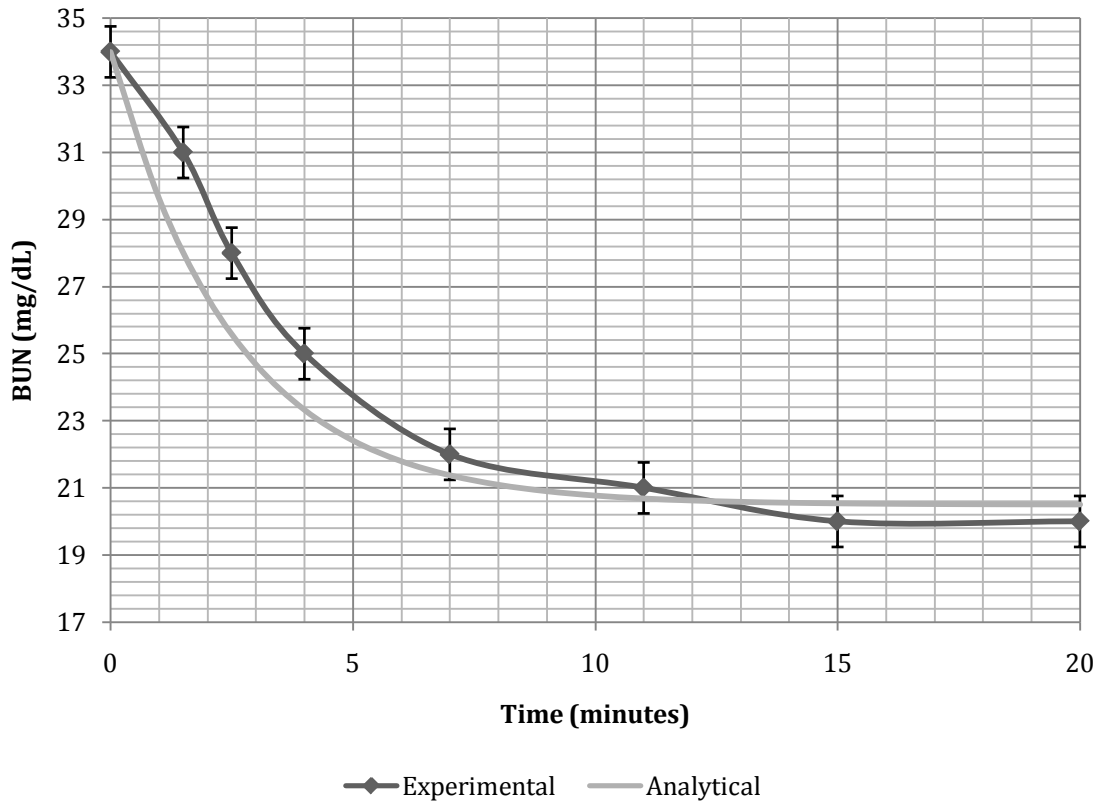


**Figure 5-4. Single-pass mode: 450 mL of porcine plasma through a ( $K_0A = 450$  mL/min) dialyzer at 100 mL/min and dialysate flow rate of 150 mL/min. The light gray line is the model and the dark gray line is the experimental results.**

In both experiments, the predicted BUN was higher than the actual value. The most obvious explanation for this is the model's inconsideration of ultrafiltration. Ultrafiltration is the transport of solutes and fluids across the membrane due to the pressure gradient (usually about 20 mmHg) in addition to the concentration gradient. Evidence of ultrafiltration can be seen in Figure 5-2 as a color change of the dialysate.

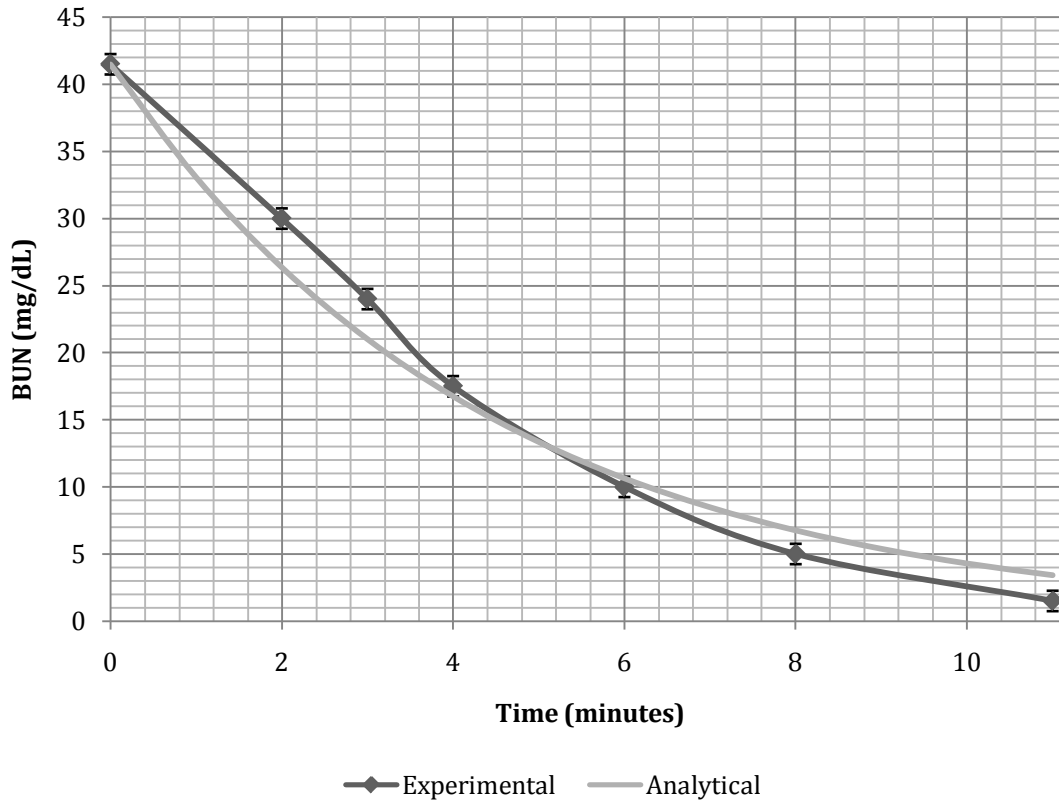


**Figure 5-5. Recirculation mode: 750 mL of porcine plasma through a dialyzer ( $K_0A = 450$  mL/min) at 100 mL/min. A fixed volume of 500 mL of dialysate was recirculated through the dialyzer at 150 mL/min. The light gray line is the model and the dark gray line is the experiment results.**

### 5.1.3 Validation via published hemodialysis data

Published data on the changing BUN of a dialysis patient is available in the work of Ziólko et al. (2000). In their study, a 23-year-old 58 kg male was dialyzed for 3.5 h. Figure 5-6 plots their results against the one-compartment model presented in this thesis. The discrepancy of the model in the first 100 minutes can be attributed to the lack of a two-compartment consideration. However, the model predicts the final blood concentration well (BUN = 34.9 mg/dL vs. 36.4 mg/dL experimental).

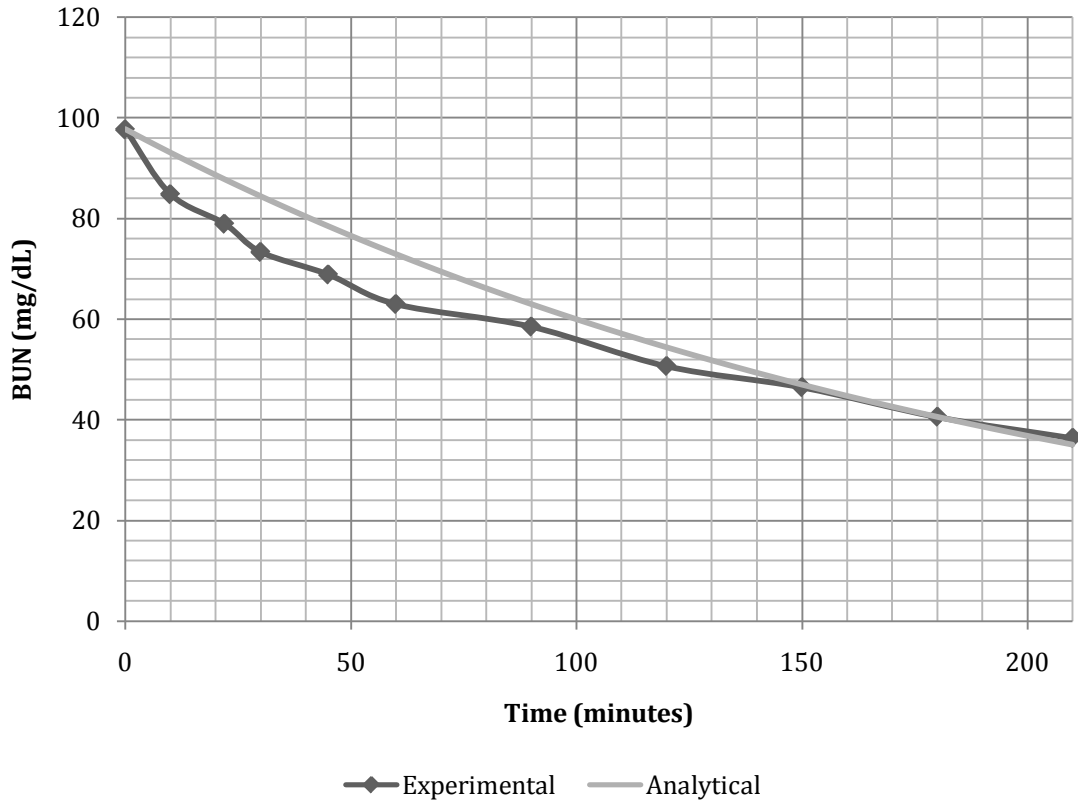


**Figure 5-6. The one-compartment Matlab model (dashed line) compared to the published results (solid line) of Ziólko et al. (2000).**

Given the validity of the model, the next step is to design a feasible portable daily hemodialysis system. The great variance in patient variables (blood volume, urea generation rate, etc.) prevents one from proposing a single system configuration for all patients.

## 5.2 Modeling basic hemodialysis scenarios

The model created can now be used to model outcomes of various hemodialysis situations.

This section will only focus on modeling basic dialyzer performance. Section 5.2 will address the effects of dose length and treatment schedules. Table 5-1 details the simulations in this section.

**Table 5-1. The simulations in Section 5.1.**

Section	Recirculation	Urea Generation	Figure
5.2.1	No	No	Figure 5-7
5.2.2	Yes	No	Figure 5-8
5.2.3	No	Yes	Figure 5-10
5.2.4	Yes	Yes	Figure 5-11

### 5.2.1 Basic system with no recirculation or urea generation

The first test to run on the model is the most basic configuration: blood and dialysate running counter current through a typical-size dialyzer until the urea has been cleared from the blood. The blood flow rate was arbitrarily set at 100 mL/min and the initial BUN was set at 500 mg/L (10.1743 mg of urea per mL of blood). Detailed test conditions are in Table 5-2.

**Table 5-2. Input parameters associated with Figure 5-7.**

Parameter	Value
Initial BUN ( $C_{Bi}$ )	500 mg/L
Blood flow rate ( $Q_B$ )	100 mL/min
$K_0A$	1,200 mL/min
Trade-off coefficient ( $\alpha$ )	0.95
Blood volume ( $V_B$ )	1,000 mL
Ultrafiltration flow rate ( $Q_F$ )	0.000 mL/min
Urea generation rate ( $\dot{G}$ )	0.000 mg/min

**Table 5-3. Output parameters associated with Figure 5-7.**

Parameter	Value
Dialysate flow rate ( $Q_D$ )	108 mL/min
Clearance ( $K$ )	95.11 mL/min
Dialysate Volume ( $V_D$ )	8,640 mL
Dialysance ( $D$ )	95.08
Final BUN	0.1689 mg/L

The results from this simulation, graphed in Figure 5-7, were not surprising. The largest rate of urea clearance is experienced in the beginning of the experiment when there is the greatest

gradient between the blood and dialysate concentrations. While the dialysate concentration of urea remains 0 mg/mL throughout the simulation, as the blood is cleaned its concentration decreases.

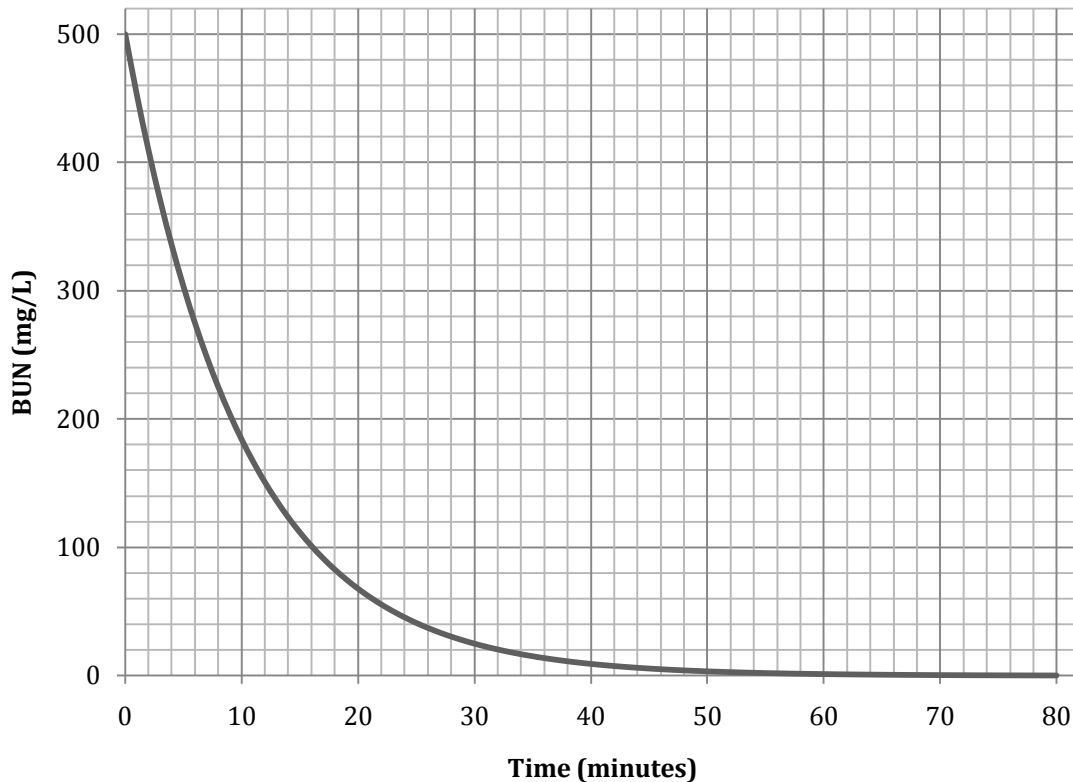


**Figure 5-7. A simple dialyzer circuit without dialysis recirculation or urea generation. The predicted BUN drops below 1 mg/L after 63 minutes. See Table 5-2 for a detailed list of the parameter values.**

The dialysance ( $D$ ) of this experiment does not change (the model predicts a value of 95.08), even as the blood concentration decreases. Since dialysance is the ratio of the concentration change of the blood to the concentration gradient between the blood and dialysate, as the concentration gradient decreases, less urea will be removed from the blood.

After 63 minutes, the BUN of the blood is predicted to drop below 1 mg/L, resulting in blood that is effectively free of urea.

The next test of the model is to recirculate the dialysate that passes through the dialyzer.

### 5.2.2 Basic system with recirculation but no urea generation

When the dialysate volume is capped and recirculated through the dialyzer, its increasing urea concentration becomes a concerning issue. As urea is transferred from the blood to the dialysate, the concentration gradient between the blood and dialysate decreases, reducing the driving force in membrane-based dialysis.

When the same variables are run through the same model as in Section 5.2.1, but the dialysate volume is capped at 2.0 L, the effects of dialysate recirculation become clear. Figure 5-8 is the plot of this simulation, which shows the final BUN of the blood settling around 167 mg/L. Also plotted (as a dashed line) are the results of the exact same simulation without dialysate recirculation. Details of the simulation are in Table 5-4 and Table 5-5.

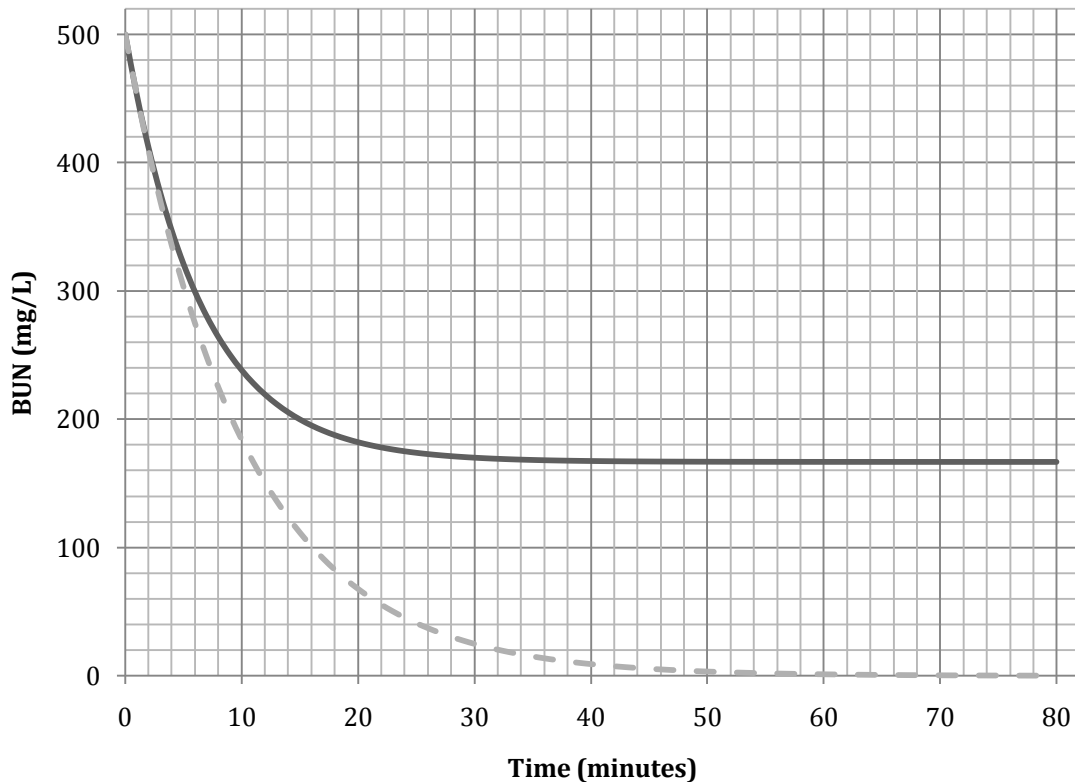


Figure 5-8. A simple dialysis circuit with dialysate recirculation, but no urea generation.

Verification of this simulation can be provided by assuming that after sufficient time the urea will be evenly distributed between the blood and dialysate volumes. Because the initial concentration of urea in the blood is 10.1743 mg/mL, and there is 1000 mL of blood, there is 10174.3 mg of urea initially in the blood. The total fluid volume in the simulation (dialysate volume and blood volume combined) is 3000 mL, so an even distribution of urea would result in a urea concentration of 3.5714 mg/mL, or a BUN reading of 166.6667 mg/L. This is exactly what the model predicts, with a BUN dropping below 167 mg/L after 44 minutes.

**Table 5-4. Input parameters associated with Figure 5-8.**

Parameter	Value
<b>Initial BUN (<math>C_{Bi}</math>)</b>	500 mg/L
<b>Blood flow rate (<math>Q_B</math>)</b>	100 mL/min
<b><math>K_0A</math></b>	1,200 mL/min
<b>Trade-off coefficient (<math>\alpha</math>)</b>	0.95
<b>Blood volume (<math>V_B</math>)</b>	1,000 mL
<b>Ultrafiltration flow rate (<math>Q_F</math>)</b>	0.000 mL/min
<b>Urea generation rate (<math>\dot{G}</math>)</b>	0.000 mg/min

**Table 5-5. Output parameters associated with Figure 5-8.**

Parameter	Value
<b>Dialysate flow rate (<math>Q_D</math>)</b>	108 mL/min
<b>Clearance (<math>K</math>)</b>	95.11 mL/min
<b>Dialysate Volume (<math>V_D</math>)</b>	2,000 mL
<b>Dialysance (<math>D</math>)</b>	95.08
<b>Final BUN</b>	166.67 mg/L

This test also raises concern for the feasibility of dialysate reuse in a hemodialysis system. The alternative to recycling 2 L of dialysate through the dialyzer is to simply use 2 L of dialysate in single-pass mode, and stop dialysis once the dialysate runs out. This will always provide the dialyzer with the maximum concentration gradient, but it will not run as long.

When the exact same parameters are run through the model as listed in Table 5-4, but the dialysate is run in a single-pass mode and shut off after 19 minutes (using 2.052 L of dialysate, approximately the same volume used in the previous test), the blood reaches a significantly lower urea concentration (63.72 mg/dL) than when the dialysate is recirculated (166.67 mg/dL). The dark line in Figure 5-9 is 2.0 L run in single-pass mode, while the dotted line is 2.0 L continuously recirculated.

In a human, there is constant urea generation (the impact of which is explored in the next section). If the dialyzer is shut off after 19 minutes, any urea that is generated is left in the blood if the dialyzer is shut off.

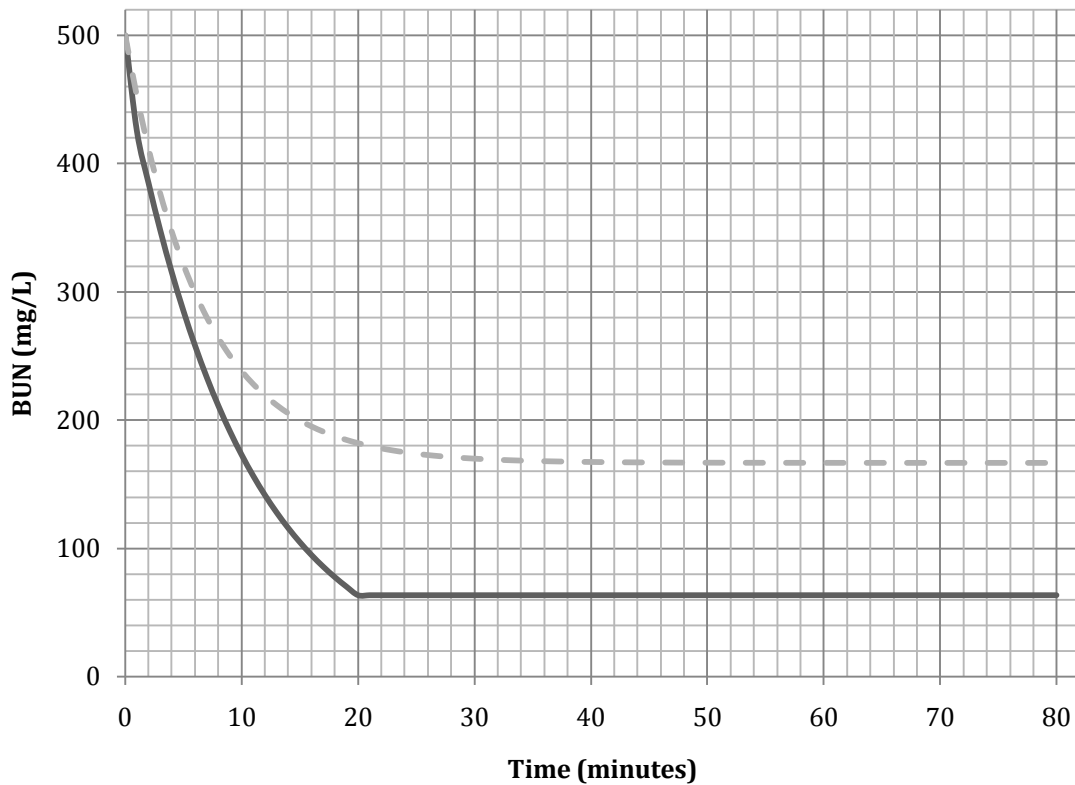


**Figure 5-9. Two liters of dialysate are used in single-pass for 19 minutes, and then the dialyzer is shut off. The dotted line is the same parameters, but the 2 L is allowed to recirculate for the full 80 minutes.**

### 5.2.3 Basic system with urea generation and no recirculation

One would expect that the steady state value of a system with urea generation would be slightly higher than a system without it – eventually there will be a balance after the dialyzer has removed all residual urea from the blood. This is exactly the case, as shown in Figure 5-10. The darker line – the case with urea generation – always has a urea concentration slightly higher and settles on a higher final value. Detailed system parameters are listed in Table 5-6 and Table 5-7.

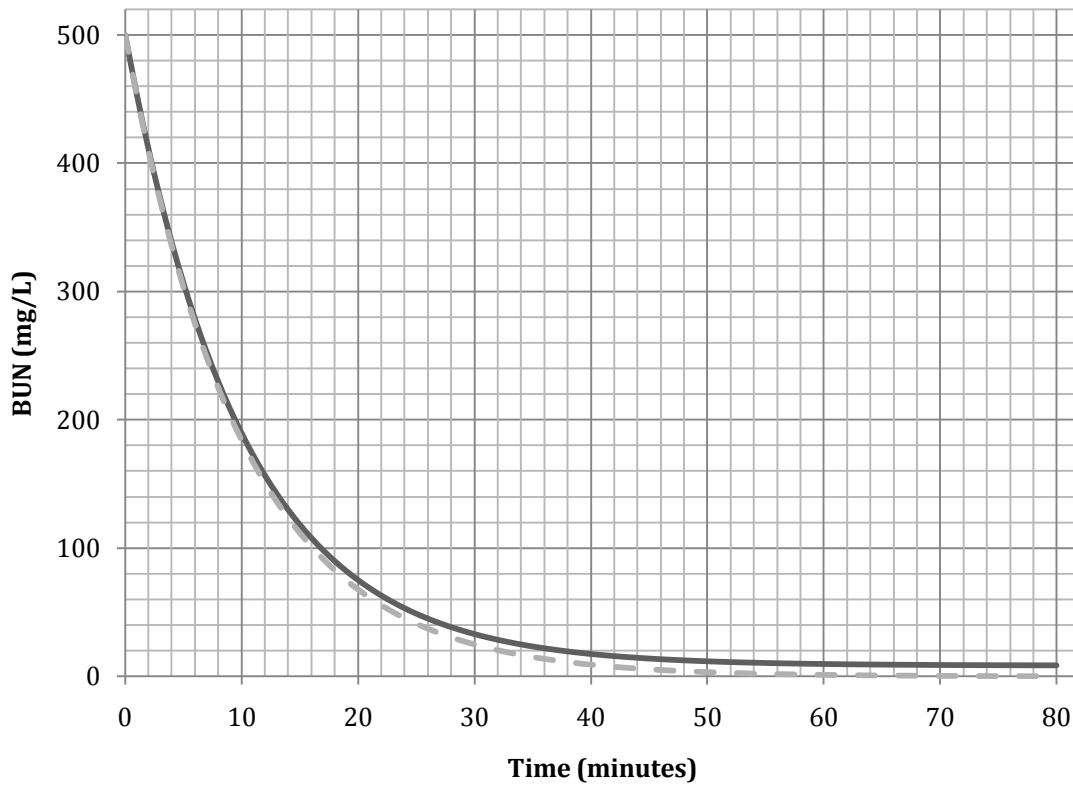


**Figure 5-10. A simple dialysis circuit with no dialysate recirculation, but a constant urea generation rate of 17.3611 mg/min. The dotted line is the expected performance when there is no urea generation.**

While this case behaves as expected, it should be noted that it had a minimal impact on the concentration of urea in the blood during dialysis. Not that including urea generation is

inconsequential: its effects become very important in a daily or weekly model of urea removal (explored in Section 5.4).

**Table 5-6. Input parameters associated with Figure 5-10.**

Parameter	Value
Initial BUN ( $C_{Bi}$ )	500 mg/L
Blood flow rate ( $Q_B$ )	100 mL/min
$K_0A$	1,200 mL/min
Trade-off coefficient ( $\alpha$ )	0.95
Blood volume ( $V_B$ )	1,000 mL
Ultrafiltration flow rate ( $Q_F$ )	0.000 mL/min
Urea generation rate ( $\dot{G}$ )	17.3611 mg/min

**Table 5-7. Output parameters associated with Figure 5-10.**

Parameter	Value
Dialysate flow rate ( $Q_D$ )	108 mL/min
Clearance ( $K$ )	95.11 mL/min
Dialysate Volume ( $V_D$ )	8,640 mL
Dialysance ( $D$ )	95.08
Final BUN	8.69 mg/L

#### 5.2.4 Basic system with recirculation and urea generation

The question arises over whether it is better to run the dialyzer in single pass mode for a shorter period, or use the same volume of dialysate and recirculate it for a longer period.

The issue of urea generation becomes more important in this discussion. While it was shown in the scenario presented in Figure 5-9 that it was beneficial to run the dialyzer in single-pass mode, there was no urea generation in that simulation. Figure 5-11 is the same simulation run with a urea generation rate of 17.361 mg/min, corresponding to a healthy human's generation rate of 25 g/day.

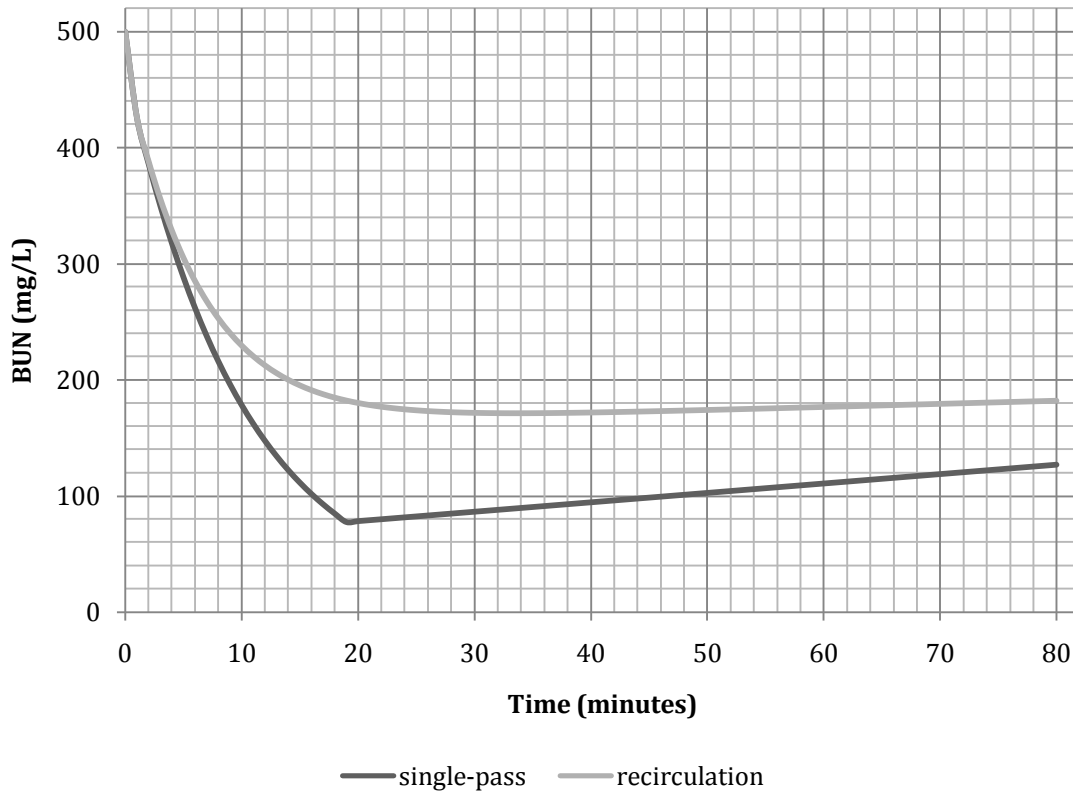


**Figure 5-11. Comparing dialysate recirculation to single-pass. Both simulations used approximately the same volume of dialysate.**

Even with this relatively high urea generation rate (dialysis patients typically lower their urea generation rate through dietary changes), after 80 minutes the single-pass simulation still has a lower urea concentration (127.08 mg/dL) than the simulation with mixing (182.06 mg/dL). In this particular scenario, the single-pass was superior. However, it is conceivable that the recirculation model could provide better urea clearances under certain conditions – perhaps when the fixed volume of dialysate is higher or the urea generation rate is greater.

The lesson to be learned from this comparison is that whenever dialysate recirculation is considered, one must also consider the results from running that same volume of dialysate through the dialyzer in single-pass mode for a shorter time. The Simulink model does not predict

automatically which method is best for the given scenario, so each needs to be tested before drawing any conclusions.

### **5.3 Steady state behavior and sample size**

Before hemodialysis scenarios are modeled, two additional behaviors of the model must be investigated. First, Section 5.3.1 explores the effect picking different initial BUNs has on the final outcome of the model. Then Section 5.3.2 examines the effect of different sample sizes in long-term hemodialysis modeling.

#### **5.3.1 Initial BUN selection and steady state behavior**

When a hemodialysis scenario is modeled, many different variables must be selected (see Section 4.7.1.1). While nearly all variables have an important impact on accurately modeling (such as the blood and dialysate flow rates), the initial BUN actually has no long-term impact on the results.

Regardless of the initial BUN, the system will decay to a steady state. In Figure 5-12, three different hemodialysis scenarios are plotted, each corresponding to a different initial BUN. All other variables were kept identical to highlight the effect of different initial BUNs.

Plots are provided corresponding to initial BUNs of 70 mg/dL, 30 mg/dL, and 10 mg/dL. Each plot decays to a steady state daily cycling between 21 mg/dL and 3 mg/dL.

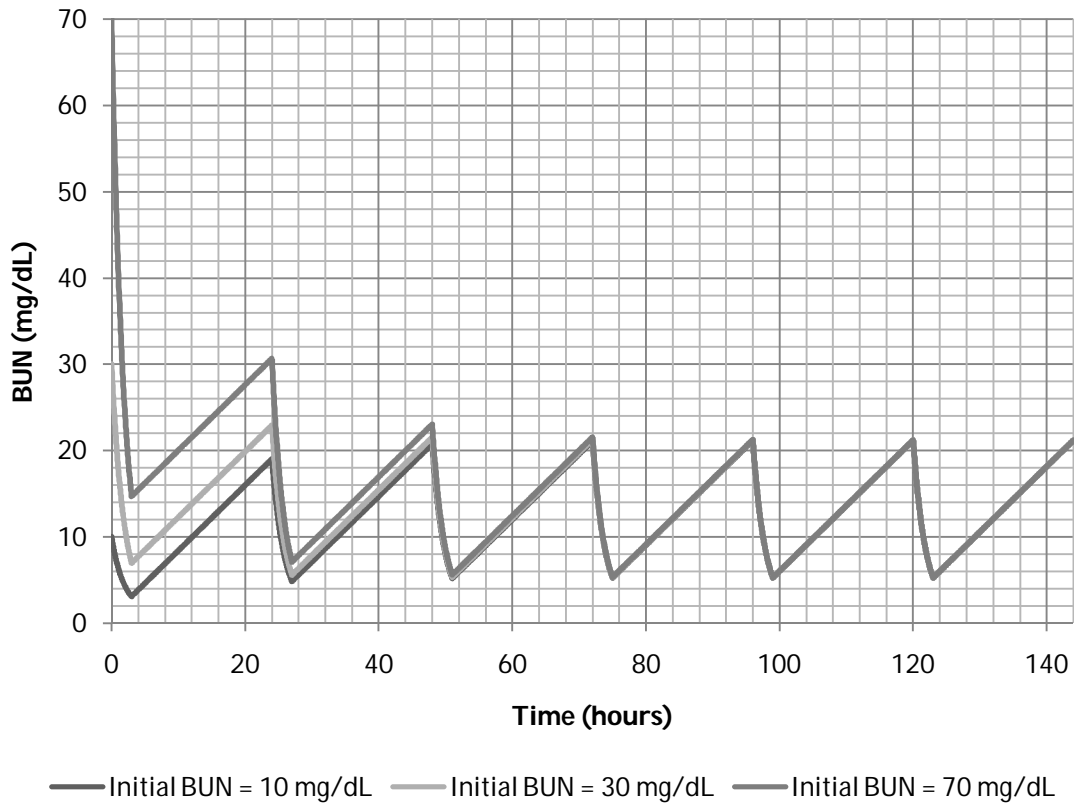


**Figure 5-12. Regardless of the initial BUN, after several days the daily BUN cycle is the same. The only difference between the plots is the initial BUN – every other parameter ( $K_0A$ ,  $Q_B$ ,  $Q_D$ , etc.) is the same.**

The peaks of the plots in Figure 5-12 seem to decay in an exponential fashion. If just the peaks are connected by a fitted curve, the exponential relationship becomes clear. Figure 5-13 plots the hemodialysis simulation results for an initial BUN of 70 mg/dL and a dashed best-fit curve connecting its peaks.

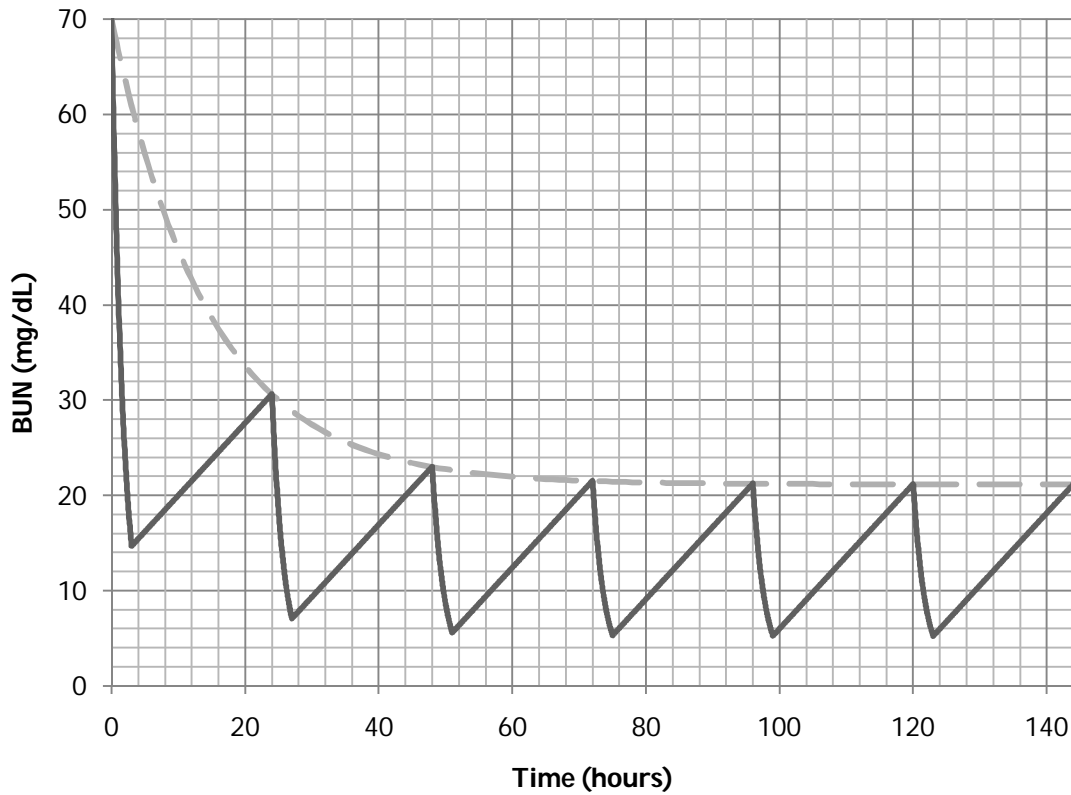


**Figure 5-13. When the peaks of the simulation corresponding to an initial BUN of 70 mg/dL are connected (dashed line) an exponential curve is formed.**

To completely examine the effect of different initial BUNs, the daily maximums from all three different initial BUN plots are plotted in Figure 5-14. Exponential curves (listed in Table 5-8) are fitted to each plot.

**Table 5-8. The curve fit equations for the plots in Figure 5-14.**

Curve Fit Equation	Initial BUN
$y = 21.185 + 48.815e^{-0.068409x}$	70 mg/dL
$y = 21.183 + 8.817e^{-0.068409x}$	30 mg/dL
$y = 21.182 - 11.182e^{-0.068409x}$	10 mg/dL

Interestingly, the time constant for each curve is the same ( $\tau = 1/-0.068409 = -14.618$ ). That means that for each set of hemodialysis conditions ( $Q_B$ ,  $Q_D$ ,  $K_0A$ , etc.) there exists a fixed time constant that dictates how quickly the patient's BUN cycle will reach a steady state condition.

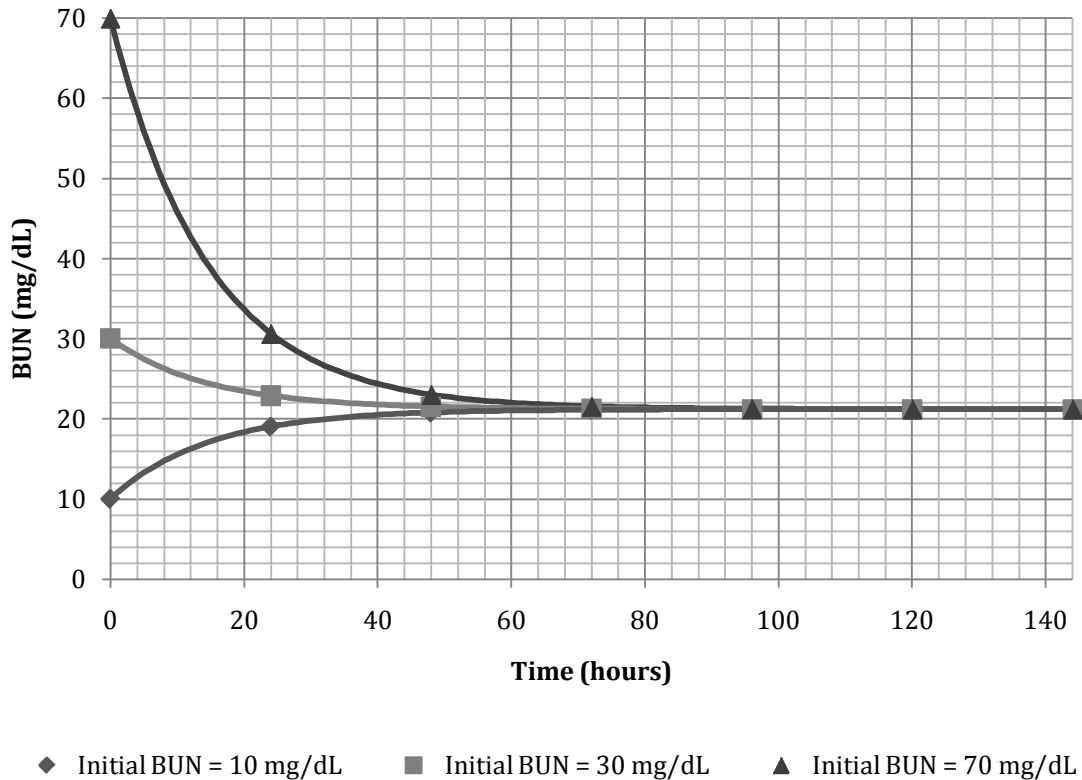


**Figure 5-14. The daily peaks of each plot in Figure 5-12 are plotted. A simple exponential curve accurately describes how each plot decays to the same steady state conditions.**

A governing property of a hemodialysis configuration is its dialysance ( $D$ ) (Equation 4-21; for details see Section 4.3.4). It is a function of the flow rates ( $Q_B$  and  $Q_D$ ) and the dialyzer ( $K_0A$ ), but not the initial BUN. If there were a way to predict how quickly a patient will reach steady state conditions, examining the relationship between the dialysance and the time constant might yield significant results.

When devising hemodialysis configurations, one can select an initial BUN that corresponds to the steady state daily maximum – even if a different value is selected, the system will decay to it anyway. In each of the simulations presented in this thesis, different initial BUNs were tested to determine the steady state value. Each simulation is plotted with an initial BUN that roughly corresponds to the steady state value.

### **5.3.2 Examining the effects of sample size in the model**

By default, the model samples and recalculates the urea concentration of the blood in one-minute intervals. However, this sample size could be too large for long-term predictions (simulating one week of dialysis would require over 10,000 samples). To test the model flexibility to other sample sizes, identical hemodialysis conditions were plotted (corresponding to the published data of Ziólko et al. (2000), Figure 5-6) at six-second, one-minute, and ten-minute intervals in Figure 5-15.

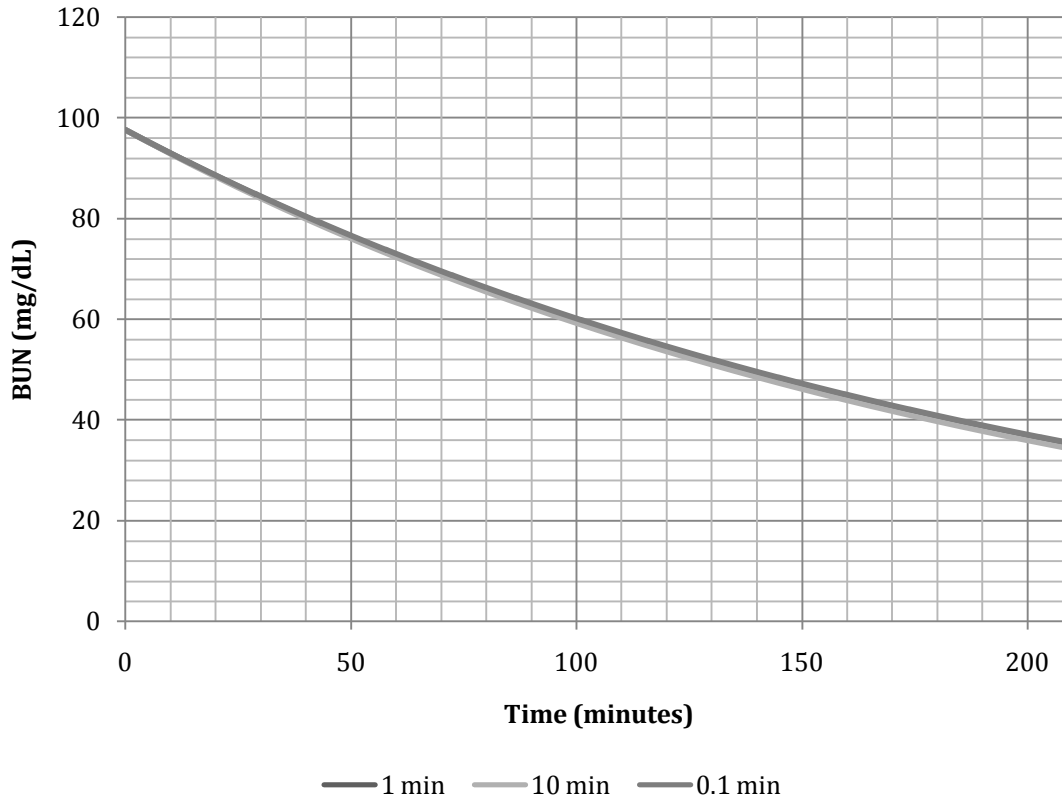


**Figure 5-15. The published hemodialysis input data (Figure 5-6) is modeled at three different time intervals: 1 min, 10 min, and 0.1 min.**

The discrepancy between the three plots is smaller than errors than can be expected from patient variability and other assumptions. The six-second interval predicted a final BUN of 35.360 mg/dL (1.04 mg/dL difference from experimental results), the one-minute interval predicted 34.869 mg/dL (1.531 mg/dL difference), and the ten-minute interval predicted 34.234 mg/dL (2.166 mg/dL difference).

The next test is to see whether using a larger interval size brings increasing discrepancy or decreasing discrepancy. Because no published data is available for a changing BUN over the course of a week, only the variance between two sample sizes can be tested. Figure 5-16 plots one- and ten-minute intervals over the course of a week.

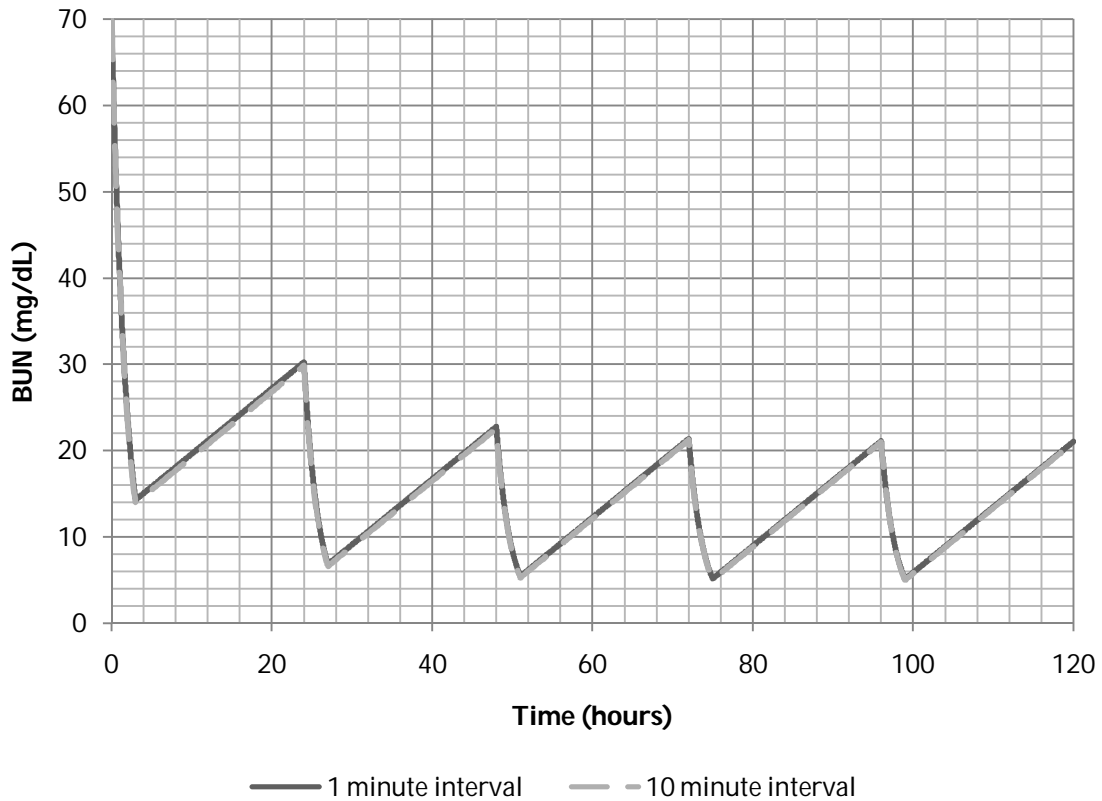


**Figure 5-16. Two different sampling sizes are plotted. The 10-minute interval line (grey, long dashes) is able to predict the final BUN calculated equally as accurate as when using 1-minute intervals.**

The one- and ten-minute intervals predicted nearly the same final BUN (21.021 and 20.904 mg/dL, respectively). Ten-minute intervals seem to have sufficient accuracy – other errors associated with hemodialysis will likely have much more influence. The difference between random points of the two plots in Figure 5-16 are plotted in Figure 5-17. As time increases, the difference between the plots decreases. While this does not indicate superior accuracy of either interval, both appear to have comparable precision.

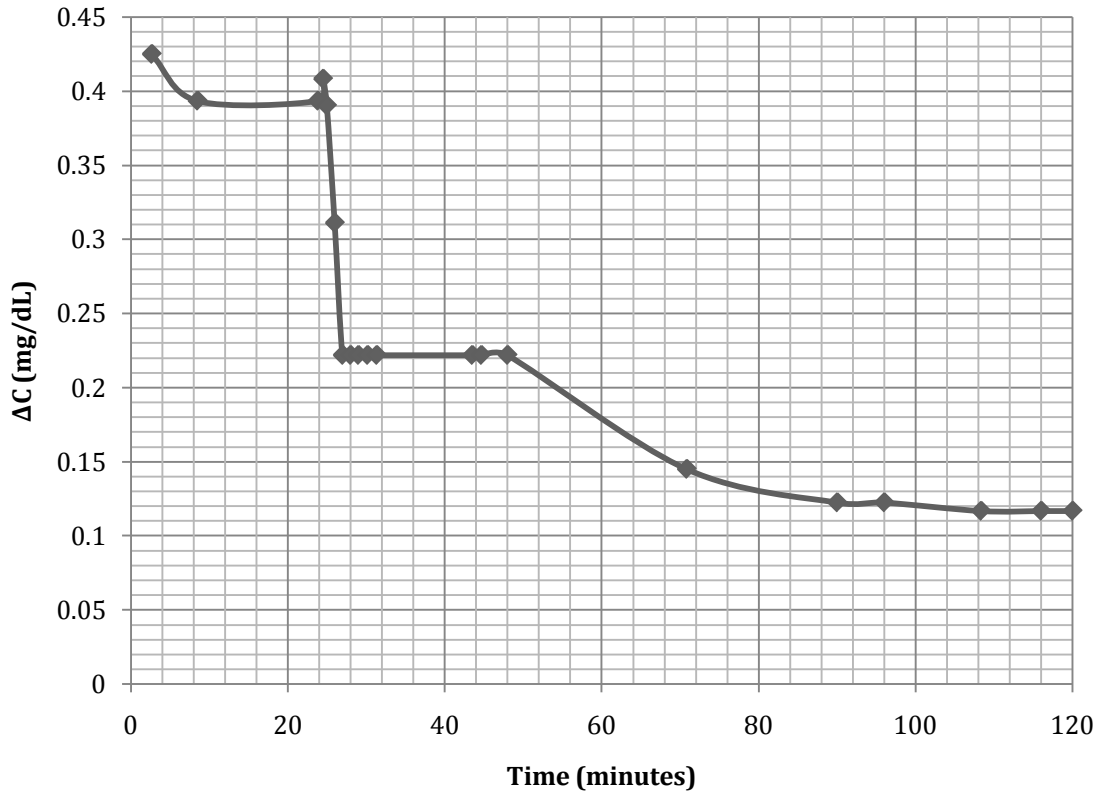


**Figure 5-17. The discrepancy between the two plots of Figure 5-16 are plotted. As time increases, the difference between the two plots decreases.**

In this thesis, one-minute intervals are used unless otherwise noted.

#### **5.4 Modeling hemodialysis**

The next step in the development of the model is to recreate human physiology, instead of a lab setup. The important difference between these two settings is that when selecting parameters for human hemodialysis, daily or weekly cycles must be taken into account.

Table 5-9 provides a summary of the situations modeled (and their associated figures) in this section.

**Table 5-9. The scenarios modeled in this section.**

	Section	Recirculation	Regeneration	Figure(s)
<b>Clinical Hemodialysis</b>	5.4.1	No	Yes	Figure 5-18
<b>Home Hemodialysis</b>	5.4.2	No	Yes	Figure 5-19 Figure 5-20
<b>Home Hemodialysis (with Recirculation)</b>	5.4.3	Yes	Yes	Figure 5-21 Figure 5-22
<b>Best- and realistic-case scenarios</b>	5.4.4	No	Yes	Figure 5-23 Figure 5-24

#### **5.4.1 Recreating a typical clinical hemodialysis scenario**

The first test of this model is to recreate traditional clinical hemodialysis. Figure 5-18 is the results from the model when parameters commonly associated with traditional dialysis are used. The blood flow rate was kept high at 300 mL/min (resulting in a trade-off dialysate flow rate of 442 mL/min), and 2-hour treatments every other day. Table 5-10 and Table 5-11 list the inputs and outputs of this simulation.

The various inputs of this model are selected to be as typical as possible. The dialyzer was chosen to be large ( $K_0A = 1600$  mL/min), because clinics are free to use the largest dialyzer available to them. Additionally, the model predicts no negative impact from choosing the largest possible dialyzer (Figure 4-9). The blood flow rate was set at 300 mL/min (Ward & Leypoldt, 2001), although higher flow rates are very common (Berkoben & Schwab, 2003) and the urea generation rate was set to 12.5 g/day – half the rate of a healthy human (Moffett, Moffett, & Schauf, 1993), to account for dietary changes patients commit to. There is not a standard treatment schedule for dialysis patients, but three times a week is often cited (Piccoli, et al., 2000) (Kjellstrand & Ing, 1998) (Daugirdas, 1993).

Determining the total fluid volume of a patient is complicated, and many different formulae are employed (Ziólko, Pietrzyk, & Grabska-Chrząstowska, 2000). The simplest (and most commonly used model) simply considers the patient's gender and dry weight, as shown in Equation 5-1.

$$V_{male} = 0.58 \times DW \quad V_{female} = 0.55 \times DW \quad (5-1)$$

In the following simulations, a fluid volume of 32,000 mL was chosen because it is the same value as the patient used in the verification of the model in Section 5.1.

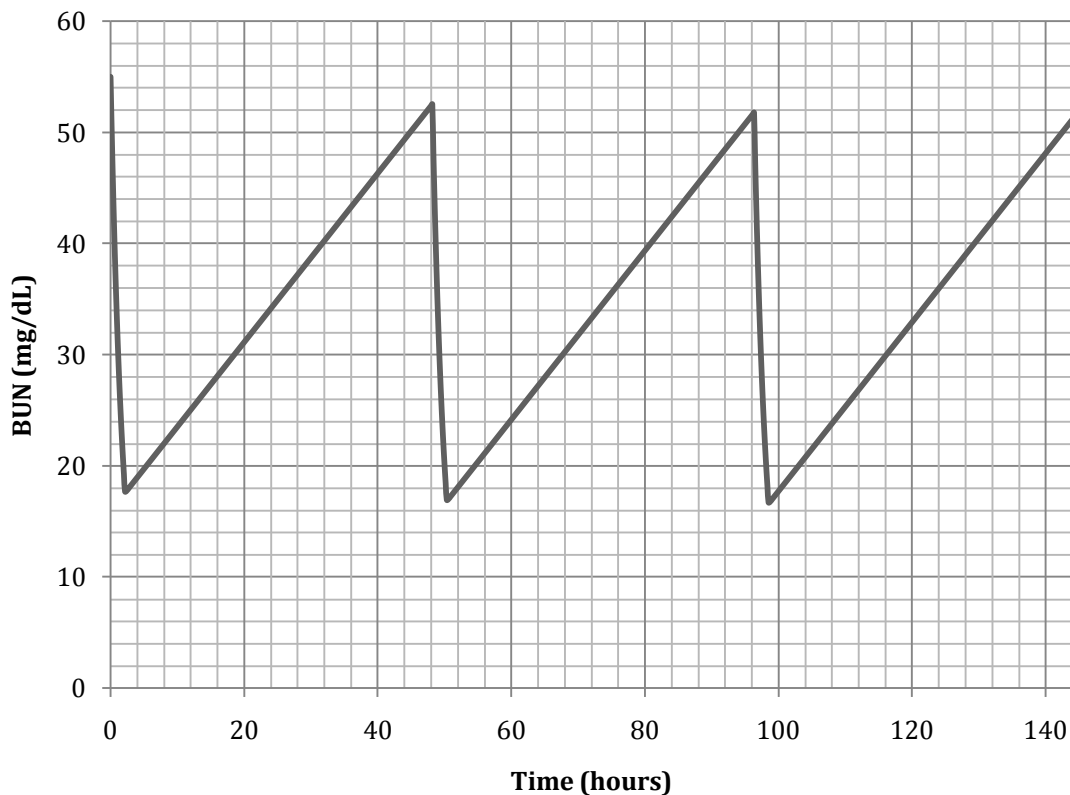


**Figure 5-18. The model predicting the results of traditional hemodialysis. The patient is dialyzed every other day for two hours.**

The results shown in Figure 5-18 are what one would expect from clinical hemodialysis. The patient begins the first treatment at the elevated BUN of 55 mg/dL, and after two hours of treatment has a reduced BUN of just below 19 mg/dL. Forty-six hours later, his or her BUN is nearing 53 mg/dL and

they are dialyzed for another two hours. This repeats every other day, and the patient's BUN never surpasses 53 mg/dL.

**Table 5-10. Input parameters used for simulation in Figure 5-18.**

Parameter	Value
<b>Initial BUN (<math>C_{Bi}</math>)</b>	55 mg/dL
<b>Blood flow rate (<math>Q_B</math>)</b>	300 mL/min
<b><math>K_0A</math></b>	1,600 mL/min
<b>Trade-off coefficient (<math>\alpha</math>)</b>	0.95
<b>Blood volume (<math>V_B</math>)</b>	32,000 mL
<b>Ultrafiltration flow rate (<math>Q_F</math>)</b>	0.000 mL/min
<b>Urea generation rate (<math>\dot{G}</math>)</b>	8.681 mg/min
<b>Treatment length (<math>t_1</math>)</b>	2 hours
<b>Time between treatment (<math>t_2</math>)</b>	46 hours
<b>Simulation sample interval</b>	10 minutes

**Table 5-11. Output parameters of simulation in Figure 5-18.**

Parameter	Value
<b>Dialysate flow rate (<math>Q_D</math>)</b>	442 mL/min
<b>Clearance (<math>K</math>)</b>	280.25 mL/min
<b>Dialysate Volume (<math>V_D</math>)</b>	53,040 mL per dose
<b>Dialysance (<math>D</math>)</b>	280.21 mL/min

#### 5.4.2 A daily hemodialysis schedule without recirculation

If patients dialyze at home, some of the parameters need to be adjusted. If blood is drawn from the venous side of the circulatory system, the blood flow rate is limited to below 100 mL/min (compared to over 300 mL/min for clinical dialysis). This reduces the rate at which urea can be cleared from the blood and lengthens the treatment, but it is a safe flow rate that can be expected at home.

Detailed inputs and outputs of this simulation are listed in Table 5-12 and Table 5-13.

Table 5-12. Input parameters associated with Figure 5-19.

Parameter	Value
Initial BUN ( $C_{Bi}$ )	45 mg/dL
Blood flow rate ( $Q_B$ )	100 mL/min
$K_0A$	1,600 mL/min
Trade-off coefficient ( $\alpha$ )	0.95
Blood volume ( $V_B$ )	32,000 mL
Ultrafiltration flow rate ( $Q_F$ )	0.000 mL/min
Urea generation rate ( $\dot{G}$ )	8.681 mg/min
Residual kidney function	0.000%
Treatment length ( $t_1$ )	3 hours
Time between treatments ( $t_2$ )	21 hours

Table 5-13. Output parameters associated with Figure 5-19.

Parameter	Value
Dialysate flow rate ( $Q_D$ )	103 mL/min
Clearance ( $K$ )	95.36 mL/min
Dialysate Volume ( $V_D$ )	25,720 mL
Dialysance ( $D$ )	95.32 mL/min

Because of the slower blood flow rate the treatment time is increased to three hours to adequately dialyze the patient, as shown in Figure 5-19. After three hours of treatment, the BUN drops just below 28 mg/dL, and then rises throughout the day to a peak of around 44 mg/dL. This simulation assumes that the patient is generating 12.5 g of urea per day, which might lie at the high end of estimations. Most dialysis patients can reduce their urea generation rate significantly through dietary changes, which would allow for shorter or less frequent dialysis treatment lengths.

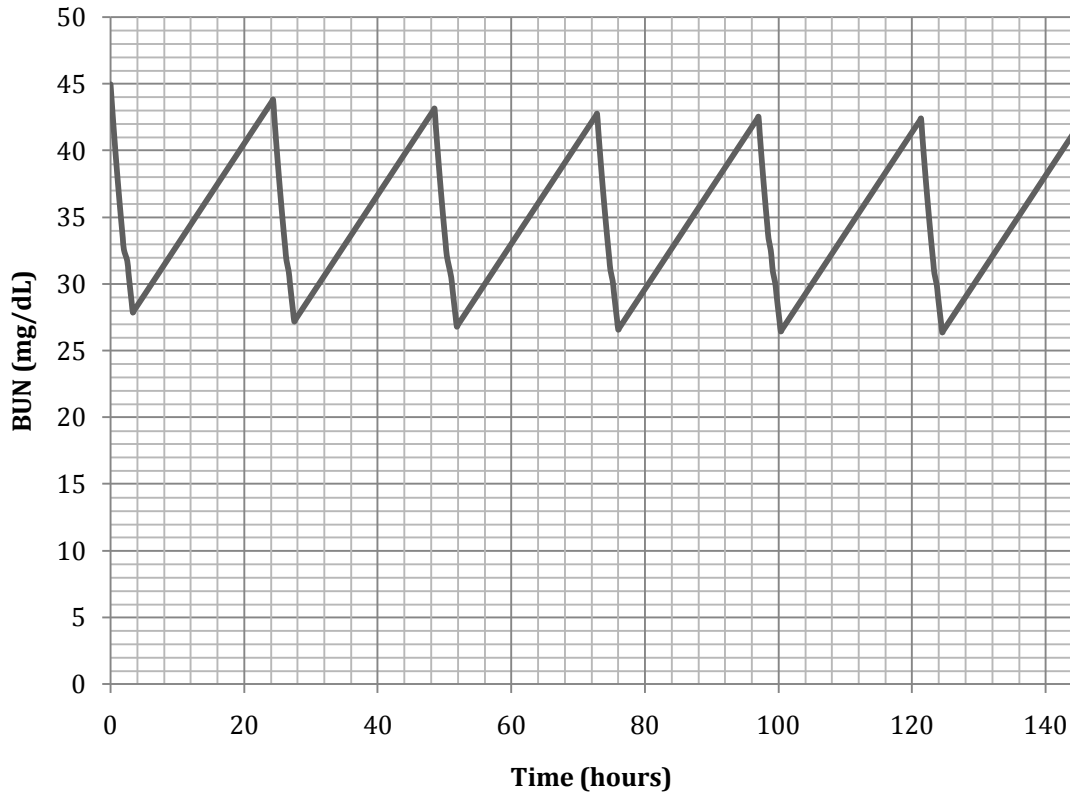


**Figure 5-19. A daily hemodialysis schedule with a limited blood flow rate.**

When the urea generation rate is halved to just 6.25 g/day (4.340 mg/min), the initial BUN raised to 48 mg/dL, and all other parameters the same as in Figure 5-19 (Table 5-12 and Table 5-13), the treatment time can be reduced to just 70 minutes per day (which also reduces the dialysate volume per dose to 7.21 L). The reduced urea generation rate (Figure 5-20) allows for a less-pronounced sawtooth pattern. Many different combinations of initial BUN and dose length were feasible; if a lower average BUN were desired a longer treatment time could be selected.

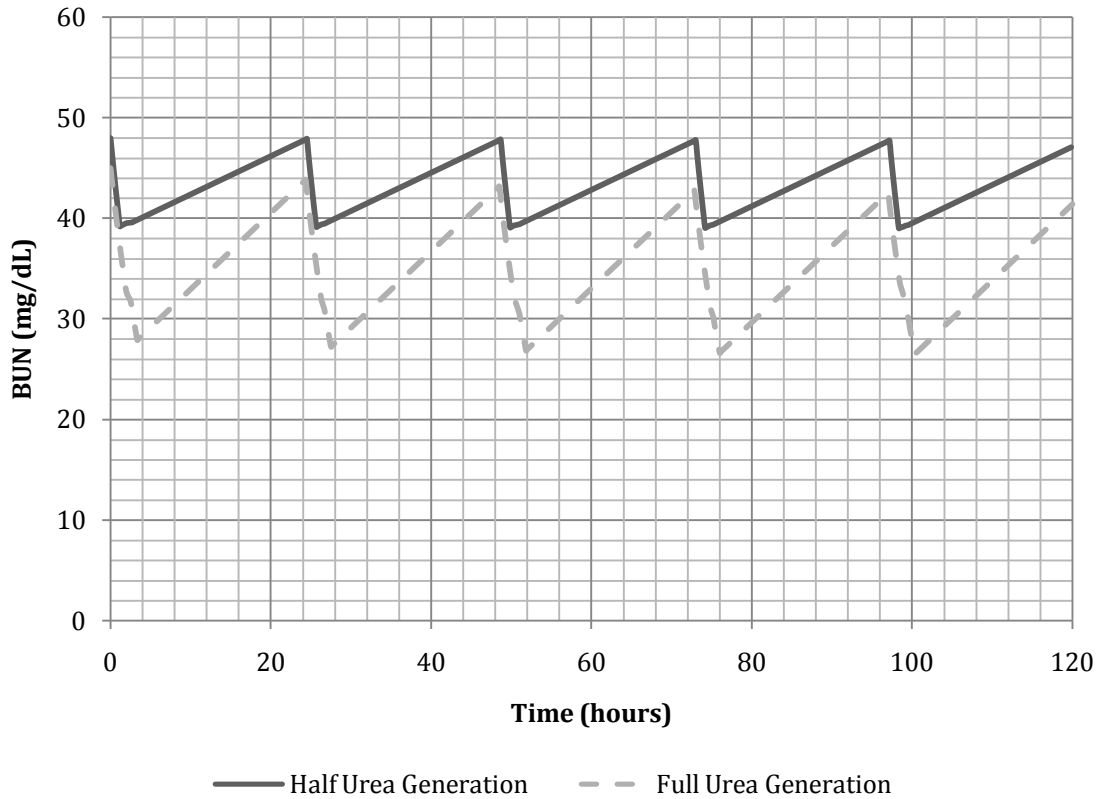


**Figure 5-20. A daily home hemodialysis schedule with a reduced urea generation rate of 6.25 g/day. The dotted line is 12.5 g/day urea generation rate.**

The next section will examine a daily treatment with dialysate recirculation.

### 5.4.3 A daily hemodialysis schedule with recirculation

The idea behind dialysate recirculation is that a reduced volume of dialysate can be used to remove urea from the blood. However, previous simulations (Figure 5-11) indicate that it is most likely better to use the dialysate in single-pass mode, even with a reduced volume.

Table 5-14. Input parameters associated with Figure 5-21.

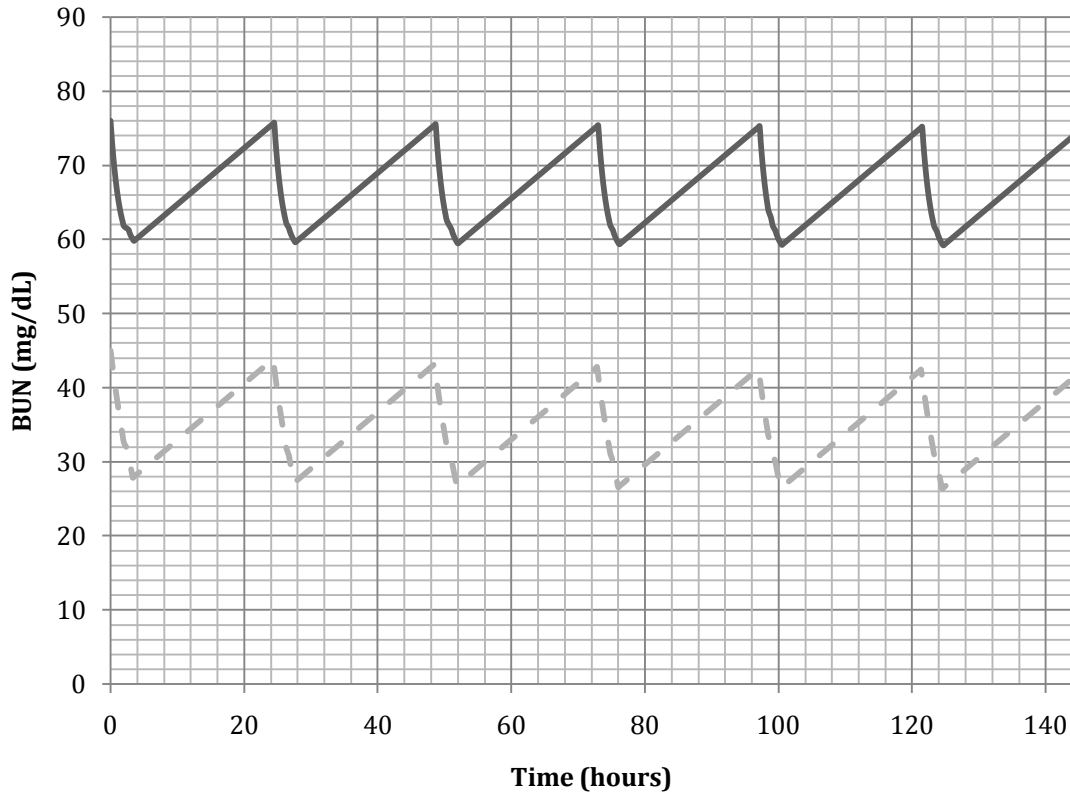
Parameter	Value
Initial BUN ( $C_{Bi}$ )	76 mg/dL
Blood flow rate ( $Q_B$ )	100 mL/min
$K_0A$	1,600 mL/min
Trade-off coefficient ( $\alpha$ )	0.95
Blood volume ( $V_B$ )	32,000 mL
Ultrafiltration flow rate ( $Q_F$ )	0.000 mL/min
Urea generation rate ( $\dot{G}$ )	8.681 mg/min
Treatment length ( $t_1$ )	3 hours
Time between treatments ( $t_2$ )	21 hours

Table 5-15. Output parameters associated with Figure 5-21.

Parameter	Value
Dialysate flow rate ( $Q_D$ )	103 mL/min
Clearance ( $K$ )	95.36 mL/min
Dialysate volume ( $V_D$ )	1,200 mL per dose
Dialysance ( $D$ )	95.32 mL/min

In Figure 5-21, two dialysis scenarios are simulated (inputs and outputs in Table 5-14 and Table 5-15). The darker line is dialysis when 12 L of dialysate are recirculated perfectly during the 3-hour dose; the dashed line is 3 hours of dialysis without recirculation (more than 12 L was used).

The difference between the two plots is considerable – the recirculated dialysate scenario never falls below a BUN of about 60 mg/mL despite a lengthy 3-hour dose. While the exact ramifications of such an elevated BUN cannot be determined from this simulation, the single-pass plot provides BUN levels that are far lower than with recirculation.



**Figure 5-21. Daily hemodialysis with a fixed amount (12 L) of dialysate recirculating per treatment. The dotted line is the same simulation without recirculation (which uses more than 12 L of dialysate, but equal treatment time).**

The poor performance of dialysate recirculation, in conjunction with the results of Figure 5-11 (which compared dialysate recirculation to a reduced dialysate dose), seems to indicate that dialysate recirculation is an ineffective way to reduce the dialysate volume.

In the previous simulation (Figure 5-21), dialysate recirculation performed much worse than the simulation without recirculation. That is easily attributed to the fact that the two scenarios had equal treatment time – but unequal dialysate volumes. An alternative way to compare them is to fix the volume of dialysate, but have different treatment times.

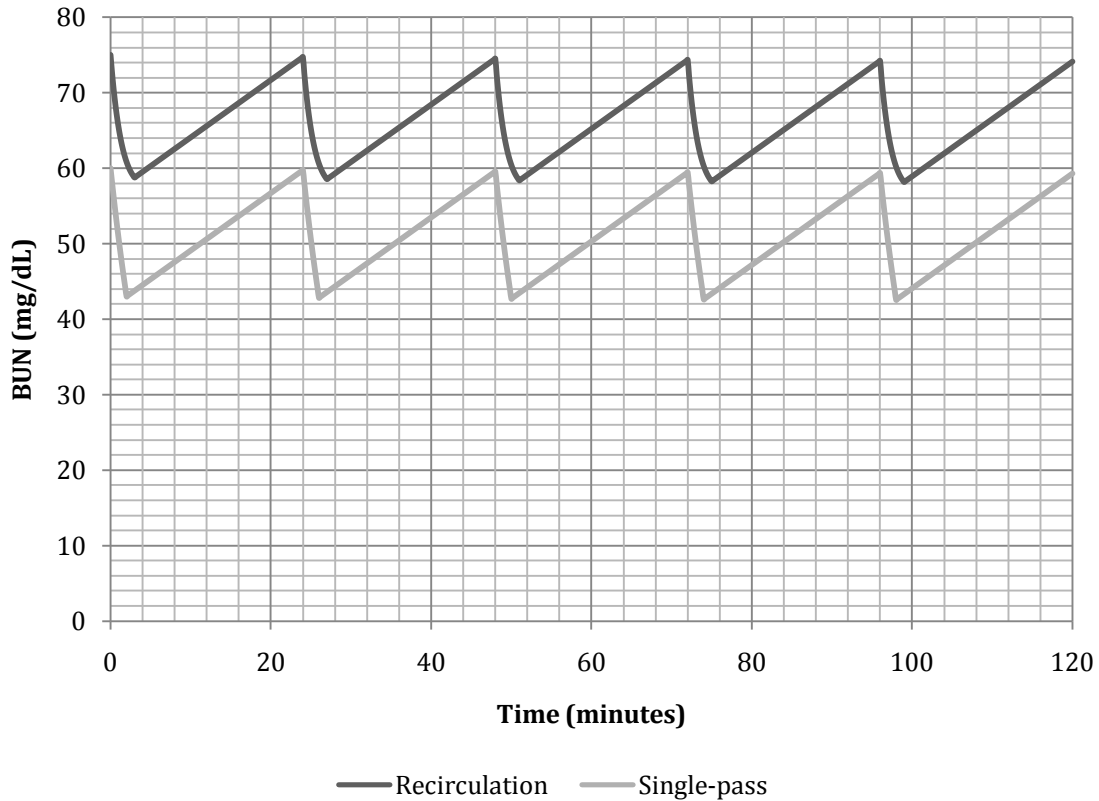


**Figure 5-22. A fixed volume of dialysate (12.36 L) is run in single-pass mode (light line) and recirculation mode (dark line). The treatment time for the single-pass simulation was shorter (2 h vs. 3 h)**

In this case (Figure 5-22), the single-pass simulation will have a shorter treatment time. In order to give the recirculation simulation the best possible performance, the dialyzer was shut off after the BUN reached an inflection point (2 hours, shown in Figure 5-22; detailed parameters in Table 5-16 and Table 5-17). Even with these more favorable conditions, it appears as though dialysate recirculation is still not superior to the single-pass simulation.

Table 5-16. Input parameters associated with Figure 5-22.

Parameter	Value
Initial BUN ( $C_{Bi}$ )	75 mg/L, 60 mg/L (single-pass)
Blood flow rate ( $Q_B$ )	100 mL/min
$K_0A$	1,600 mL/min
Trade-off coefficient ( $\alpha$ )	0.95
Blood volume ( $V_D$ )	32,000 mL
Ultrafiltration flow rate ( $Q_F$ )	0.000 mL/min
Urea generation rate ( $\dot{G}$ )	8.681 mg/min
Treatment length ( $t_1$ )	3 hours, 2 hours (single-pass)
Time between treatments ( $t_2$ )	21 hours, 22 hours (single-pass)

Table 5-17. Output parameters associated with Figure 5-22.

Parameter	Value
Dialysate flow rate ( $Q_D$ )	103 mL/min
Clearance ( $K$ )	95.36 mL/min
Dialysate volume ( $V_D$ )	12,360 mL per dose
Dialysance ( $D$ )	95.32 mL/min

#### 5.4.4 Recommended system configurations

Considering the results of the previous simulations, some final system configurations can be made. Because of the great variety of patient conditions – size, residual renal function, acceptable BUN ranges, etc. – not every possible concept can be presented. Fortunately, the model created in Chapter 4 can easily be reprogrammed to investigate a specific case not presented in this thesis.

Three cases are developed: a best-case scenario, in which every parameter is chosen to favor a portable hemodialysis system; a realistic-case scenario, in which every parameter is chosen in line with expected patient variables, and a worst-case scenario.

For example, in the best-case scenario, the largest dialyzer and blood flow rate are chosen, while the smallest urea generation rate and blood volume are selected as well (Table 5-18). In the worst-

case scenario, the opposite values are picked (Table 5-20). The results of these two cases are shown in Figure 5-23 and Figure 5-24.

It can be difficult to compare competing designs because they may have different treatment lengths or time between treatments. An example of this is Figure 5-20: a precursory examination might lead one to think that the dashed gray line is a superior treatment regimen because it corresponds to a lower average patient BUN throughout the week.

However, a strong argument can be made for the solid dark gray line. Its treatment time is only 70 minutes – compared to 180 minutes for the dash gray line. In the case of Figure 5-20, the only difference between each simulation's initial conditions was the urea generation rate ( $\dot{G}$ ). Because of the reduced urea generation rate, a shorter treatment time was possible.

Such tradeoffs must be made when suggesting treatment regimens. In the graphs that follow, two very reasonable options might be available – a higher average BUN with shorter treatment time, or a lower average BUN with longer treatment times. It is impossible to quantify these choices into any sort of model since preference will vary from patient to patient. To that end, such choices were made in the development of each simulation and are not easily visible to the reader.

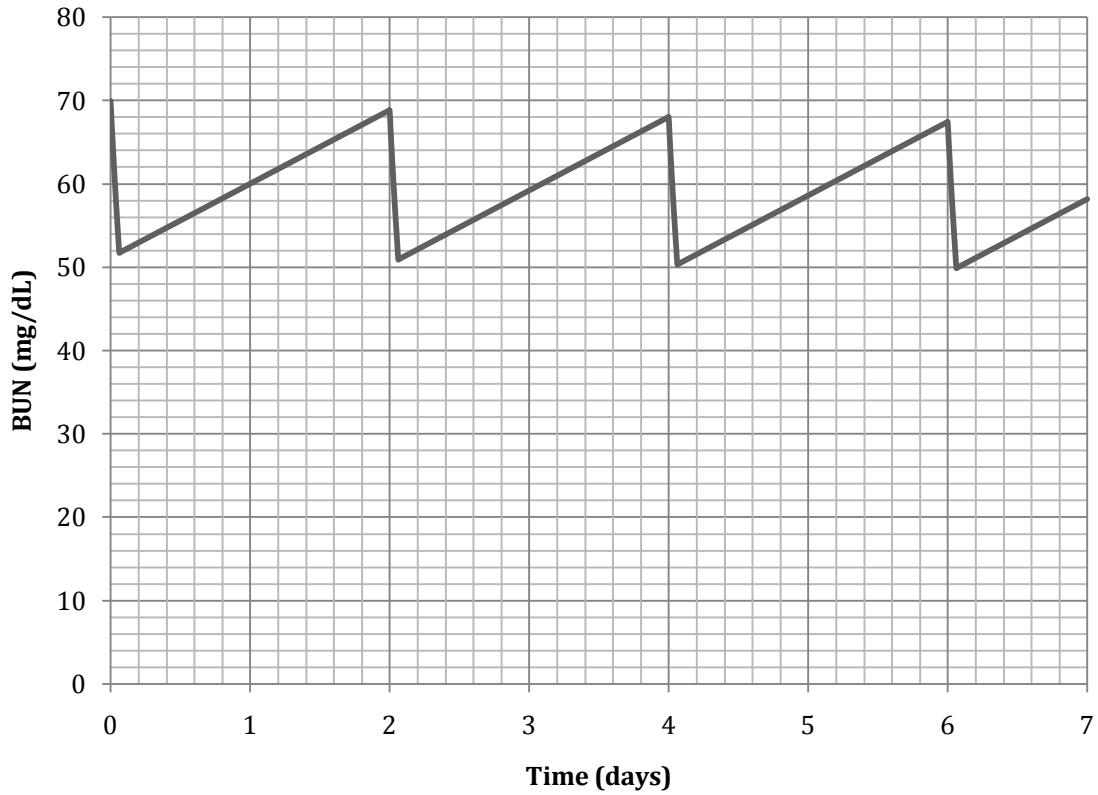


**Figure 5-23. The best-case scenario.**

In the best-case scenario (Figure 5-23), the treatment time was able to be just 90 minutes every other day and used about 9 L of dialysate while maintaining a BUN between 50 and 70 mg/dL. This simulation relied on a low body weight (47 kg) in predicting the total fluid volume to dialyze; along with such other optimal variables, that realization of a regimen as presented in Figure 5-23 is not possible. However, this was meant to represent the *best* scenario, not a typical situation.

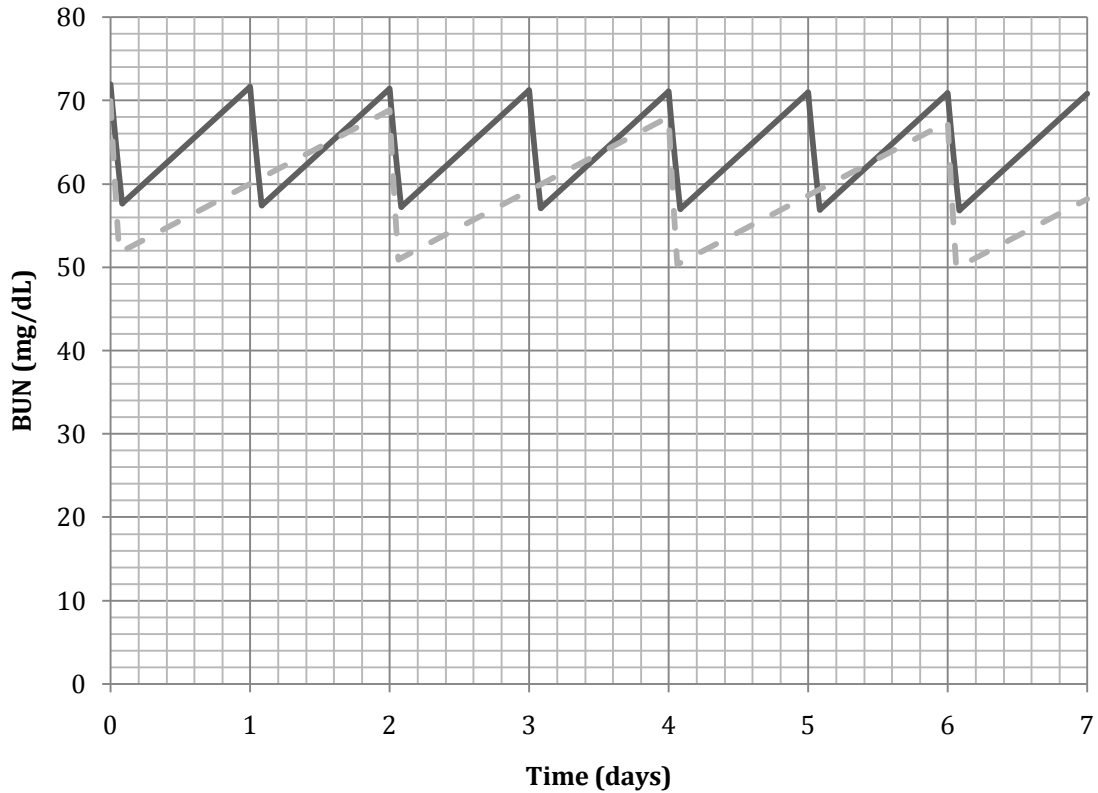


**Figure 5-24. A realistic scenario.**

In a more realistic case (Figure 5-24), the treatment time was 2 hours every day, and used 11 L of dialysate per dose. This simulation used much more practical variables – including disregarding any residual kidney function and ultrafiltration, both of which would provide increased clearances. The simulated patient weighed 63 kg.

Perhaps also important to the design of a portable hemodialysis system is the rate at which dialysate is expended. In the case of Figure 5-24, the patient would use about 6 L of dialysate per hour – low enough that portability becomes a real possibility.

Table 5-18. Input parameters for a best-case scenario.

Parameter	Value
Initial BUN ( $C_{Bi}$ )	70 mg/dL
Blood flow rate ( $Q_B$ )	100 mL/min
$K_0A$	1,600 mL/min
Trade-off coefficient ( $\alpha$ )	0.95
Blood volume ( $V_B$ )	28,000 mL
Ultrafiltration flow rate ( $Q_F$ )	0.000 mL/min
Urea generation rate ( $\dot{G}$ )	4.3403 mg/min
Treatment length ( $t_1$ )	1.5 hours
Time between treatments ( $t_2$ )	46.5 hours
Residual kidney function ( $GFR\%$ )	15.000%

Table 5-19. Output parameters for a best-case scenario.

Parameter	Value
Dialysate flow rate ( $Q_D$ )	103 mL/min
Clearance ( $K$ )	95.36 mL/min
Dialysate volume ( $V_D$ )	9,270 mL per dose
Dialysance ( $D$ )	95.32 mL/min

Table 5-20. Input parameters for a realistic scenario.

Parameter	Value
Initial BUN ( $C_{Bi}$ )	72 mg/L
Blood flow rate ( $Q_B$ )	80 mL/min
$K_0A$	800 mL/min
Trade-off coefficient ( $\alpha$ )	0.95
Blood volume ( $V_B$ )	38,000 mL
Ultrafiltration flow rate ( $Q_F$ )	0.000 mL/min
Urea generation rate ( $\dot{G}$ )	8.68056 mg/min
Treatment length ( $t_1$ )	2 hours
Time between treatments ( $t_2$ )	22 hours
Residual kidney function ( $GFR\%$ )	0.000%

**Table 5-21. Output parameters for a realistic scenario.**

<b>Parameter</b>	<b>Value</b>
<b>Dialysate flow rate (<math>Q_D</math>)</b>	91 mL/min
<b>Clearance (<math>K</math>)</b>	76.1 mL/min
<b>Dialysate volume (<math>V_D</math>)</b>	10,920 mL per dose
<b>Dialysance (<math>D</math>)</b>	76.09 ml/min

Finally, a worst-case scenario can be examined. In this case, the smallest dialyzer ( $K_0A = 800$  mL/min), the lowest blood flow rate ( $Q_B = 80$  mL/min), a large patient ( $V_B = 53$  L corresponding to a body weight of 91 kg or 200 lbs), and the trade-off dialysate flow rate ( $Q_D = 91$  mL/min) is selected.

With these inputs, a daily hemodialysis system is still possible. By increasing the range of BUN values to 80–90 mg/dL, a daily treatment length of 90 minutes (using 8.19 L of dialysate per dose) is possible, as shown in Figure 5-25.

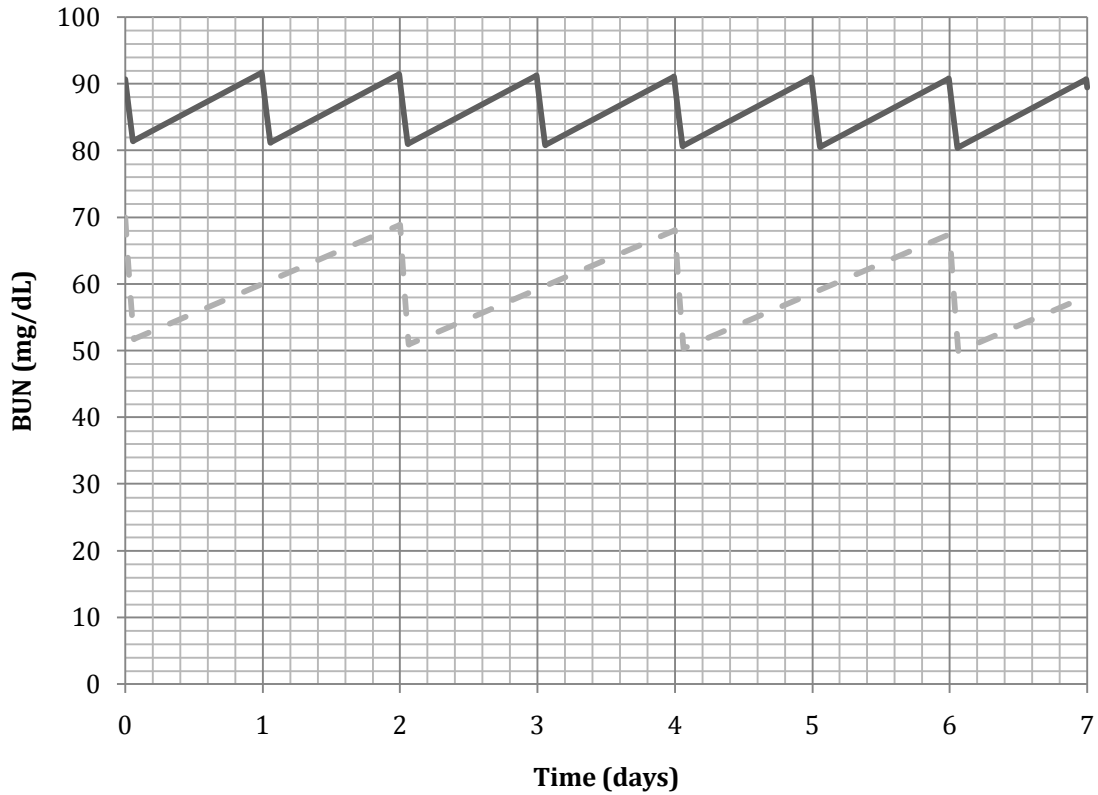


Figure 5-25. The worst-case scenario.

The inputs and outputs of Figure 5-25 are listed in Table 5-22 and Table 5-23, respectively.

Table 5-22. Input parameters for a worst-case scenario.

Parameter	Value
Initial BUN ( $C_{Bi}$ )	91 mg/L
Blood flow rate ( $Q_B$ )	80 mL/min
$K_0A$	800 mL/min
Trade-off coefficient ( $\alpha$ )	0.95
Blood volume ( $V_B$ )	53,000 mL
Ultrafiltration flow rate ( $Q_F$ )	0.000 mL/min
Urea generation rate ( $\dot{G}$ )	8.68056 mg/min
Treatment length ( $t_1$ )	1.5 hours
Time between treatments ( $t_2$ )	22.5 hours
Residual kidney function ( $GFR\%$ )	0.000%

Table 5-23. Output parameters for a worst-case scenario.

Parameter	Value
Dialysate flow rate ( $Q_D$ )	91 mL/min
Clearance ( $K$ )	76.1 mL/min
Dialysate volume ( $V_D$ )	8,190 mL per dose
Dialysance ( $D$ )	76.09 ml/min

## 5.5 Conclusion

This chapter sought to provide relevant product concepts (Section 5.4) following verification of the model (Section 5.1) and investigation of model behavior (Sections 5.2 and 5.3).

The model provided results as accurate as other published models (Ziólko, Pietrzyk, & Grabska-Chrzastowska, 2000) when using actual hemodialysis data. The *in vitro* experiments also provided results that were predicted by the model.

The exploration of steady state behavior and the discovery of a unique time constant associated with each set of dialysis inputs could provide, with some future work (Section 6.4), new ways for patients to choose their treatment schedule.

The research question this chapter focused on was:

*Is a portable hemodialysis system possible? What are the detailed system configurations that are possible?*

With such a large variety of dialysis patients in the world, it is impossible to conclude this chapter with one definitive system configuration. However, the examples presented at the end of this chapter (Section 5.4) show that patient BUN levels can be maintained within acceptable ranges while only using as little as 9 L of dialysate per dose. Because the dialysate volume is the heaviest

component – and therefore the largest barrier to the development of a portable system – a possible system that only uses 9 L makes a strong case to pursue the development of a portable system.

However, this model makes several assumptions (Section 4.7.3), and additional assumptions in the application of the model that have not been discussed. Specifically, this model only predicts the daily change of the patient's urea levels, and disregards all other solutes of interest. This was done for two reasons: first, urea is the solute primarily targeted by dialysis; and second, the model's prediction of different solutes relies on publication of dialyzer  $K_0A$  specifications for additional solutes. Nearly all dialyzer manufacturers publish  $K_0A$  only for urea, limiting the application of this model to other solutes. If more detailed dialyzer specifications were available, other solutes could be modeled.

While basic parameters of a portable hemodialysis concept have been established, many more factors would need to be considered in order to develop a prototype. Because it relies on traditional, dialyzer-based dialysis, 40 years of experience could be leveraged to address biocompatibility, safety, legal, and manufacturing issues that would undoubtedly be raised.

However, if the device were to be wearable, additional research would be needed. There are considerable safety issues concerning a device that continuously draws blood from its user. Additionally, the weight would become such a stringent design requirement that some sort of dialysate regeneration would be needed for a successful system.

## CHAPTER SIX

### CLOSURE AND CONTRIBUTIONS

The broad goal of this thesis was to develop a superior renal replacement therapy using systematic engineering principles. Chapter 3 provided a thorough functional analysis of the human kidney and current hemodialysis; both of which led to an RRT concept. Chapter 4 developed a system model that was used in Chapter 5 to create system concepts.

In Chapter 1, three research questions were posed as the framework of this thesis. A hypothesis was provided with each research question. In Section 6.1, each hypothesis will be addressed in the context of the work completed in this thesis.

#### **6.1 Answering the research questions**

The purpose of this research was to determine the possibility of developing an alternative to traditional renal replacement therapies (dialysis), and to explore how traditional dialysis could be modified to make it more portable.

This research was divided into three research questions, which are now tested.

##### **6.1.1 Research question one**

The first research question was addressed in Chapter 3.

**Research Question 1:**

*Can a renal replacement therapy be developed that provides an alternative filtration method while matching or exceeding current hemodialysis performance?*

**Hypothesis 1:**

*A renal replacement system that more closely mimics the behavior of a human kidney can provide a more effective treatment.*

In Chapter 3, an alternative to traditional hemodialysis was developed by reverse engineering the human kidney. It was discovered there was a striking functional difference between the human kidney and hemodialysis: the human kidney filters nearly everything out of the blood and then reabsorbs only the needed solutes, while hemodialysis attempts to remove only the bad solutes from the blood in one pass.

The kidney uses two passes to clean the blood – a large filtering stage, and then a reabsorption stage. This idea was the foundation of the bio-artificial concept developed in Chapter 3. The concept separates out the plasma, filters the desirable solutes through electrophoresis, and then returns the desirable solutes and other additives (water, sodium, etc.) to the plasma filtrate. The filtrate is then returned to the patient.

The limitations of current hemodialysis are well understood – its use for the last forty years has led to research that has exploited all its potential. The goal of this research question was to determine whether developing an alternative RRT was possible given today's technology.

To that end, this thesis addressed the first research question. The key was to show that the approach to designing a renal replacement system had to be changed. By mimicking the kidney's functionality, an exacting filter (the largest hurdle towards an improved RRT and something that

researchers have been unable to develop) is no longer needed. The challenge with the proposed bio-inspired concept is not how to best remove solutes from the blood, but how to best add them in – a fundamental difference.

However, without actually constructing such a system, no definitive answer can be provided for the first research question. At this point, enough is known to claim that traditional concentration-based dialysis is unlikely to see any major performance improvements – its long-time use has fleshed out seemingly all possible advances. A behaviorally-novel method is needed to gain significant increases in performance.

### **6.1.2 Research question two**

The second research question was addressed in Chapter 4.

#### **Research Question 2:**

*Can a detailed hemodialysis system model be created that accurately takes into account different patient and dialysis variables?*

#### **Hypothesis 2:**

*By improving upon the work of Sargent & Gotch (1989), a detailed computer model can be created that offers optimization of the fundamental dialysis equations and considers patient variables.*

Following the dialyzer physics detailed by Sargent & Gotch (1989), a detailed system model was created in Chapter 4. The model was further augmented with considerations for dialysate recirculation, dialysate regeneration, treatment schedules, ultrafiltration, trade-off considerations, and urea generation.

These additional inputs and considerations are necessary because the model is used to design a system under very strict design constraints. Because a portable system can only provide minimal clearances, considering the body's residual kidney function and other attributes is essential. A key difference between the model created in this thesis and published models is the context in which they were created – specifically, most models are created to simulate current hemodialysis practice. The model in this work is unique because it was created to explore all possibilities for hemodialysis system design.

### **6.1.3 Research question three**

The third research question was addressed in Chapter 5.

#### **Research Question 3:**

*Is a portable hemodialysis system possible? What are the detailed system configurations that are possible?*

#### **Hypothesis 3:**

*By exploring the physics that govern hemodialysis, portable system configurations can be developed that meet the needs of chronic renal failure patients.*

The augmentations of the model and the flexibility of Matlab Simulink allowed for a detailed exploration of hemodialysis concepts in Chapter 5. The primary limitation of a portable system is its weight; the concepts created all were designed with the goal of minimizing the total dialysate volume.

The model was explored and the inputs were set knowingly to produce concepts that would have the smallest possible dialysate volume through trial and error. The concepts created used about

10 L of dialysate per treatment, a reasonable amount, although the definition of *portable* is subjective.

Tricks could be deployed to reduce the 10 L figure; if treatment lasts 90 minutes, then dialysate weight could be viewed as 3 L per half hour – the patient could cycle dialysate volumes every half hour during treatment. While not everyone might agree that 10 L of dialysate is portable, most would probably concur that a 3 L system was.

In the end, the ultimate solution to the portability problem lies in regenerating dialysate, as has been employed by other research groups. A dialysate regeneration system is not commercially available and would require significant additional research to achieve. Its development is further described in Section 6.4 as future work.

## **6.2 Contributions**

Hemodialysis has existed in relatively the same form for the last fifty years. One of the overall goals of this thesis was to examine a novel way to re-imagine renal replacement therapies. In that scope, several contributions have been made.

### **6.2.1 A functional analysis of kidney behavior and a related renal replacement therapy concept**

The functional analysis of the human renal system in Chapter 3 provides a unique look at how the kidney functions, combining commonly available medical information into a single functional model. The kidney's method of filtering wastes is contrasted against the methods employed by artificial renal systems – highlighting how substantially different each system functions.

In an attempt to create a superior alternative renal replacement therapy, the kidney's functional behavior is mimicked in a novel renal replacement system. The proposed bio-inspired concept

provides a therapy that is functionally similar to the human renal system, and as a result, might provide superior treatment.

Today's treatments are insufficient because they require exact filtering. By mimicking the kidney, a concept is developed that does not require exacting one-stage filtering, but instead requires a multistage solute-replacement stage. While the proposed system is designed with a yet-to-be developed technology (electrophoresis has not been successfully implemented in this fashion, but it is feasible), which limited the development of that concept in this thesis, the option is left to future research.

### **6.2.2 A thorough one-compartment model of hemodialysis**

Many one-compartment models of hemodialysis have been developed (Ziółko, Pietrzyk, & Grabska-Chrzastowska, 2000). The model presented in this thesis provides several novel additions to traditional one-compartment models.

Models available in published literature do not account for urea generation, dialysate recirculation, automatic determination of dialysate flow rate (based upon input blood flow rate and dialyzer properties), residual kidney function, and extended use (longer than one session). These features were included in the model presented in Chapter 4. With the addition of these features, and the power of Simulink, the robust hemodialysis concepts presented in Chapter 5 were possible.

It was necessary to extend the work of previous models to develop a portable hemodialysis system. The design of a portable hemodialysis system has such stringent constraints on it that it is necessary to consider every possible source of urea generation and depletion in order to create feasible design concepts.

For example, patients with 15% residual kidney function may be on dialysis, but previous models did not account for their [limited] natural ability to clear urea. This can add up to several grams of urea cleared per day, which in turn has a direct impact on the treatment lengths and dialysis schedule.

The model's unique determination of the dialysate flow rate is very important, too. Traditional dialysis wisdom says that the dialysate flow rate should be twice the blood flow rate (Ward & Leyboldt, 2001). However, at the blood flow rates encountered in a portable system this rule breaks down – in fact, at low blood flow rates the dialysate flow rate should roughly match the blood flow rate. Having a higher dialysate flow rate does not have a negative impact, but there is a trade-off that is needed. The model automatically attempts to find a dialysate flow rate that balances clearance and total dialysate volume needed for treatment.

Consideration of dialysate recirculation is also unique among models in published literature. Dialysate recirculation is an easy way to reduce the total weight of the system (by reducing the overall dialysate volume), but the results of such theoretical investigations did not gather promising results. In fact, it was shown in Chapter 5 that given a fixed reduced volume of dialysate, it is best to just run the dialysate in single-pass mode at the ideal flow rate, rather than let the dialysate dwell in recirculation mode for any time length.

### **6.2.3 Relating a time constant to a given set of hemodialysis inputs**

One of the more interesting results of the examination of steady state behavior of dialysis (Section 5.3) was the relation of a time constant to a given set of hemodialysis inputs. Basically, this thesis revealed that all of the hemodialysis inputs – flow rates, dialyzer properties, patient urea generation, etc. – can be lumped into two variables: a time constant,  $\tau$ , and the initial BUN ( $C_{Bi}$ ), as shown in Equation 6-1.

$$Y(\tau, C_{Bi}) = f(C_{Di}, K_0A, Q_B, Q_D, \dot{G}, GFR\%, V_D, V_B, t_1, t_2) \quad (6-1)$$

Because a unique time constant has been identified that lumps together all the input parameters associated with hemodialysis, patients and could have a much easier time relating all the variables, making the choice of a proper therapy (dose length and schedule) much easier. The time constants in this thesis were determined by manual inspection of output plots of the model. A simple method to reduce all the input variables into one time constant is not examined in this thesis and is left as future work.

#### **6.2.4 Feasible concepts of a portable hemodialysis system**

The model exploration in Chapter 5 yielded many feasible concepts for a portable hemodialysis system. If someone were to continue the work of this thesis, these concepts would be the natural starting point.

Because of the model's comprehensiveness, these concepts have a strong value toward the embodiment design of a hemodialysis system. Most importantly, this thesis has shown that portable hemodialysis concepts are possible without large changes in technology.

### **6.3 Scope and limitations of this research**

Two major limitations exist in this thesis. In Chapter 3, the bio-inspired concept that was generated was never experimentally tested, so its full benefits and limitations are not fully known.

The model created in Chapter 4 is a one-compartment model; two compartment models more accurately predict post-dialysis BUN but provide equally-accurate results for long term (several days) hemodialysis modeling (Ziólko, Pietrzyk, & Grabska-Chrząstowska, 2000).

Finally, the most important limitation of this work is the patient variation that is impossible to account for when developing concepts in Chapter 5 from the model created in Chapter 4. The most obvious limitation is the range of patient sizes and their total blood volume, which has a significant effect on each dose length. To account for this variation, different scenarios were tested at the end of Chapter 5 that dealt with a range of patient sizes, although it is clear that there is no “one size fits all” concept for hemodialysis.

More challenging, however, was determining the acceptable amount of urea to maintain in patients when modeling potential concepts. Unlike weight variations, of which there is considerable published data, determining values for acceptable BUN ranges is much less precise. Healthy humans have BUN levels in the 7–12 mg/dL range, but hemodialysis patients can run their BUN up to 1000 mg/dL between doses.

Choosing an acceptable BUN range for a portable hemodialysis concept was not easy. Patients with high BUN levels experience symptoms of fatigue and poor fortitude, but how poorly they feel at particle BUN levels varies from patient to patient and is not readily available in published data. Furthermore, choosing the range has a significant impact on the dose length and other hemodialysis inputs.

To that end, BUN ranges were kept as low as possible without sacrificing portability – generally in the 70–100 mg/dL range.

#### **6.4 Future work**

The following directions for future work have been identified.

#### **6.4.1 Dialysate regeneration**

A dialysate regeneration system is necessary for a most portable hemodialysis system. The concepts developed in this thesis do not rely on a dialysate regeneration system; with one, the overall system weight could be significantly reduced.

Dialysate regeneration would require dialysate to pass through a filtering system after leaving the dialyzer. The complications from cleaning used dialysate arise from urea's inability to be absorbed by activated carbon. While nearly all other solutes can be cleaned from dialysate with activated carbon, urea must first be converted to urease via a chemical reaction, and then absorbed with charcoal.

Only one company has developed a dialysate cleaning system, and it is not commercially available. It would be possible to develop a proprietary dialysate cleaning system to reduce the dialysate required per treatment significantly.

#### **6.4.2 System optimization and sensitivity analysis**

The inputs of the simulations performed in this thesis were selected with designer intuition. However, a thorough study could be performed that detailed the exact relationship between all the different variables in a hemodialysis system – the focus in this thesis was primarily on the relationship between the blood and dialysate flow rates.

The model could be reconfigured in reverse: the designer would specify his or her desired output system parameters, and the model would select the best inputs to meet those needs.

#### **6.4.3 Improved pump design**

In Chapter 4, the efficiencies of pumps currently available for hemodialysis machines were examined. Their efficiencies were found to be below 0.5%. This was a surprising result; it is

surmised that minimal investigation and design work could create a pump that doubled or tripled the currently available efficiency.

A graduate student in this laboratory has already begun the work to design a more efficient pump for hemodialysis, based upon the deficiencies outlined in this thesis.

#### **6.4.4 Dialyzer-free dialysis**

The ultimate “future work” to note is the development of a renal replacement system that does not rely on a dialyzer. While it should not be the goal to blindly reject membrane dialysis, research seems to indicate that to significantly improve the clearance of solutes from patients with ESRD, an alternative renal replacement therapy must be created.

To that end, a concept for an alternative method to remove solutes was systematically developed in Chapter 3. That concept relied on electrophoresis to remove more accurately solutes; however, any number of new technologies might provide a superior renal replacement system.

## APPENDIX A

### GLOSSARY OF TERMS

<b>Bowman's capsule</b>	The part of the nephron surrounding the glomerulus.
<b>brake power</b>	The power required to operate a pump. Different from <i>fluid power</i> , which is the power associated with the moving fluid.
<b>CAPD</b>	Continuous Ambulatory Peritoneal Dialysis. Peritoneal dialysis where the dialysate fluid is injected into the abdomen, and then drained several hours later.
<b>CCPD</b>	Continuous Cycling Peritoneal Dialysis. Peritoneal dialysis where the dialysate fluid is continuously cycled through the abdomen.
<b>centrifugal pump</b>	A pump that relies on an impeller inside the fluid to provide a pressure rise.
<b>collecting ducts</b>	Ducts that form the final stage of the nephron; they exit to the ureter.
<b>convection</b>	The movement of particles across a membrane due to pressure gradients.
<b>diabetes</b>	A disease in which the pancreas stops producing insulin, causing high blood glucose levels. Often leads to renal disease.
<b>dialysance</b>	The magnitude of flux out of the blood to be expected per unit of concentration driving force between the blood and dialysate in the dialyzer.
<b>dialysate</b>	The solution that runs on the opposite side of membrane during dialysis. Solutes in the blood pass through the membrane and into the dialysate due to a concentration gradient.
<b>distal tubule</b>	The part of the nephron between the loop of Henle and the collecting ducts.
<b>electrophoresis</b>	The separation of particles based upon their electrical charge. As a fluid flows between two oppositely charged plates, the particles in the fluid stream migrate depending on their charge.
<b>endocrine</b>	Glands that secrete hormones into the blood.
<b>fluid power</b>	The power of the fluid leaving a pump.

<b>glomerulus</b>	The small tuft of blood capillaries that are surrounded by the Bowman's capsule. Blood flows from the capillaries to the Bowman's capsule. With the Bowman's capsule they form the renal corpuscle.
<b>glomerular filtration rate</b>	The rate at which blood is filtered across the glomerulus. A typical value for a healthy adult is 125 mL/min.
<b>glucose degradation products</b>	Solutes in peritoneal dialysis fluid that degrade the body's peritoneum. After several years of exposure to GDPs, peritoneal dialysis patients are often forced to switch to traditional hemodialysis.
<b>hemodiafiltration</b>	A renal replacement therapy that combines hemodialysis and hemofiltration.
<b>hemofiltration</b>	A renal replacement therapy that uses <i>convection</i> as waste removal process. Often used in intensive care settings due to the high water-loss associated with it.
<b>heparin</b>	A common blood anticoagulant often used during hemodialysis.
<b>hirudin</b>	An anticoagulant used before the advent of heparin in the 1940s.
<b>hollow fiber dialyzer</b>	Today's most common type of dialyzer. Thousands of small tubules carry blood through a counter flow of dialysate.
<b>homeostasis</b>	A balanced state of being: proper regulation of solutes and processes in the body.
<b>loop of Henle</b>	The section of the nephron between proximal and distal tubules.
<b>Matlab</b>	Computing software used to solve mathematical problems.
<b>MEMS</b>	Micro ElectroMechanical Systems are very small devices, with parts on the scale of micrometers.
<b>nephron</b>	The basic functional unit of the kidney. Each nephron is composed of a renal corpuscle, Bowman's capsule, proximal tubule, distal tubule, and collecting ducts.
<b>nephrectomised</b>	The state of having one's kidneys removed.
<b>peritoneal dialysis</b>	Dialysis that relies on the body's peritoneum as a membrane. Dialysate fluid is pumped in and out the abdomen.
<b>peritoneum</b>	The membrane that forms the lining of the abdomen. Used in peritoneal dialysis as the barrier between the blood and dialysate.

<b>persaltic pump</b>	A type of positive displacement pump that is used during hemodialysis. Medical tubing is squeezed by rollers to create the pressure gradient.
<b>positive displacement pump</b>	Any type of pump that creates a rise in pressure by cyclic filling and emptying of a volume. Rotary pumps, the pumps most commonly used in hemodialysis, are positive displacement pumps.
<b>proximal tubule</b>	The section of a nephron after the Bowman's capsule and before the loop of Henle.
<b>recirculation</b>	When dialysate is reused after it has passed through the dialyzer.
<b>renal corpuscle</b>	The corpuscle formed by both the Bowman's capsule and the glomerulus.
<b>renal replacement therapy</b>	Any form of treatment that attempts to emulate the function of the kidneys.
<b>shunt</b>	An artificial connection between a vein and an artery that provides the blood for hemodialysis.
<b>sieving coefficient</b>	The ratio between the change of concentrations of the blood and dialysate.
<b>single-pass</b>	When dialysate is passed through the dialyzer just once during hemodialysis.
<b>transmembrane pressure</b>	The pressure difference between the blood and dialysate inside of a dialyzer during dialysis.
<b>tubule</b>	A very small tube, either inside of a dialyzer or a part of a nephron.
<b>ultrafiltration</b>	The convective process that occurs during dialysis.
<b>urea</b>	A byproduct of protein metabolism in humans. Must be cleaned from the blood (via the kidneys or dialysis) to avoid death.
<b>urease</b>	The chemical used in the REDY sorbent system that processes urea in the dialysate.
<b>uremia</b>	The buildup of toxins in the blood that are normally removed by healthy kidneys.
<b>vasa recta</b>	A collection of blood capillaries in the nephron that extend into the medulla.

## APPENDIX B

### MATLAB CODE

The Simulink code is provided below in two columns.

```
Model {
  Name "reconciled"
  Version 7.1
  MdlSubVersion 0
  GraphicalInterface {
    NumRootInputs 0
    NumRootOutputs 0
    ParameterArgumentNames ""
    ComputedModelVersion "1.64"
    NumModelReferences 0
    NumTestPointedSignals 0
  }
  SavedCharacterEncoding "windows-1252"
  SaveDefaultBlockParams on
  SampleTimeColors off
  LibraryLinkDisplay "none"
  WideLines off
  ShowLineDimensions off
  ShowPortDataTypes off
  ShowLoopsOnError on
  IgnoreBidirectionalLines off
  ShowStorageClass off
  ShowTestPointIcons on
  ShowSignalResolutionIcons on
  ShowViewerIcons on
  SortedOrder off
  ExecutionContextIcon off
  ShowLinearizationAnnotations on
  ScopeRefreshTime 0.035000
  OverrideScopeRefreshTime on
  DisableAllScopes off
  DataTypeOverride "UseLocalSettings"
  MinMaxOverflowLogging "UseLocalSettings"
  MinMaxOverflowArchiveMode "Overwrite"
  BlockNameDataTip off
  BlockParametersDataTip off
  BlockDescriptionStringDataTip off
  ToolBar on
  StatusBar on
  BrowserShowLibraryLinks off
  BrowserLookUnderMasks off
  Created "Wed Aug 27 13:12:11 2008"
  Creator "Jeff"
  UpdateHistory "UpdateHistoryNever"
  ModifiedByFormat "%<Auto>"
  LastModifiedBy "Jeff"
  ModifiedDateFormat "%<Auto>"
  LastModifiedDate "Tue Jan 20 16:23:02 2009"
  RTWModifiedDateStamp 0
  ModelVersionFormat "1.%<AutoIncrement:64>"
  ConfigurationManager "None"
  SimulationMode "normal"
  LinearizationMsg "none"
  Profile off
  ParamWorkspaceSource "MATLABWorkspace"
  AccelSystemTargetFile "accel.tlc"
  AccelTemplateMakefile "accel_default_tmf"
  AccelMakeCommand "make_rtw"
  TryForcingSFcnDF off
  RecordCoverage off
  CovPath "/"
  CovSaveName "covdata"
  CovMetricSettings "dw"
  CovNameIncrementing off
  CovHtmlReporting on
  covSaveCumulativeToWorkspaceVar on
  CovSaveSingleToWorkspaceVar on
  CovCumulativeVarName "covCumulativeData"
  CovCumulativeReport off
  CovReportOnPause on
  CovModelRefEnable "Off"
  ExtModeBatchMode off
  ExtModeEnableFloating on
  ExtModeTrigType "manual"
  ExtModeTrigMode "normal"
  ExtModeTrigPort "1"
  ExtModeTrigElement "any"
  ExtModeTrigDuration 1000
  ExtModeTrigDurationFloating "auto"
  ExtModeTrigHoldOff 0
  ExtModeTrigDelay 0
  ExtModeTrigDirection "rising"
  ExtModeTrigLevel 0
  ExtModeArchiveMode "off"
  ExtModeAutoIncOneShot off
  ExtModeIncDirWhenArm off
  ExtModeAddSuffixToVar off
  ExtModeWriteAllDataToWs off
  ExtModeArmWhenConnect on
  ExtModeSkipDownloadWhenConnect off
  ExtModeLogAll on
  ExtModeAutoUpdateStatusClock on
  BufferReuse on
  ShowModelReferenceBlockVersion off
  ShowModelReferenceBlockIO off
  Array {
    Type "Handle"
    Dimension 1
    Simulink.ConfigSet {
      $ObjectID 1
      Version "1.4.0"
      Array {
        Type "Handle"
        Dimension 7
        Simulink.SolverCC {
          $ObjectID 2
          Version "1.4.0"
          StartTime "0.0"
          StopTime "720"
          AbsTol "auto"
          FixedStep "auto"
          InitialStep "auto"
          MaxNumMinSteps "-1"
          MaxOrder 5
          ZcThreshold "auto"
          ConsecutiveZCsStepRelTol "10*128*eps"
          MaxConsecutiveZCs "1000"
          ExtrapolationOrder 4
          NumberNewtonIterations 1
          MaxStep "auto"
          MinStep "auto"
          MaxConsecutiveMinStep "1"
          RelTol "1e-3"
          SolverMode "Auto"
          Solver "ode45"
          SolverName "ode45"
          ShapePreserveControl "DisableAll"
          ZeroCrossControl "UseLocalSettings"
          ZeroCrossAlgorithm "Non-adaptive"
          AlgebraicLoopSolver "TrustRegion"
          SolverResetMethod "Fast"
          PositivePriorityOrder off
          AutoInsertRateTranBlk off
          SampleTimeConstraint "Unconstrained"
          InsertRTBMode "Whenever possible"
        }
      }
    }
  }
  Simulink.DataIOCC {
    $ObjectID 3
    Version "1.4.0"
    Decimation "1"
    ExternalInput "[t, u]"
    FinalStateName "xFinal"
    InitialState "xInitial"
    LimitDataPoints off
    MaxDataPoints "1000"
    LoadExternalInput off
    LoadInitialState off
    SaveFinalState off
    SaveFormat "Array"
    SaveOutput on
    SaveState off
    SignalLogging on
    InspectSignalLogs off
    SaveTime on
    StateSaveName "xout"
    TimeSaveName "tout"
    OutputSaveName "yout"
    SignalLoggingName "logsout"
    OutputOption "RefineOutputTimes"
```

```

OutputTimes          "[]"
Refine                "1"
}
Simulink.OptimizationCC {
  $objectID          4
  Array {
    Type              "Cell"
    Dimension          5
    Cell               "ZeroExternalMemoryAtStartup"
    Cell               "ZeroInternalMemoryAtStartup"
    Cell               "InitFltsAndDbIsToZero"
    Cell               "OptimizeModelRefInitCode"
    Cell               "NoFixptDivByZeroProtection"
    PropName           "DisabledProps"
  }
  Version             "1.4.0"
  BlockReduction      on
  BooleanDataType     on
  ConditionallyExecuteInputs on
  InlineParams        off
  InlineInvariantSignals off
  OptimizeBlockIOStorage on
  BufferReuse          on
  EnhancedBackFolding off
  EnforceIntegerDowncast on
  ExpressionFolding   on
  ExpressionDepthLimit 2147483647
  FoldNonRolledExpr   on
  LocalBlockOutputs   on
  RollThreshold        5
  SystemCodeInlineAuto off
  StateBitsets         off
  DataBitsets          off
  UseTempVars          off
  ZeroExternalMemoryAtStartup on
  ZeroInternalMemoryAtStartup on
  InitFltsAndDbIsToZero on
  NoFixptDivByZeroProtection off
  EfficientFloat2IntCast off
  OptimizeModelRefInitCode off
  LifeSpan             "inf"
  BufferReusableBoundary on
  SimCompilerOptimization "Off"
  AccelVerboseBuild    off
}
Simulink.DebuggingCC {
  $objectID          5
  Version             "1.4.0"
  RTPrefix            "error"
  ConsistencyChecking "none"
  ArrayBoundsChecking "none"
  SignalInfNanChecking "none"
  SignalRangeChecking "none"
  ReadBeforeWriteMsg  "UseLocalSettings"
  WriteAfterWriteMsg  "UseLocalSettings"
  WriteAfterReadMsg   "UseLocalSettings"
  AlgebraicLoopMsg    "warning"
  ArtificialAlgebraicLoopMsg "warning"
  SaveWithDisabledLinksMsg "warning"
  SaveWithParameterizedLinksMsg "warning"
  CheckSSIInitialOutputMsg on
  CheckExecutionContextPreStartOutputMsg off
  CheckExecutionContextRuntimeOutputMsg off
  SignalResolutionControl "UseLocalSettings"
  BlockPriorityViolationMsg "warning"
  MinStepSizeMsg      "warning"
  TimeAdjustmentMsg   "none"
  MaxConsecutiveZCsMsg "error"
  SolverPrmCheckMsg    "warning"
  InheritedTsInSrcMsg "warning"
  DiscreteInheritContinuousMsg "warning"
  MultiTaskDSMMsg     "error"
  MultiTaskCondExecSysMsg "error"
  MultiTaskRateTransMsg "error"
  SingleTaskRateTransMsg "none"
  TasksWithSamePriorityMsg "warning"
  SigSpecEnsureSampleTimeMsg "warning"
  CheckMatrixSingularityMsg "none"
  IntegerOverflowMsg   "warning"
  Int32ToFloatingConvMsg "warning"
  ParameterDowncastMsg "error"
  ParameterOverflowMsg  "error"
  ParameterUnderflowMsg "none"
  ParameterPrecisionLossMsg "warning"
  ParameterTunabilityLossMsg "warning"
  UnderSpecifiedDataTypeMsg "none"
  UnnecessaryDatatypeConvMsg "none"
  VectorMatrixConversionMsg "none"
  InvalidFcnCallConnMsg "error"
  FcnCallInpInsideContextMsg "Use local settings"
  SignalLabelMismatchMsg "none"
  UnconnectedInputMsg   "warning"
  UnconnectedOutputMsg  "warning"
  UnconnectedLineMsg    "warning"
  SFcnCompatibilityMsg  "none"
  UniqueDataStoreMsg    "none"
  BusObjectLabelMismatch "warning"
  RootOutputRequireBusObject "warning"
  AssertControl          "UseLocalSettings"
  EnableOverflowDetection off
  ModelReferenceIOMsg    "none"
  ModelReferenceVersionMismatchMsg "none"
}
ModelReferenceIOMismatchMessage "none"
ModelReferenceCSMismatchMessage "none"
ModelReferenceSimTargetVerbose off
UnknownTsInhSupMsg              "warning"
ModelReferenceDataLoggingMessage "warning"
ModelReferenceSymbolNameMessage "warning"
ModelReferenceExtraNoncontSigs "error"
StateNameClashWarn               "warning"
StrictBusMsg                      "Warning"
LoggingUnavailableSignals "error"
BlockIODiagnostic                 "none"
}
Simulink.HardwareCC {
  $objectID          6
  Version             "1.4.0"
  ProdBitPerChar     8
  ProdBitPerShort    16
  ProdBitPerInt      32
  ProdBitPerLong     32
  ProdIntDivRoundTo "Undefined"
  ProdEndianness     "Unspecified"
  ProdWordSize       32
  ProdShiftRightIntArith on
  ProdHWDeviceType   "32-bit Generic"
  TargetBitPerChar   8
  TargetBitPerShort  16
  TargetBitPerInt    32
  TargetBitPerLong   32
  TargetShiftRightIntArith on
  TargetIntDivRoundTo "Undefined"
  TargetEndianness   "Unspecified"
  TargetWordSize     32
  TargetTypeEmulationWarnSuppressLevel 0
  TargetPreprocMaxBitsSint 32
  TargetPreprocMaxBitsUint 32
  TargetHWDeviceType "Specified"
  TargetUnknown      off
  ProdEqTarget       on
}
Simulink.ModelReferenceCC {
  $objectID          7
  Version             "1.4.0"
  UpdateModelReferenceTargets
  "IfOutOfDateOrStructuralChange"
  CheckModelReferenceTargetMessage "error"
  ModelReferenceNumInstancesAllowed "Multi"
  ModelReferenceSigSizeVariationType "Always allowed"
  ModelReferencePassRootInputsByReference on
  ModelReferenceMinAlgLoopOccurrences off
}
Simulink.RTWCC {
  $BackupClass       8
  $objectID          8
  Array {
    Type              "Cell"
    Dimension          6
    Cell               "IncludeHyperlinkInReport"
    Cell               "GenerateTraceInfo"
    Cell               "GenerateTraceReport"
    Cell               "GenerateTraceReportS1"
    Cell               "GenerateTraceReportSf"
    Cell               "GenerateTraceReportEml"
    PropName           "DisabledProps"
  }
  Version             "1.4.0"
  SystemTargetFile   "grt.tlc"
  GenCodeOnly        off
  MakeCommand         "make_rtw"
  GenerateMakefile   on
  TemplateMakefile   "grt_default_tmf"
  GenerateReport     off
  SaveLog            off
  RTWVerbose         on
  RetainRTWFile      off
  ProfileTLC         off
  TLCDiagnostic      off
  TLCDebug           off
  TLCCoverage        off
  TLCAssert          off
  ProcessScriptMode  "Default"
  ConfigurationMode  "Optimized"
  ConfigAtBuild      off
  IncludeHyperlinkInReport off
  LaunchReport       off
  TargetLang         "C"
  IncludeBusHierarchyInRTWFileBlockHierarchyMap off
  IncludeERTFirstTime off
  GenerateTraceInfo  off
  GenerateTraceReport off
  GenerateTraceReportS1 off
  GenerateTraceReportSf off
  GenerateTraceReportEml off
  GenerateCodeInfo   off
  RTWCompilerOptimization "Off"
  Array {
    Type              "Handle"
    Dimension          2
    Simulink.CodeAppCC {
      $objectID          9
      Array {
        Type              "Cell"
        Dimension          16

```



```

LockScale off
RndMeth "Floor"
SaturateOnIntegerOverflow on
SampleTime "-1"
}
Block {
BlockType Inport
Port "1"
UseBusObject off
BusObject "BusObject"
BusOutputAsStruct off
PortDimensions "-1"
SampleTime "-1"
OutMin "[]"
OutMax "[]"
DataType "auto"
OutDataType "fixdt(1,16,0)"
OutScaling "[]"
OutDataTypeStr "Inherit: auto"
SignalType "auto"
SamplingMode "auto"
LatchByDelayingOutsideSignal off
LatchByCopyingInsideSignal off
Interpolate on
}
Block {
BlockType Integrator
ExternalReset "none"
InitialConditionSource "internal"
InitialCondition "0"
LimitOutput off
UpperSaturationLimit "inf"
LowerSaturationLimit "-inf"
ShowSaturationPort off
ShowStatePort off
AbsoluteTolerance "auto"
IgnoreLimit off
ZeroCross "on"
ContinuousStateAttributes ""
}
Block {
BlockType Outport
Port "1"
UseBusObject off
BusObject "BusObject"
BusOutputAsStruct off
PortDimensions "-1"
SampleTime "-1"
OutMin "[]"
OutMax "[]"
DataType "auto"
OutDataType "fixdt(1,16,0)"
OutScaling "[]"
OutDataTypeStr "Inherit: auto"
SignalType "auto"
SamplingMode "auto"
OutputWhenDisabled "held"
InitialOutput "[]"
}
Block {
BlockType Product
Inputs "2"
Multiplication "Element-wise (.*)"
CollapseMode "All dimensions"
CollapseDim "1"
InputSameDT on
OutMin "[]"
OutMax "[]"
OutDataTypeMode "Same as first input"
OutDataType "fixdt(1,16,0)"
OutScaling "[]"
OutDataTypeStr "Inherit: Same as first input"
LockScale off
RndMeth "Zero"
SaturateOnIntegerOverflow on
SampleTime "-1"
}
Block {
BlockType Scope
ModelBased off
TickLabels "OneTimeTick"
ZoomMode "on"
Grid "on"
TimeRange "auto"
YMin "-5"
YMax "5"
SaveToWorkspace off
SaveName "ScopeData"
LimitDataPoints on
MaxDataPoints "5000"
Decimation "1"
SampleInput off
SampleTime "-1"
}
Block {
BlockType "S-Function"
FunctionName "system"
SFunctionModules ""
PortCounts "[]"
SFunctionDeploymentMode off
}
Block {
BlockType SubSystem
ShowPortLabels "FromPortIcon"
Permissions "ReadWrite"
PermitHierarchicalResolution "All"
TreatAsAtomicUnit off
CheckFcnCallInpInsideContextMsg off
SystemSampleTime "-1"
RTWFcnNameOpts "Auto"
RTWFileNameOpts "Auto"
RTWMemSecFuncInitTerm "Inherit from model"
RTWMemSecFuncExecute "Inherit from model"
RTWMemSecDataConstants "Inherit from model"
RTWMemSecDataInternal "Inherit from model"
RTWMemSecDataParameters "Inherit from model"
SimViewingDevice off
DataTypeOverride "UseLocalSettings"
MinMaxOverflowLogging "UseLocalSettings"
}
Block {
BlockType Sum
IconShape "rectangular"
Inputs "++"
CollapseMode "All dimensions"
CollapseDim "1"
InputSameDT on
AccumDataTypeStr "Inherit: Inherit via internal rule"
OutMin "[]"
OutMax "[]"
OutDataTypeMode "Same as first input"
OutDataType "fixdt(1,16,0)"
OutScaling "[]"
OutDataTypeStr "Inherit: Same as first input"
LockScale off
RndMeth "Floor"
SaturateOnIntegerOverflow on
SampleTime "-1"
}
Block {
BlockType ToWorkspace
VariableName "simulink_output"
MaxDataPoints "1000"
Decimation "1"
SampleTime "0"
FixptAsFi off
}
Block {
BlockType Terminator
}
Block {
BlockType UnitDelay
X0 "0"
SampleTime "1"
StateMustResolveToSignalObject off
RTWStateStorageClass "Auto"
}
Block {
BlockType Constant
Value "1"
VectorParams1D on
SamplingMode "Sample based"
OutMin "[]"
OutMax "[]"
OutDataTypeMode "Inherit from 'Constant value'"
OutDataType "fixdt(1,16,0)"
ConRadixGroup "Use specified scaling"
OutScaling "[]"
OutDataTypeStr "Inherit: Inherit from 'Constant value'"
SampleTime "inf"
FramePeriod "inf"
}
Block {
BlockType DiscretePulseGenerator
PulseType "Sample based"
TimeSource "Use simulation time"
Amplitude "1"
Period "2"
PulseWidth "1"
PhaseDelay "0"
SampleTime "1"
VectorParams1D on
}
}
AnnotationDefaults {
HorizontalAlignment "center"
VerticalAlignment "middle"
ForegroundColor "black"
BackgroundColor "white"
DropShadow off
FontName "Helvetica"
FontSize 10
FontWeight "normal"
FontAngle "normal"
UseDisplayTextAsClickCallback off
}
}
LineDefaults {
FontName "Helvetica"
FontSize 9
FontWeight "normal"
FontAngle "normal"
}
}
System {
Name "reconciled"
}

```

```

Location                [2, 72, 1598, 1149]
Open                    on
ModelBrowserVisibility off
ModelBrowserWidth      212
ScreenColor             "white"
PaperOrientation        "landscape"
PaperPositionMode      "auto"
PaperType               "usletter"
PaperUnits              "inches"
TiledPaperMargins      [0.500000, 0.500000, 0.500000, 0.500000]
TiledPageScale         1
ShowPageBoundaries    off
ZoomFactor              "100"
ReportName              "simulink-default.rpt"
Block {
  BlockType             SubSystem
  Name                  "Account for residual\nkidney function"
  Ports                 [2, 1]
  Position               [360, 641, 445, 719]
  ForegroundColor       "blue"
  PermitHierarchicalResolution "ExplicitOnly"
  MinAlgLoopOccurrences off
  PropExecContextOutsideSubsystem off
  RTWSystemCode         "Auto"
  FunctionWithSeparateData off
  Opaque                off
  Array {
    Type                "Handle"
    Dimension            0
    PropName             "AvailSigsLoadSave"
  }
  RequestExecContextInheritance off
  MaskHideContents     off
  MaskType              "Stateflow"
  MaskDescription       "Embedded MATLAB block"
  MaskDisplay           "disp('fcn');"
  MaskSelfModifiable  on
  MaskIconFrame         on
  MaskIconOpaque       off
  MaskIconRotate       "none"
  MaskIconUnits        "autoscale"
  System {
    Name                "Account for
residual\nkidney function"
    Location             [257, 457, 812, 717]
    Open                 off
    ModelBrowserVisibility off
    ModelBrowserWidth  200
    ScreenColor          "white"
    PaperOrientation     "landscape"
    PaperPositionMode   "auto"
    PaperType            "usletter"
    PaperUnits           "inches"
    TiledPaperMargins   [0.500000, 0.500000, 0.500000,
0.500000]
    TiledPageScale      1
    ShowPageBoundaries  off
    ZoomFactor          "100"
    Block {
      BlockType          Inport
      Name               "UGR"
      Position           [20, 101, 40, 119]
      IconDisplay        "Port number"
    }
    Block {
      BlockType          Inport
      Name               "GFR"
      Position           [20, 136, 40, 154]
      Port               "2"
      IconDisplay        "Port number"
      OutDataType        "sfix(16)"
      OutScaling         "2^0"
    }
    Block {
      BlockType          Demux
      Name               " Demux "
      Ports              [1, 1]
      Position           [270, 160, 320, 200]
      Outputs            "1"
    }
    Block {
      BlockType          "S-Function"
      Name               " SFunction "
      Tag                "Stateflow S-Function"
    }
    Ports                [2, 2]
    Position              [180, 100, 230, 160]
    FunctionName          "sf_sfunsfun"
    PortCounts            "[2 2]"
    EnableBusSupport     on
    Port {
      PortNumber         2
      Name               "urea_gen"
      RTWStorageClass    "Auto"
      DataLoggingName    "SignalName"
    }
  }
  Block {
    BlockType           Terminator
    Name                " Terminator "
    Position            [460, 171, 480, 189]
  }
}
Block {
  BlockType             BlockType
  Name                  "Blood Flow Rate"
  Position              [200, 450, 230, 480]
  Value                 "1000"
  OutDataType           "sfix(16)"
  OutScaling            "2^0"
}
Block {
  BlockType             UnitDelay
  Name                  "Blood concentration\ndelay"
  Position              [820, 598, 855, 632]
  X0                    "1.607142856"
}
Block {
  BlockType             SubSystem
  Name                  "Calculate B and D\nconcentration changes"
  Ports                 [10, 3]
  Position               [790, 382, 955, 543]
  ForegroundColor       "blue"
  PermitHierarchicalResolution "ExplicitOnly"
  MinAlgLoopOccurrences off
  PropExecContextOutsideSubsystem off
  RTWSystemCode         "Auto"
  FunctionWithSeparateData off
  Opaque                off
  Array {
    Type                "Handle"
    Dimension            0
    PropName             "AvailSigsLoadSave"
  }
  RequestExecContextInheritance off
  MaskHideContents     off
  MaskType              "Stateflow"
  MaskDescription       "Embedded MATLAB block"
  MaskDisplay           "disp('Dialyance');"
  MaskSelfModifiable  on
  MaskIconFrame         on
  MaskIconOpaque       off
  MaskIconRotate       "none"
  MaskIconUnits        "autoscale"
  System {
    Name                "Calculate B and
D\nconcentration changes"
    Location             [257, 457, 812, 717]
    Open                 off
    ModelBrowserVisibility off
    ModelBrowserWidth  200
    ScreenColor          "white"
    PaperOrientation     "landscape"
    PaperPositionMode   "auto"
    PaperType            "usletter"
    PaperUnits           "inches"
    TiledPaperMargins   [0.500000, 0.500000, 0.500000,
0.500000]
    TiledPageScale      1
    ShowPageBoundaries  off
    ZoomFactor          "100"
    Block {
      BlockType          Inport
      Name               "urea_gen"
      Position           [460, 101, 480, 119]
      IconDisplay        "Port number"
      OutDataType        "sfix(16)"
      OutScaling         "2^0"
    }
    Line {
      SrcBlock           " SFunction "
      SrcPort            1
      DstBlock           " Demux "
      DstPort            1
    }
    Line {
      SrcBlock           "UGR"
      SrcPort            1
      DstBlock           " SFunction "
      DstPort            1
    }
    Line {
      SrcBlock           "GFR"
      SrcPort            1
      DstBlock           " SFunction "
      DstPort            2
    }
    Line {
      Name               "urea_gen"
      Labels              [0, 0]
      SrcBlock           " SFunction "
      SrcPort            2
      DstBlock           "urea_gen"
      DstPort            1
    }
    Line {
      SrcBlock           " Demux "
      SrcPort            1
      DstBlock           " Terminator "
      DstPort            1
    }
  }
}
Block {
  BlockType             BlockType
  Name                  "Blood Flow Rate"
  Position              [200, 450, 230, 480]
  Value                 "1000"
  OutDataType           "sfix(16)"
  OutScaling            "2^0"
}
Block {
  BlockType             UnitDelay
  Name                  "Blood concentration\ndelay"
  Position              [820, 598, 855, 632]
  X0                    "1.607142856"
}
Block {
  BlockType             SubSystem
  Name                  "Calculate B and D\nconcentration changes"
  Ports                 [10, 3]
  Position               [790, 382, 955, 543]
  ForegroundColor       "blue"
  PermitHierarchicalResolution "ExplicitOnly"
  MinAlgLoopOccurrences off
  PropExecContextOutsideSubsystem off
  RTWSystemCode         "Auto"
  FunctionWithSeparateData off
  Opaque                off
  Array {
    Type                "Handle"
    Dimension            0
    PropName             "AvailSigsLoadSave"
  }
  RequestExecContextInheritance off
  MaskHideContents     off
  MaskType              "Stateflow"
  MaskDescription       "Embedded MATLAB block"
  MaskDisplay           "disp('Dialyance');"
  MaskSelfModifiable  on
  MaskIconFrame         on
  MaskIconOpaque       off
  MaskIconRotate       "none"
  MaskIconUnits        "autoscale"
  System {
    Name                "Calculate B and
D\nconcentration changes"
    Location             [257, 457, 812, 717]
    Open                 off
    ModelBrowserVisibility off
    ModelBrowserWidth  200
    ScreenColor          "white"
    PaperOrientation     "landscape"
    PaperPositionMode   "auto"
    PaperType            "usletter"
    PaperUnits           "inches"
    TiledPaperMargins   [0.500000, 0.500000, 0.500000,
0.500000]
    TiledPageScale      1
    ShowPageBoundaries  off
    ZoomFactor          "100"
    Block {
      BlockType          Inport
      Name               "urea_gen"
      Position           [460, 101, 480, 119]
      IconDisplay        "Port number"
      OutDataType        "sfix(16)"
      OutScaling         "2^0"
    }
    Line {
      SrcBlock           " SFunction "
      SrcPort            1
      DstBlock           " Demux "
      DstPort            1
    }
    Line {
      SrcBlock           "UGR"
      SrcPort            1
      DstBlock           " SFunction "
      DstPort            1
    }
    Line {
      SrcBlock           "GFR"
      SrcPort            1
      DstBlock           " SFunction "
      DstPort            2
    }
    Line {
      Name               "urea_gen"
      Labels              [0, 0]
      SrcBlock           " SFunction "
      SrcPort            2
      DstBlock           "urea_gen"
      DstPort            1
    }
    Line {
      SrcBlock           " Demux "
      SrcPort            1
      DstBlock           " Terminator "
      DstPort            1
    }
  }
}
Block {
  BlockType             BlockType
  Name                  "Blood Flow Rate"
  Position              [200, 450, 230, 480]
  Value                 "1000"
  OutDataType           "sfix(16)"
  OutScaling            "2^0"
}
Block {
  BlockType             UnitDelay
  Name                  "Blood concentration\ndelay"
  Position              [820, 598, 855, 632]
  X0                    "1.607142856"
}
Block {
  BlockType             SubSystem
  Name                  "Calculate B and D\nconcentration changes"
  Ports                 [10, 3]
  Position               [790, 382, 955, 543]
  ForegroundColor       "blue"
  PermitHierarchicalResolution "ExplicitOnly"
  MinAlgLoopOccurrences off
  PropExecContextOutsideSubsystem off
  RTWSystemCode         "Auto"
  FunctionWithSeparateData off
  Opaque                off
  Array {
    Type                "Handle"
    Dimension            0
    PropName             "AvailSigsLoadSave"
  }
  RequestExecContextInheritance off
  MaskHideContents     off
  MaskType              "Stateflow"
  MaskDescription       "Embedded MATLAB block"
  MaskDisplay           "disp('Dialyance');"
  MaskSelfModifiable  on
  MaskIconFrame         on
  MaskIconOpaque       off
  MaskIconRotate       "none"
  MaskIconUnits        "autoscale"
  System {
    Name                "Calculate B and
D\nconcentration changes"
    Location             [257, 457, 812, 717]
    Open                 off
    ModelBrowserVisibility off
    ModelBrowserWidth  200
    ScreenColor          "white"
    PaperOrientation     "landscape"
    PaperPositionMode   "auto"
    PaperType            "usletter"
    PaperUnits           "inches"
    TiledPaperMargins   [0.500000, 0.500000, 0.500000,
0.500000]
    TiledPageScale      1
    ShowPageBoundaries  off
    ZoomFactor          "100"
    Block {
      BlockType          Inport
      Name               "urea_gen"
      Position           [460, 101, 480, 119]
      IconDisplay        "Port number"
      OutDataType        "sfix(16)"
      OutScaling         "2^0"
    }
    Line {
      SrcBlock           " SFunction "
      SrcPort            1
      DstBlock           " Demux "
      DstPort            1
    }
    Line {
      SrcBlock           "UGR"
      SrcPort            1
      DstBlock           " SFunction "
      DstPort            1
    }
    Line {
      SrcBlock           "GFR"
      SrcPort            1
      DstBlock           " SFunction "
      DstPort            2
    }
    Line {
      Name               "urea_gen"
      Labels              [0, 0]
      SrcBlock           " SFunction "
      SrcPort            2
      DstBlock           "urea_gen"
      DstPort            1
    }
    Line {
      SrcBlock           " Demux "
      SrcPort            1
      DstBlock           " Terminator "
      DstPort            1
    }
  }
}
Block {
  BlockType             BlockType
  Name                  "Blood Flow Rate"
  Position              [200, 450, 230, 480]
  Value                 "1000"
  OutDataType           "sfix(16)"
  OutScaling            "2^0"
}
Block {
  BlockType             UnitDelay
  Name                  "Blood concentration\ndelay"
  Position              [820, 598, 855, 632]
  X0                    "1.607142856"
}
Block {
  BlockType             SubSystem
  Name                  "Calculate B and D\nconcentration changes"
  Ports                 [10, 3]
  Position               [790, 382, 955, 543]
  ForegroundColor       "blue"
  PermitHierarchicalResolution "ExplicitOnly"
  MinAlgLoopOccurrences off
  PropExecContextOutsideSubsystem off
  RTWSystemCode         "Auto"
  FunctionWithSeparateData off
  Opaque                off
  Array {
    Type                "Handle"
    Dimension            0
    PropName             "AvailSigsLoadSave"
  }
  RequestExecContextInheritance off
  MaskHideContents     off
  MaskType              "Stateflow"
  MaskDescription       "Embedded MATLAB block"
  MaskDisplay           "disp('Dialyance');"
  MaskSelfModifiable  on
  MaskIconFrame         on
  MaskIconOpaque       off
  MaskIconRotate       "none"
  MaskIconUnits        "autoscale"
  System {
    Name                "Calculate B and
D\nconcentration changes"
    Location             [257, 457, 812, 717]
    Open                 off
    ModelBrowserVisibility off
    ModelBrowserWidth  200
    ScreenColor          "white"
    PaperOrientation     "landscape"
    PaperPositionMode   "auto"
    PaperType            "usletter"
    PaperUnits           "inches"
    TiledPaperMargins   [0.500000, 0.500000, 0.500000,
0.500000]
    TiledPageScale      1
    ShowPageBoundaries  off
    ZoomFactor          "100"
    Block {
      BlockType          Inport
      Name               "urea_gen"
      Position           [460, 101, 480, 119]
      IconDisplay        "Port number"
      OutDataType        "sfix(16)"
      OutScaling         "2^0"
    }
    Line {
      SrcBlock           " SFunction "
      SrcPort            1
      DstBlock           " Demux "
      DstPort            1
    }
    Line {
      SrcBlock           "UGR"
      SrcPort            1
      DstBlock           " SFunction "
      DstPort            1
    }
    Line {
      SrcBlock           "GFR"
      SrcPort            1
      DstBlock           " SFunction "
      DstPort            2
    }
    Line {
      Name               "urea_gen"
      Labels              [0, 0]
      SrcBlock           " SFunction "
      SrcPort            2
      DstBlock           "urea_gen"
      DstPort            1
    }
    Line {
      SrcBlock           " Demux "
      SrcPort            1
      DstBlock           " Terminator "
      DstPort            1
    }
  }
}
Block {
  BlockType             BlockType
  Name                  "Blood Flow Rate"
  Position              [200, 450, 230, 480]
  Value                 "1000"
  OutDataType           "sfix(16)"
  OutScaling            "2^0"
}
Block {
  BlockType             UnitDelay
  Name                  "Blood concentration\ndelay"
  Position              [820, 598, 855, 632]
  X0                    "1.607142856"
}
Block {
  BlockType             SubSystem
  Name                  "Calculate B and D\nconcentration changes"
  Ports                 [10, 3]
  Position               [790, 382, 955, 543]
  ForegroundColor       "blue"
  PermitHierarchicalResolution "ExplicitOnly"
  MinAlgLoopOccurrences off
  PropExecContextOutsideSubsystem off
  RTWSystemCode         "Auto"
  FunctionWithSeparateData off
  Opaque                off
  Array {
    Type                "Handle"
    Dimension            0
    PropName             "AvailSigsLoadSave"
  }
  RequestExecContextInheritance off
  MaskHideContents     off
  MaskType              "Stateflow"
  MaskDescription       "Embedded MATLAB block"
  MaskDisplay           "disp('Dialyance');"
  MaskSelfModifiable  on
  MaskIconFrame         on
  MaskIconOpaque       off
  MaskIconRotate       "none"
  MaskIconUnits        "autoscale"
  System {
    Name                "Calculate B and
D\nconcentration changes"
    Location             [257, 457, 812, 717]
    Open                 off
    ModelBrowserVisibility off
    ModelBrowserWidth  200
    ScreenColor          "white"
    PaperOrientation     "landscape"
    PaperPositionMode   "auto"
    PaperType            "usletter"
    PaperUnits           "inches"
    TiledPaperMargins   [0.500000, 0.500000, 0.500000,
0.500000]
    TiledPageScale      1
    ShowPageBoundaries  off
    ZoomFactor          "100"
    Block {
      BlockType          Inport
      Name               "urea_gen"
      Position           [460, 101, 480, 119]
      IconDisplay        "Port number"
      OutDataType        "sfix(16)"
      OutScaling         "2^0"
    }
    Line {
      SrcBlock           " SFunction "
      SrcPort            1
      DstBlock           " Demux "
      DstPort            1
    }
    Line {
      SrcBlock           "UGR"
      SrcPort            1
      DstBlock           " SFunction "
      DstPort            1
    }
    Line {
      SrcBlock           "GFR"
      SrcPort            1
      DstBlock           " SFunction "
      DstPort            2
    }
    Line {
      Name               "urea_gen"
      Labels              [0, 0]
      SrcBlock           " SFunction "
      SrcPort            2
      DstBlock           "urea_gen"
      DstPort            1
    }
    Line {
      SrcBlock           " Demux "
      SrcPort            1
      DstBlock           " Terminator "
      DstPort            1
    }
  }
}

```





```

Name "Dialyzer Dialysate\nPressure"
Position [500, 345, 530, 375]
Value "50"
OutDataType "sfix(16)"
OutScaling "2^0"
}
Block {
BlockType Integrator
Name "Integrator"
Ports [1, 1]
Position [635, 200, 665, 230]
}
Block {
BlockType Constant
Name "Kidney GFR%"
Position [285, 685, 315, 715]
Value "0"
OutDataType "sfix(16)"
OutScaling "2^0"
}
Block {
BlockType Constant
Name "KoA"
Position [200, 505, 230, 535]
Value "16000"
OutDataType "sfix(16)"
OutScaling "2^0"
}
Block {
BlockType SubSystem
Name "Optimize Dialysate Flow Rate"
Ports [2, 2]
Position [325, 439, 450, 546]
ForegroundColor "blue"
PermitHierarchicalResolution "ExplicitOnly"
MinAlgLoopOccurrences off
PropExecContextOutsideSubsystem off
RTWSystemCode "Auto"
FunctionWithSeparateData off
Opaque off
Array {
Type "Handle"
Dimension 0
PropName "AvailSigsLoadSave"
}
RequestExecContextInheritance off
MaskHideContents off
MaskType "Stateflow"
MaskDescription "Embedded MATLAB block"
MaskDisplay "disp('Dialysate');"
MaskSelfModifiable on
MaskIconFrame on
MaskIconOpaque off
MaskIconRotate "none"
MaskIconUnits "autoscale"
System {
Name "Optimize Dialysate Flow
Rate"
Location [257, 457, 812, 717]
Open off
ModelBrowserVisibility off
ModelBrowserWidth 200
ScreenColor "white"
PaperOrientation "landscape"
PaperPositionMode "auto"
PaperType "usletter"
PaperUnits "inches"
TiledPaperMargins [0.500000, 0.500000, 0.500000,
0.500000]
TiledPageScale 1
ShowPageBoundaries off
ZoomFactor "100"
Block {
BlockType Inport
Name "Qb"
Position [20, 101, 40, 119]
IconDisplay "Port number"
OutDataType "sfix(16)"
OutScaling "2^0"
}
Block {
BlockType Inport
Name "KoA"
Position [20, 136, 40, 154]
Port "2"
IconDisplay "Port number"
}
Block {
BlockType Demux
Name " Demux "
Ports [1, 1]
Position [270, 220, 320, 260]
Outputs "1"
}
Block {
BlockType "S-Function"
Name " SFunction "
Tag "Stateflow S-Function"
reconciled 2"
Ports [2, 3]
Position [180, 100, 230, 220]
FunctionName "sf_sfun"
}

```

```

PortCounts "2 3"
EnableBusSupport on
Port {
PortNumber 2
Name "Qd"
RTWStorageClass "Auto"
DataLoggingNameMode "SignalName"
}
Port {
PortNumber 3
Name "K"
RTWStorageClass "Auto"
DataLoggingNameMode "SignalName"
}
Block {
BlockType Terminator
Name " Terminator "
Position [460, 231, 480, 249]
}
Block {
BlockType Outport
Name "Qd"
Position [460, 101, 480, 119]
IconDisplay "Port number"
}
Block {
BlockType Outport
Name "K"
Position [460, 136, 480, 154]
Port "2"
IconDisplay "Port number"
OutDataType "sfix(16)"
OutScaling "2^0"
}
Line {
SrcBlock " SFunction "
SrcPort 1
DstBlock " Demux "
DstPort 1
}
Line {
SrcBlock "Qb"
SrcPort 1
DstBlock " SFunction "
DstPort 1
}
Line {
SrcBlock "KoA"
SrcPort 1
DstBlock " SFunction "
DstPort 2
}
Line {
Name "Qd"
Labels [0, 0]
SrcBlock " SFunction "
SrcPort 2
DstBlock "Qd"
DstPort 1
}
Line {
Name "K"
Labels [0, 0]
SrcBlock " SFunction "
SrcPort 3
DstBlock "K"
DstPort 1
}
Line {
SrcBlock " Demux "
SrcPort 1
DstBlock " Terminator "
DstPort 1
}
}
Block {
BlockType Product
Name "Product"
Ports [2, 1]
Position [580, 197, 610, 228]
InputSameDT off
OutDataTypeMode "Inherit via internal rule"
OutDataType "sfix(16)"
OutScaling "2^0"
OutDataTypeStr "Inherit: Inherit via internal rule"
SaturateOnIntegerOverflow off
}
Block {
BlockType Product
Name "Product1"
Ports [2, 1]
Position [660, 312, 690, 343]
InputSameDT off
OutDataTypeMode "Inherit via internal rule"
OutDataType "sfix(16)"
OutScaling "2^0"
OutDataTypeStr "Inherit: Inherit via internal rule"
SaturateOnIntegerOverflow off
}
Block {
}

```

```

BlockType      Scope
Name           "Scope"
Ports         [1]
Position       [1340, 324, 1370, 356]
Floating      off
Location      [1, 46, 1601, 1169]
Open          off
NumInputPorts "1"
List {
  ListType    AxesTitles "%<SignalLabel>"
  axes1
}
TimeRange     "110" "1440"
YMin          "110"
YMax          "300"
SaveName      "ScopeData1"
DataFormat    "StructureWithTime"
SampleTime    "0"
}
Block {
BlockType      Scope
Name           "Scope1"
Ports         [1]
Position       [1130, 824, 1160, 856]
Floating      off
Location      [1, 46, 1601, 1169]
Open          off
NumInputPorts "1"
List {
  ListType    AxesTitles "%<SignalLabel>"
  axes1
}
SaveName      "ScopeData2"
DataFormat    "StructureWithTime"
SampleTime    "0"
}
Block {
BlockType      SubSystem
Name           "Select proper\ndialysate volume"
Ports         [2, 1]
Position       [760, 204, 840, 251]
ForegroundColor "blue"
PermitHierarchicalResolution "ExplicitOnly"
MinAlgLoopOccurrences off
PropExecContextOutsideSubsystem off
RTWSystemCode "Auto"
FunctionWithSeparateData off
Opaque        off
Array {
  Type        "Handle"
  Dimension   0
  PropName    "AvailSigsLoadSave"
}
RequestExecContextInheritance off
MaskHideContents off
MaskType      "Stateflow"
MaskDescription "Embedded MATLAB block"
MaskDisplay   "disp('fcn');"
MaskSelfModifiable on
MaskIconFrame on
MaskIconOpaque off
MaskIconRotate "none"
MaskIconUnits "autoscale"
System {
  Name        "Select"
  Location    [257, 457, 812, 717]
  Open        off
  ModelBrowserVisibility off
  ModelBrowserWidth 200
  ScreenColor "white"
  PaperOrientation "landscape"
  PaperPositionMode "auto"
  PaperType      "usletter"
  PaperUnits     "inches"
  TiledPaperMargins [0.500000, 0.500000, 0.500000,
0.500000]
  TiledPageScale 1
  ShowPageBoundaries off
  ZoomFactor      "100"
  Block {
    BlockType      Inport
    Name           "d1"
    Position       [20, 101, 40, 119]
    IconDisplay    "Port number"
    OutDataType    "sfix(16)"
    OutScaling     "2^0"
  }
  Block {
    BlockType      Inport
    Name           "d2"
    Position       [20, 136, 40, 154]
    Port          "2"
    IconDisplay    "Port number"
  }
}
Block {
BlockType      Demux
Name           "Demux "
Ports         [1, 1]
Position       [270, 160, 320, 200]
Outputs       "1"
}
Block {

```

```

BlockType      "S-Function"
Name           " SFunction "
Tag           "Stateflow S-Function"
Ports         [2, 2]
Position       [180, 100, 230, 160]
FunctionName   "sf_sfun"
PortCounts    "[2 2]"
EnableBusSupport on
Port {
  PortNumber    2
  Name          "d_act"
  RTWStorageClass "Auto"
  DataLoggingNameMode "SignalName"
}
Block {
BlockType      Terminator
Name           " Terminator "
Position       [460, 171, 480, 189]
}
Block {
BlockType      Outport
Name           "d_act"
Position       [460, 101, 480, 119]
IconDisplay    "Port number"
OutDataType    "sfix(16)"
OutScaling     "2^0"
}
Line {
SrcBlock      " SFunction "
SrcPort       1
DstBlock      " Demux "
DstPort       1
}
Line {
SrcBlock      "d1"
SrcPort       1
DstBlock      " SFunction "
DstPort       1
}
Line {
SrcBlock      "d2"
SrcPort       1
DstBlock      " SFunction "
DstPort       2
}
Line {
Name          "d_act"
Labels       [0, 0]
SrcBlock     " SFunction "
SrcPort      2
DstBlock     "d_act"
DstPort      1
}
Line {
SrcBlock      " Demux "
SrcPort       1
DstBlock      " Terminator "
DstPort       1
}
}
Block {
BlockType      Sum
Name           "Subtract"
Ports         [2, 1]
Position       [595, 317, 625, 348]
Inputs        "+-"
InputSameDT   off
OutDataTypeMode "Inherit via internal rule"
OutDataType    "sfix(16)"
OutScaling     "2^-10"
OutDataTypeStr "Inherit: Inherit via internal rule"
SaturateOnIntegerOverflow off
}
Block {
BlockType      ToWorkspace
Name           "To Workspace"
Position       [1330, 395, 1390, 425]
VariableName   "y"
MaxDataPoints "inf"
SampleTime    "-1"
SaveFormat     "Array"
}
Block {
BlockType      ToWorkspace
Name           "To Workspace1"
Position       [1130, 275, 1190, 305]
VariableName   "y1"
MaxDataPoints "inf"
SampleTime    "-1"
SaveFormat     "Array"
}
Block {
BlockType      Constant
Name           "Total Blood VolumeVn(mL)"
Position       [620, 470, 650, 500]
Value          "32000"
OutDataType    "sfix(16)"
OutScaling     "2^0"
}
}

```



```

    DstBlock          "Calculate B and          Points          [230, 0; 0, 20]
D\nconcentration changes"  DstBlock          "Product1"
    DstPort          9                      DstPort          1
  }
  Line {
    SrcBlock          "Product"
    SrcPort          1
    DstBlock          "Integrator"
    DstPort          1
  }
  Line {
    SrcBlock          "Total Dialysate\nVolume (mL)"
    SrcPort          1
    Points            [10, 0]
    Branch {
      Points          [15, 0; 0, -30]
      DstBlock        "Calculate B and D\nconcentration
changes"             DstPort          8
    }
    Branch {
      Points          [0, -290]
      DstBlock        "Select proper\nDialysate volume"
      DstPort          2
    }
  }
  Line {
    SrcBlock          "Calculate B and
D\nconcentration changes"  SrcPort          2
    SrcPort          2
    Points            [15, 0]
    DstBlock          "Dialysate
concentration\nDelay"      DstBlock          1
    DstPort          1
  }
  Line {
    SrcBlock          "Dialysate
concentration\nDelay"      SrcPort          1
    SrcPort          1
    Points            [50, 0; 0, 75; -55, 0]
    Branch {
      Points          [-270, 0; 0, -225]
      DstBlock        "Calculate B and D\nconcentration
changes"             DstPort          6
    }
    Branch {
      Points          [0, 145]
      DstBlock        "Scope1"
      DstPort          1
    }
  }
  Line {
    SrcBlock          "Select proper\nDialysate
volume"                  SrcPort          1
    SrcPort          1
    DstBlock          "Convert mL\nTo L"
    DstPort          1
  }
  Line {
    SrcBlock          "Convert mL\nTo L"
    SrcPort          1
    SrcPort          1
    Points            [-85, 0]
    DstBlock          "Total Dialysate\n(L)"
    DstPort          1
  }
  Line {
    SrcBlock          "Convert urea concentration
(mg/mL)\nTO BUN"        SrcPort          1
    SrcPort          1
    Points            [30, 0]
    Branch {
      DstBlock        "To Workspace"
      DstPort          1
    }
    Branch {
      Points          [0, -70]
      DstBlock        "Scope"
      DstPort          1
    }
  }
  Line {
    SrcBlock          "Dialyzer Blood\nPressure"
    SrcPort          1
    DstBlock          "Subtract"
    DstPort          1
  }
  Line {
    SrcBlock          "Dialyzer Dialysate\nPressure"
    SrcPort          1
    Points            [0, -20]
    DstBlock          "Subtract"
    DstPort          2
  }
  Line {
    SrcBlock          "Subtract"
    SrcPort          1
    DstBlock          "Product1"
    DstPort          2
  }
  Line {
    SrcBlock          "Ultrafiltration\nCoefficient"
    SrcPort          1
  }
}

D\nconcentration changes"  DstBlock          "Product1"
DstPort          1
}
Line {
  SrcBlock          "Product1"
  SrcPort          1
  Points            [30, 0; 0, 65]
  DstBlock          "Calculate B and
D\nconcentration changes"  DstBlock          1
  DstPort          1
}
}
# Finite State Machines
# Stateflow Version 7.1 (R2008a) dated Feb 7 2008, 21:38:28
#
Stateflow {
  machine {
    id                1
    name              "reconciled"
    created            "27-Aug-2008 13:50:43"
    isLibrary          0
    firstTarget        52
    sfVersion          71014000.000003
  }
  chart {
    id                2
    name              "Account for residual\nkidney function"
    windowPosition    [352.266 253.688 200.25 189.75]
    viewLimits        [0 156.75 0 153.75]
    screen            [1 1 1600 1200 1.3333333333333333]
    treeNode          [0 3 0 0]
    firstTransition    5
    firstJunction      4
    viewObj           2
    machine           1
    ssIdHighWaterMark 6
    decomposition     CLUSTER_CHART
    type              EML_CHART
    firstData         6
    chartFileNumber   1
    disableImplicitCasting 1
    eml {
      name            "fcn"
    }
  }
  state {
    id                3
    labelString        "eML_blk_kernel()"
    position           [18 64.5 118 66]
    fontSize           12
    chart             2
    treeNode          [2 0 0 0]
    superState        SUBCHART
    subviewer         2
    ssIdNumber        1
    type              FUNC_STATE
    decomposition     CLUSTER_STATE
    eml {
      isEML           1
      script           "function urea_gen = fcn(UGR,
GFR)\n% This block supports the Embedded MATLAB subset.\n% See the help
menu for details. \n\nurea_gen = (1-GFR)*UGR;\n"
      editorLayout    "100 M4x1[806 216 671 364]"
    }
  }
  junction {
    id                4
    position           [23.5747 49.5747 7]
    chart             2
    linkNode          [2 0 0]
    subviewer         2
    ssIdNumber        3
    type              CONNECTIVE_JUNCTION
  }
  transition {
    id                5
    labelString        "{eML_blk_kernel();}"
    labelPosition     [32.125 19.875 102.544 14.964]
    fontSize          12
    src {
      intersection    [0 0 1 0 23.5747 14.625 0 0]
    }
    dst {
      id              4
      intersection    [7 0 -1 -1 23.5747 42.5747 0 0]
    }
    midPoint          2
    chart             [2 0 0]
    linkNode          [23.575 23.575 14.625 34.575]
    dataLimits        2
    subviewer         SMART
    drawStyle         2
    executionOrder    1
    ssIdNumber        2
  }
  data {

```

```

id 6
ssIdNumber 6
name "UGR"
linkNode [2 0 7]
scope INPUT_DATA
machine 1
props {
  array {
    size "-1"
  }
  type {
    method SF_INHERITED_TYPE
    primitive SF_DOUBLE_TYPE
    isSigned 1
    wordLength "16"
  }
  complexity SF_COMPLEX_INHERITED
  frame SF_FRAME_INHERITED
}
dataType "Inherit: Same as Simulink"
}
data {
id 7
ssIdNumber 4
name "GFR"
linkNode [2 6 8]
scope INPUT_DATA
machine 1
props {
  array {
    size "-1"
  }
  type {
    method SF_INHERITED_TYPE
    primitive SF_DOUBLE_TYPE
  }
  complexity SF_COMPLEX_INHERITED
}
dataType "Inherit: Same as Simulink"
}
data {
id 8
ssIdNumber 5
name "urea_gen"
linkNode [2 7 0]
scope OUTPUT_DATA
machine 1
props {
  array {
    size "-1"
  }
  type {
    method SF_INHERITED_TYPE
    primitive SF_DOUBLE_TYPE
  }
  complexity SF_COMPLEX_INHERITED
  frame SF_FRAME_NO
}
dataType "Inherit: Same as Simulink"
}
instance {
id 9
name "Account for residual\nkidney function"
machine 1
chart 2
}
chart {
id 10
name "Optimize Dialysate Flow Rate"
windowPosition [352.266 253.688 200.25 189.75]
viewLimits [0 156.75 0 153.75]
screen [1 1 1600 1200 1.3333333333333333]
treeNode [0 11 0 0]
firstTransition 13
firstJunction 12
viewObj 10
machine 1
ssIdHighWaterMark 10
decomposition CLUSTER_CHART
type EML_CHART
firstData 14
chartFileNumber 2
disableImplicitCasting 1
eml {
  name "Dialysate"
}
}
state {
id 11
labelString "eML_blk_kernel()"
position [18 64.5 118 66]
fontSize 12
chart 10
treeNode [10 0 0 0]
superState SUBCHART
subviewer 10
ssIdNumber 1
type FUNC_STATE
decomposition CLUSTER_STATE
eml {
  isEML 1
  script "function [Qd,K] =
Dialysate(Qb, KoA)\n\n% a = Qb;\n% c = KoA;\n% \n% b = 1;\n% jmax =

```

```

0;\n% \n% while b < 1000\n% J = (a)*((exp((c)*(1-(a/b)))/(a)-
1))/((exp((c)*(1-(a/b)))/(a))-(a/b));\n% if J > jmax\n%
jmax = J;\n% end\n% b = b+1.000001;\n% end\n% \n% d = 5;\n% L =
0;\n% P = 0.95*jmax;\n% \n% while L < P\n% d = d+1.001;\n% L =
(a)*((exp((c)*(1-(a/d)))/(a))-1))/((exp((c)*(1-(a/d)))/(a))-
(a/d));\n% if d > 1000\n% break\n% end\n% end\n% \n% K
= L;\n% Qd = round(d);\n% Qd = 1030;\n% K=1;\n%
}
editorLayout "100 M4x1[139 133 1122 930]"
}
junction {
id 12
position [23.5747 49.5747 7]
chart 10
linkNode [10 0 0]
subviewer 10
ssIdNumber 3
type CONNECTIVE_JUNCTION
}
transition {
id 13
labelString "eML_blk_kernel();"
labelPosition [32.125 19.875 102.544 14.964]
fontSize 12
src {
  intersection [0 0 1 0 23.5747 14.625 0 0]
}
dst {
  id 12
  intersection [7 0 -1 -1 23.5747 42.5747 0 0]
}
midPoint [23.5747 24.9468]
chart 10
linkNode [10 0 0]
dataLimits [23.575 23.575 14.625 34.575]
subviewer 10
drawStyle SMART
executionOrder 1
ssIdNumber 2
}
data {
id 14
ssIdNumber 8
name "Qd"
linkNode [10 0 15]
scope OUTPUT_DATA
machine 1
props {
  array {
    size "-1"
  }
  type {
    method SF_INHERITED_TYPE
    primitive SF_DOUBLE_TYPE
    isSigned 1
    wordLength "16"
  }
  complexity SF_COMPLEX_INHERITED
  frame SF_FRAME_NO
}
dataType "Inherit: Same as Simulink"
}
data {
id 15
ssIdNumber 4
name "Qb"
linkNode [10 14 16]
scope INPUT_DATA
machine 1
props {
  array {
    size "-1"
  }
  type {
    method SF_INHERITED_TYPE
    primitive SF_DOUBLE_TYPE
  }
  complexity SF_COMPLEX_INHERITED
}
dataType "Inherit: Same as Simulink"
}
data {
id 16
ssIdNumber 5
name "K"
linkNode [10 15 17]
scope OUTPUT_DATA
machine 1
props {
  array {
    size "-1"
  }
  type {
    method SF_INHERITED_TYPE
    primitive SF_DOUBLE_TYPE
  }
  complexity SF_COMPLEX_INHERITED
  frame SF_FRAME_NO
}
dataType "Inherit: Same as Simulink"
}
data {
id 17

```

```

ssIdNumber      7
name            "KoA"
linkNode       [10 16 0]
scope          INPUT_DATA
machine        1
props {
  array {
    size        "-1"
  }
  type {
    method      SF_INHERITED_TYPE
    primitive   SF_DOUBLE_TYPE
    isSigned    1
    wordLength  "16"
  }
  complexity   SF_COMPLEX_INHERITED
  frame       SF_FRAME_INHERITED
}
dataType      "Inherit: Same as Simulink"
}
instance {
  id          18
  name       "Optimize Dialysate Flow Rate"
  machine    1
  chart     10
}
chart {
  id        19
  name     "Select proper\ndialysate volume"
  windowPosition [352.266 253.688 200.25 189.75]
  viewLimits  [0 156.75 0 153.75]
  screen     [1 1 1600 1200 1.33333333333333]
  treeNode  [0 20 0 0]
  firstTransition 22
  firstJunction  21
  viewObj       19
  machine       1
  ssIdHighWaterMark 6
  decomposition CLUSTER_CHART
  type         EML_CHART
  firstData    23
  chartFileNumber 3
  disableImplicitCasting 1
  eml {
    name      "fcn"
  }
}
state {
  id        20
  labelString "eML_blk_kernel()"
  position  [18 64.5 118 66]
  fontSize  12
  chart    19
  treeNode [19 0 0 0]
  superState SUBCHART
  subviewer  19
  ssIdNumber 1
  type      FUNC_STATE
  decomposition CLUSTER_STATE
  eml {
    isEML      1
    script     "function d_act = fcn(d1,
d2)\n% This block supports the Embedded MATLAB subset.\n% See the help
menu for details. \n\nif d1<d2\n  d_act = d1;\nelse d_act =
d2;\nend\n"
  }
  editorLayout "100 M4x1[594 516 671 364]"
}
junction {
  id        21
  position  [23.5747 49.5747 7]
  chart    19
  linkNode [19 0 0]
  subviewer 19
  ssIdNumber 3
  type      CONNECTIVE_JUNCTION
}
transition {
  id        22
  labelString "eML_blk_kernel();"
  labelPosition [32.125 19.875 102.544 14.964]
  fontSize  12
  src {
    intersection [0 0 1 0 23.5747 14.625 0 0]
  }
  dst {
    id        21
    intersection [7 0 -1 -1 23.5747 42.5747 0 0]
  }
  midPoint  [23.5747 24.9468]
  chart    19
  linkNode [19 0 0]
  dataLimits [23.575 23.575 14.625 34.575]
  subviewer 19
  drawStyle SMART
  executionOrder 1
  ssIdNumber 2
}
data {
  id        23
  ssIdNumber 4
  name     "d1"
  linkNode [19 0 24]
}

```

```

scope          INPUT_DATA
machine        1
props {
  array {
    size        "-1"
  }
  type {
    method      SF_INHERITED_TYPE
    primitive   SF_DOUBLE_TYPE
  }
  complexity   SF_COMPLEX_INHERITED
  dataType     "Inherit: Same as Simulink"
}
data {
  id          24
  ssIdNumber  5
  name       "d_act"
  linkNode   [19 23 25]
  scope     OUTPUT_DATA
  machine   1
  props {
    array {
      size        "-1"
    }
    type {
      method      SF_INHERITED_TYPE
      primitive   SF_DOUBLE_TYPE
    }
    complexity   SF_COMPLEX_INHERITED
    frame       SF_FRAME_NO
  }
  dataType     "Inherit: Same as Simulink"
}
data {
  id          25
  ssIdNumber  6
  name       "d2"
  linkNode   [19 24 0]
  scope     INPUT_DATA
  machine   1
  props {
    array {
      size        "-1"
    }
    type {
      method      SF_INHERITED_TYPE
      primitive   SF_DOUBLE_TYPE
      isSigned    1
      wordLength  "16"
    }
    complexity   SF_COMPLEX_INHERITED
    frame       SF_FRAME_INHERITED
  }
  dataType     "Inherit: Same as Simulink"
}
instance {
  id          26
  name       "Select proper\ndialysate volume"
  machine    1
  chart     19
}
chart {
  id        27
  name     "Calculate B and D\nconcentration changes"
  windowPosition [367.266 238.688 200.25 189.75]
  viewLimits  [0 156.75 0 153.75]
  screen     [1 1 1600 1200 1.33333333333333]
  treeNode  [0 28 0 0]
  firstTransition 30
  firstJunction  29
  viewObj       27
  machine       1
  ssIdHighWaterMark 18
  decomposition CLUSTER_CHART
  type         EML_CHART
  firstData    31
  chartFileNumber 4
  disableImplicitCasting 1
  eml {
    name      "Dialyance"
  }
}
state {
  id        28
  labelString "eML_blk_kernel()"
  position  [18 64.5 118 66]
  fontSize  12
  chart    27
  treeNode [27 0 0 0]
  superState SUBCHART
  subviewer 27
  ssIdNumber 1
  type      FUNC_STATE
  decomposition CLUSTER_STATE
  eml {
    isEML      1
    script     "function [bconc, dconc, D] =
Dialyance(Qf, Qb, Qd, KoA, cbi, cdi, Vb, Vd, urea_gen, sched)\n\n% a =
(exp(1)) + ((KoA * (1 - (Qb/Qd)))/(Qb)) - (1);\n% b = (exp(1) + ((KoA
* (1 - (Qb/Qd)))/(Qb)))/(Qb);\n% c = 1/Qd;\n\n% D = (a)/(b-c);\n\nif
sched == 0\n  cdi=0;\nend\n\nif Qb == Qd\n  Qd = Qd + 1;\nend\n\n% a =
Qb;\n% b = Qd;\n% c = KoA;\n% nf = ((c)*(1-(a/b)))/(a);\n\n% D = (exp(f)-

```

```

1)/((exp(f/a)-(1/b));\n\nmgd_total = cbi * Vb;\n\nmgd_total = cdi *
Vd;\n\nncbo = (cbi - (D/Qb)*(cbi-cdi);\n\n% cdo = ((D/Qd)*(cbi-cdi)) +
cdi;\n\nmg_removed = (cbo-cbi)*(Qb) + (Qf)*(cbo);\n\nif sched == 0\n
mg_removed = 0;\n\nend\n\nnew_total = mg_total - mg_removed +
urea_gen;\n\nnbconc = new_total / Vb;\n\nnewd_total = mgd_total +
mg_removed;\n\nndconc = newd_total / Vd;"
editorLayout "100 M4x1[806 216 1616 1186]"
}
}
junction {
id 29
position [23.5747 49.5747 7]
chart 27
linkNode [27 0 0]
subviewer 27
ssIdNumber 3
type CONNECTIVE_JUNCTION
}
transition {
id 30
labelString "{eML_blk_kernel()};"
labelPosition [32.125 19.875 102.544 14.964]
fontSize 12
src {
intersection [0 0 1 0 23.5747 14.625 0 0]
}
dst {
id 29
intersection [7 0 -1 -1 23.5747 42.5747 0 0]
}
midPoint [23.5747 24.9468]
chart 27
linkNode [27 0 0]
dataLimits [23.575 23.575 14.625 34.575]
subviewer 27
drawStyle SMART
executionOrder 1
ssIdNumber 2
}
data {
id 31
ssIdNumber 18
name "Qf"
linkNode [27 0 32]
scope INPUT_DATA
machine 1
props {
array {
size "-1"
}
type {
method primitive SF_INHERITED_TYPE
isSigned 1
wordLength "16"
}
complexity SF_COMPLEX_INHERITED
frame SF_FRAME_INHERITED
}
dataType "Inherit: Same as Simulink"
}
data {
id 32
ssIdNumber 4
name "Qb"
linkNode [27 31 33]
scope INPUT_DATA
machine 1
props {
array {
size "-1"
}
type {
method primitive SF_INHERITED_TYPE
isSigned 1
wordLength "16"
}
complexity SF_COMPLEX_INHERITED
frame SF_FRAME_INHERITED
}
dataType "Inherit: Same as Simulink"
}
data {
id 33
ssIdNumber 11
name "Qd"
linkNode [27 32 34]
scope INPUT_DATA
machine 1
props {
array {
size "-1"
}
type {
method primitive SF_INHERITED_TYPE
isSigned 1
wordLength "16"
}
complexity SF_COMPLEX_INHERITED
frame SF_FRAME_NO
}
dataType "Inherit: Same as Simulink"
}
data {

```

```

id 34
ssIdNumber 5
name "bconc"
linkNode [27 33 35]
scope OUTPUT_DATA
machine 1
props {
array {
size "-1"
}
type {
method primitive SF_INHERITED_TYPE
isSigned 1
wordLength "16"
}
complexity SF_COMPLEX_INHERITED
frame SF_FRAME_NO
}
dataType "Inherit: Same as Simulink"
}
data {
id 35
ssIdNumber 17
name "dconc"
linkNode [27 34 36]
scope OUTPUT_DATA
machine 1
props {
array {
size "-1"
}
type {
method primitive SF_INHERITED_TYPE
isSigned 1
wordLength "16"
}
complexity SF_COMPLEX_INHERITED
frame SF_FRAME_NO
}
dataType "Inherit: Same as Simulink"
}
data {
id 36
ssIdNumber 7
name "KoA"
linkNode [27 35 37]
scope INPUT_DATA
machine 1
props {
array {
size "-1"
}
type {
method primitive SF_INHERITED_TYPE
isSigned 1
wordLength "16"
}
complexity SF_COMPLEX_INHERITED
frame SF_FRAME_INHERITED
}
dataType "Inherit: Same as Simulink"
}
data {
id 37
ssIdNumber 8
name "cbi"
linkNode [27 36 38]
scope INPUT_DATA
machine 1
props {
array {
size "-1"
}
type {
method primitive SF_INHERITED_TYPE
isSigned 1
wordLength "16"
}
complexity SF_COMPLEX_INHERITED
frame SF_FRAME_INHERITED
}
dataType "Inherit: Same as Simulink"
}
data {
id 38
ssIdNumber 15
name "cdi"
linkNode [27 37 39]
scope INPUT_DATA
machine 1
props {
array {
size "-1"
}
type {
method primitive SF_INHERITED_TYPE
isSigned 1
wordLength "16"
}
complexity SF_COMPLEX_INHERITED
frame SF_FRAME_NO
}
dataType "Inherit: Same as Simulink"
}
data {
id 39
ssIdNumber 16
name "cdo"
linkNode [27 38 40]
scope INPUT_DATA
machine 1
props {
array {
size "-1"
}
type {
method primitive SF_INHERITED_TYPE
isSigned 1
wordLength "16"
}
complexity SF_COMPLEX_INHERITED
frame SF_FRAME_NO
}
dataType "Inherit: Same as Simulink"
}

```



```

    }
    complexity SF_COMPLEX_INHERITED
  }
  dataType "Inherit: Same as Simulink"
}
data {
  id 50
  ssIdNumber 5
  name "bun"
  linkNode [45 49 0]
  scope OUTPUT_DATA
  machine 1
  props {
    array {
      size "-1"
    }
    type {
      method SF_INHERITED_TYPE
      primitive SF_DOUBLE_TYPE
    }
    complexity SF_COMPLEX_INHERITED
    frame SF_FRAME_NO
  }
  dataType "Inherit: Same as Simulink"
}
instance {
  id 51
  name "Convert urea concentration (mg//ml)\nto
BUN"
  machine 1
  chart 45
}
target {
  id 52
  name "sfun"
  description "Default Simulink S-Function
Target."
  machine 1
  linkNode [1 0 0]
}
}

```

## REFERENCES

- Abel, J. J., Rowntree, L. G., & Turner, B. B. (1913). On the removal of diffusible substances from the circulating blood by means of dialysis. *Transactions of the Association of American Physicians*, (pp. 51–54). Washington, DC.
- Ahrenholz, P., Winkler, R. E., Ramlow, W., Tiess, M., & Muller, W. (1997). On-line hemodiafiltration with pre- and post-dilution: a comparison of efficacy. *International Journal of Artificial Organs*, 20 (2), 81–90.
- Asahi Kasei Medical Company. (n.d.). *Continuous Renal Replacement Therapy (CRRT)*. Retrieved February 2009, 27, from Therapeutic Apheresis & CRRT: <http://www.asahi-kasei.co.jp/medical/en/apheresis/therapies/crrt.html>
- Baker, J. M., Gardner, J. F., Gaumond, R. P., Geselowitz, D. B., & Snyder, A. J. (1998). Relation between geometry and pump efficiency in a positive-displacement blood pump with cylindrical blood chamber and brushless DC motor. *Proceedings of the Annual Northeast Bioengineering Conference*, 113.
- Baxter Healthcare Corporation. (n.d.). *Xenium Dialyzers*. Retrieved August 7, 2008, from <http://www.baxter.com/products/renal/hemodialysis/sub/xenium.pdf>
- Berkoben, M. J., & Schwab, S. J. (2003). Hemodialysis Vascular Access. In W. L. Henrich (Ed.), *Principles and Practice of Dialysis* (3rd Edition ed., pp. 45–63). Lippincott Williams & Wilkins.
- Canaud, B., Bragg-Gresham, J. L., Marshall, M. R., Desmeules, S., Gillespie, B. W., Depner, T., et al. (2006). Mortality risk for patients receiving hemodiafiltration versus hemodialysis: European results from DOPPS. *Kidney International*, 69, 2087–2093.
- Cheung, A. K., Rocco, M. V., Yan, G., Leypoldt, J. K., Levin, N. W., Greene, T., et al. (2006). Serum beta-2 microglobulin levels predict mortality in dialysis patients: results of the HEMO study. *Journal of the American Society of Nephrology*, 17, 546–555.
- Daugirdas, J. T. (1993). Second generation logarithmic estimates of single-pool variable volume Kt/V: an analysis of error. *Journal of the American Society of Nephrology*, 4, 1205–1213.
- Davita, Inc. (2008, May 27). Retrieved from <http://www.davita.com/dialysis>
- Dember, L. M., & Jaber, B. L. (2006). Dialysis-related amyloidosis: late finding or hidden epidemic? *Seminars in Dialysis* (19), 105–109.
- Di Paolo, N., & Sacchi, G. (1989). Peritoneal vascular changes in continuous ambulatory peritoneal dialysis (CAPD): an in vivo model for the study of diabetic microangiopathy. *Peritoneal Dialysis International*, 9 (1), 41–45.

- Dijk, P. C., & Jager, K. J. (2001). Renal replacement therapy in Europ: the results of a collaborative effort by the ERA-EDTA registry and six national or regional registries. *Nephrology Dialysis Transplantation*, *16*, 1120–1129.
- Drukker, W. (1989). Haemodialysis: A Historical Review. In J. F. Maher (Ed.), *Replacement of Renal Function by Dialysis: A Textbook of Dialysis* (3rd ed., pp. 20-86). Springer.
- Eloot, S., De Wachter, D., Van Tricht, I., & Verdonck, P. (2002). Computational flow modeling in hollow-fiber dialyzers. *Artificial Organs*, *26* (7), 590–599.
- Fissell, W. H., Fleischman, A. J., Humes, H. D., & Roy, S. (2007). Development of continuous implantable renal replacement: past and future. *Translational Research*, *150* (6), 327–336.
- Forni, L. G., & Hilton, P. J. (1997). Continuous hemofiltration in the treatment of acute renal failure. *The New England Journal of Medicine*, *336* (9), 1303–1309.
- Francisco, A. M. (2006). Challenges and future of renal replacement therapy. *Hemodialysis International*, *10*, S19–S23.
- Gottschalk, C. W., & Fellner, S. K. (1997). History of the Science of Dialysis. *Am J Nephrol*, *17*, 289–298.
- Gura, V., & Rambod, E. (2007). *Patent No. 7309323 B2*. United States.
- Gura, V., Beizai, M., & Polaschegg, H. (2005). Continuous Renal Replacement Therapy for End-Stage Renal Disease. *Contrib Nephrol*, *149*, 325–333.
- Humes, H. D., MacKay, S. M., Funke, A. J., & Buffington, D. A. (1999). Tissue engineering of a bioartificial renal tubule assist device: In vitro transport and metabolic characteristics. *Kidney International*, *55*, 2502–2514.
- Jennette, J. C., Hepinstall, R. H., Olson, J. L., Schwartz, M. M., & Silva, F. G. (2006). *Hepinstall's Pathology of the Kidney* (6th ed.). Wolters Kluwer Health.
- Jiang, H.-L., Xue, W.-J., Li, D.-Q., Yin, A.-P., Xin, X., Li, C.-M., et al. (2005). Influence of continuous veno-venous hemofiltration on the course of acute pancreatitis. *World Journal of Gastroenterology*, *11* (31), 4815–4822.
- Jirka, T., Cesare, S., Benedetto, D., Change, M. P., Ponce, P., Richards, N., et al. (2006). Mortality risk for patients receiving hemodiafiltration versus haemodialysis. *Kidney International*, *70*, 1524.
- John, S., & Eckhardt, K.-U. (2006). Renal replacement therapy in the treatment of acute renal failure - intermittent and continuous. *Seminars in Dialysis*, *19* (6), 455–464.
- Kaazempur-Mofrad, M. R., Vacanti, J. P., Krebs, N. J., & Borenstein, J. T. (2004, June 6-10). A MEMS-based renal replacment system. *Solid-State Sensor, Actuator and Microsystems Workshop*, 67–70.

- Kerr, P. B., Argiles, A., Flavier, J. L., Canaud, B., & Mion, C. M. (1992). Comparison of hemodialysis and hemodiafiltration: a long term longitudinal study. *Kidney International*, 41 (4), 1035–40.
- Kjellstrand, C. M., & Ing, T. (1998). Daily hemodialysis: history and revival of a superior dialysis method. *ASIAO Journal*, 4 (3), 117–122.
- Kolff, W. J. (1965). First clinical experience with the artificial kidney. *Ann Intern Med*, 62, 608–619.
- Leonard, E. F., Cortell, S., & Vitale, N. G. (2005). Membraneless Dialysis – Is It Possible? (C. Ronco, A. Brendolan, & N. W. Levin, Eds.) *Contributions to Nephrology*, 149, 343–353.
- Locatelli, F., & Buoncristiani, U. (2005). Dialysis dose and frequency. *Nephrology Dialysis Transplantation*, 20, 285–296.
- Lornoy, W., Becaus, Y., Billioux, J. M., Sierens, L., & Malderen, P. V. (1998). Remarkable removal of beta-2-microglobulin by on-line hemodiafiltration. *American Journal of Nephrology*, 18 (2), 105–108.
- Maduell, F. (2005). Hemodiafiltration. *Hemodialysis International*, 47–55.
- Marenzi, G., Marana, I., Lauri, G., Assanelli, E., Grazi, M., Campodonico, J., et al. (2003). The prevention of radiocontrast-agent-induced nephropathy by hemofiltration. *The New England Journal of Medicine*, 349 (14), 1333.
- McIntyre, C. W. (2007). Update on peritoneal dialysis solutions. *Kidney International*, 71, 486–490.
- Moffett, D., Moffett, S., & Schauf, C. (1993). *Human Physiology: Foundations and Frontiers* (2nd ed.). Dubuque, Iowa: Wm. C. Brown Publishers.
- Murray, G., Delorme, E., & Thomas, N. (1947). Development of an artificial kidney. *Archives of Surgery*, 55 (5), 505–522.
- National Kidney Foundation, Inc. (2002). *Kidney disease outcome quality initiative clinical practice guidelines for chronic kidney disease: evaluation, classification, and stratification*.
- Omega. (n.d.). *Omegaflex OEM Style Peristaltic Pumps*. Retrieved May 1, 2008, from <http://www.omega.com/Green/pdf/FPU100.pdf>
- Paskalev, D. N. (2001). Georg Haas (1886-1971): The Forgotten Dialysis Pioneer. *Dialysis & Transplantation*, 30 (12), 828–832.
- Petrie, J. J., Ng, T. G., & Hawley, C. M. (2008). Review article: is it time to embrace haemodiafiltration for centre-based haemodialysis. *Nephrology*, 13, 269–277.
- Piccoli, G. B., Bechis, F., Iacuzzo, C., Anania, P., Iadarola, A. M., Mezza, E., et al. (2000). Why our patients like daily hemodialysis. *Hemodialysis International*, 4, 47–50.
- Polaschegg, H.-D., & Levin, N. W. (1996). *Replacement of Renal Function by Dialysis*. Dordrecht, The Netherlands: Kluwer Academic Publishers.

- Rippe, B., Simonsen, O., Heimbürger, O., Christensson, A., Haraldsson, B., Stelin, G., et al. (2001). Long-term clinical effects of a peritoneal dialysis fluid with less glucose degradation products. *Kidney International*, 59, 348–357.
- (1996). Hemodialysis Fluid Composition. In C. Ronco, A. Fabris, & M. Feriani, *Replacement of Renal Function by Dialysis* (4th ed., p. 257). Springer.
- Ross, S. M. (1974). A mathematical model of mass transport in a long permeable tube with radial convection. *Journal of Fluid Mechanics*, 63, 157–175.
- Saito, A., Aung, T., Sekiguchi, K., Sato, Y., Vu, D. M., Inagaki, M., et al. (2006). Present status and perspectives of bioartificial kidneys. *Journal of Artificial Organs*, 9, 130–135.
- Sargent, A. J., & Gotch, A. F. (1989). Principles and Biophysics of Dialysis. In C. Jacobs, C. M. Kjellstrand, K. M. Koch, & J. F. Winchester (Eds.), *Replacement of Renal Function by Dialysis* (3 ed., p. 38). New York: Springer-Verlag New York, LLC.
- Saudan, P., Niederberger, M., De Seigneux, S., Romand, J., Pugin, J., Perneger, T., et al. (2006). Adding a dialysis dose to continuous hemofiltration increases survival in patients with acute renal failure. *Kidney International*, 70, 1312–1317.
- Suzuki, Y., Kohori, F., & Sakai, K. (2001). Computer-aided design of hollow-fiber dialyzers. *Journal of Artificial Organs*, 4, 326–330.
- Tiranathanagul, K., Brodie, J., & Humes, D. H. (2006). Bioartificial kidney in the treatment of acute renal failure associated with sepsis. *Nephrology*, 11 (4), 285–291.
- Tiranathanagul, K., Eiam-Ong, S., & Humes, H. D. (2005). The future of renal support: high-flux dialysis to bioartificial kidneys. *Critical Care Clinics*, 21 (4), 379–394.
- Ward, R. A., & Leypoldt, J. K. (2001). What clinically important advances in understanding and improving dialyzer function have occurred recently? *Seminars in Dialysis*, 14 (3), 160–162.
- Ward, R. A., Schmidt, B., Hullin, J., Hillerbrand, G. F., & Samtleben, W. (2000). A comparison of on-line hemodiafiltration and high-flux hemodialysis: a prospective clinical study. *Journal of the American Society of Nephrology*, 9, 2344–50.
- Witowski, J., Jörres, A., Korybalska, K., Ksiazek, K., Wisniewska-Elnur, J., Bender, T. O., et al. (2003). Glucose degradation products in peritoneal dialysis fluids: Do they harm? *Kidney International*, 63, S148–S151.
- YassineMrabet. (2008, January 17). *File:Hemodialysis-en.svg*. Retrieved February 27, 2009, from Wikipedia: <http://en.wikipedia.org/wiki/File:Hemodialysis-en.svg>
- Ziólko, M., Pietrzyk, J. A., & Grabska-Chrzastowska, J. (2000). Accuracy of hemodialysis modeling. *Kidney International*, 57, 1152–1163.